JAERI-M
9856

ANNUAL REPORT OF THE OSAKA LABORATORY FOR RADIATION CHEMISTRY JAPAN ATOMIC ENERGY RESEARCH INSTITUTE

(No. 14)

April 1, 1980 - March 31, 1981

December 1981

Osaka Laboratory for Radiation Chemistry

日本原子力研究所
Japan Atomic Energy Research Institute

JAERI-Mレポートは，日本原子力研究所が不定期に公刊している研究報告書です。
入手の問合わせは，日本原子力研究所技術情報部情報資料課（〒319-11茨城県那珂郡東海村）あて，お申しこしください。なお，このほかに財団法人原子力弘済会資料センター（〒319-11 茨城県那珂郡東海村日本原子力研究所内）で複写による実費頒布をおこなっております。

JAERI-M reports are issued irregularly.
Inquiries about availability of the reports should be addressed to Information Section, Division of Technical Information, Japan Atomic Energy Research Institute, Tokai-mura, Naka-gun, Ibaraki-ken 319-11, Japan.

編集兼発行　日本原子力研究所
印　　刷　いばらき印刷㈱

Osaka Laboratory for Radiation Chemistry
Japan Atomic Energy Research Institute
25-1 Mii-minami machi, Neyagawa
Osaka, Japan

JAERI-M 9856

ANNUAL REPORT OF THE OSAKA LABORATORY FOR RADIATION CHEMISTRY JAPAN ATOMIC ENERGY RESEARCH INSTITUTE

(No. 14)

April 1, 1980 - March 31, 1981

(Received November 28, 1981)

This report describes research activities of Osaka Laboratory for Radiation Chemistry, JAERI during one year period from April 1, 1980 through March 31, 1981. The latest report, for 1980, is JAERI-M 9214.

Detailed descriptions of the activities are presented in the following subjects: studies on reactions of carbon monoxide, hydrogen and methane; polymerization under the irradiation of high dose rate electron beams; modification of polymers, degradation, cross-linking, and grafting.

Previous reports in this series are:

Annual Report,	JARRP,	Vol. 1	1958/1959*
Annual Report,	JARRP,	Vol. 2	1960
Annual Report,	JARRP,	Vol. 3	1961
Annual Report,	JARRP,	Vol. 4	1962
Annual Report,	JARRP,	Vol. 5	1963
Annual Report,	JARRP,	Vol. 6	1964
Annual Report,	JARRP,	Vol. 7	1965
Annual Report,	JARRP,	Vol. 8	1966
Annual Report,	No. 1,	JAERI 5018	1967
Annual Report,	No. 2,	JAERI 5022	1968
Annual Report,	No. 3,	JAERI 5026	1969
Annual Report,	No. 4,	JAERI 5027	1970
Annual Report,	No. 5,	JAERI 5028	1971
Annual Report,	No. 6,	JAERI 5029	1972
Annual Report,	No. 7,	JAERI 5030	1973
Annual Report,	No. 8,	JAERI-M 6260	1974
Annual Report,	No. 9,	JAERI-M 6702	1975
Annual Report,	No.10,	JAERI-M 7355	1976
Annual Report,	No.11,	JAERI-M 7949	1977
Annual Report,	No.12,	JAERI-M 8569	1978
Annual Report,	No.13,	JAERI-M 9214	1979

* Year of the activities

Keywords: Electron Beam Irradiation, γ-Irradiation, Carbon Monoxide-Hydrogen Reaction, Methane, Radiation-Induced Reaction, Polymerization, Emulsion Polymerization, Grafting, Polymer Modification, Cross-Linking, Vinyl Monomer, Dienes, Polystyrene, Polyvinyl Chloride Powder, Radiation Chemistry

JAERI－M 9856

昭和５５年度日本原子力研究所　大阪研究所年報

日本原子力研究所・高崎研究所・大阪研究所

（１９８１年 11月 28 日受理）

本報告は、大阪研究所において昭和５５年度に行なわれた研究活動を述べたものである。主な研究題目は、一酸化炭素、水素およびメタンの反応ならびにそれに関連した研究、高線量率電子線照射による重合反応の研究、ポリマーの改質および上記の研究と関連して重合反応、高分子分解、架橋ならびにグラフト重合に関する基礎的研究などである。

日本放射線高分子研究協会年報　Vol. 1			1958/1959
日本放射線高分子研究協会年報　Vol. 2			1960
日本放射線高分子研究協会年報　Vol. 3			1961
日本放射線高分子研究協会年報　Vol. 4			1962
日本放射線高分子研究協会年報　Vol. 5			1963
日本放射線高分子研究協会年報　Vol. 6			1964
日本放射線高分子研究協会年報　Vol. 7			1965
日本放射線高分子研究協会年報　Vol. 8			1966
日本原子力研究所大阪研における放射線化学の基礎研究No.1	JAERI	5018	1967
日本原子力研究所大阪研における放射線化学の基礎研究No.2	JAERI	5022	1968
日本原子力研究所大阪研における放射線化学の基礎研究No.3	JAERI	5026	1969
日本原子力研究所大阪研における放射線化学の基礎研究No.4	JAERI	5027	1970
日本原子力研究所大阪研における放射線化学の基礎研究No.5	JAERI	5028	1971
日本原子力研究所大阪研における放射線化学の基礎研究No.6	JAERI	5029	1972
日本原子力研究所大阪研における放射線化学の基礎研究No.7	JAERI	5030	1973
Annual Report, Osaka Lab., JAERI, No.8	JAERI－M	6260	1974
Annual Report, Osaka Lab., JAERI, No.9	JAERI－M	6702	1975
Annual Report, Osaka Lab., JAERI, No.10	JAERI－M	7355	1976
Annual Report, Osaka Lab., JAERI, No.11	JAERI－M	7949	1977
Annual Report, Osaka Lab., JAERI, No.12	JAERI－M	8569	1978
Annual Report, Osaka Lab., JAERI, No.13	JAERI－M	9214	1979

CONTENTS

目　　次

I. INTRODUCTION

Osaka Laboratory was founded in 1958 as a laboratory of the Japanese Association for Radiation Research on Polymers (JARRP), which was organized and sponsored by some fifty companies interested in radiation chemistry of polymers. The JARRP was merged with Japan Atomic Energy Research Institute (JAERI) on June 1, 1967, and the laboratory has been operated as Osaka Laboratory for Radiation Chemistry, Takasaki Radiation Chemistry Establishment, JAERI. The research activities of Osaka Laboratory have been oriented towards the fundamental research on applied radiation chemistry.

The results of the research activities of the Laboratory were published from 1958 until 1966 in the Annual Reports of JARRP which consisted essentially of original papers. During the period between 1967 and 1973, the publication had been continued as JAERI Report which also consisted mainly of original papers. From 1974, the Annual Report has been published as JAERI-M Report which contains no original papers, but presents outlines of the current research activities in some detail. Readers who wish to have more information are advised to contact with individuals whose names appear under subjects.

The present annual report covers the research activities of the Laboratory between April 1, 1980 and March 31, 1981.

Most of the studies carried out in the Laboratory are continuation from the previous year, emphasis being laid on two fields; one is "Effect of radiation on the reaction of carbon monoxide, methane and hydrogen" and the other, "Radiation-induced polymerization by high dose rate electron beams".

In order to elucidate the mechanism of selectivity toward hydrocarbon formation and of sensitization of the reaction in the presence of silica gel in the radiation chemical reaction of carbon monoxide-hydrogen mixture, extensive studies have been carried out on the structure and the reactivity with hydrogen of the carbonaceous solid which is formed from CO by

the irradiation in the presence of silica gel. The amorphous carbonaceous solid has a composition indicated by $(C_5O)_n$ and contains more carbon than that obtained by the same procedure without silica gel, which has a formula of $(C_3O_2)_n$. Silica gel sensitizes strongly both the reaction producing the carbonaceous solid and the hydrogenation reaction of the carbonaceous solid. Studies have also been carried out on the radiation-induced reaction of mixture of carbon monoxide and hydrogen containing acetaldehyde without the presence of solid in an attempt to know the fate of acetaldehyde once formed by radiation and the result indicated that a considerable amount of acetaldehyde was converted to acetic acid by the irradiation.

In the study to know the effect of dose on the G value of ethylene formation at 200°C, it was found that the G (C_2H_4) value increased with decreasing dose and the maximum G (C_2H_4) value was ca. 3 at 0.03 Mrad. From the molecular weight distribution of the hydrocarbon products obtained by large dose, it was suggested that methane is converted to hydrogen and higher hydrocarbons as the final products obtained by continued irradiation.

The irradiation study of methane was carried out in the temperature range from 100°C to 600°C. The maximum G value (ca. 13) of ethane formation was found at 550°C, where thermal decomposition producing hydrogen and carbon begins to occur significantly.

The mixture of methane and carbon monoxide was irradiated with electron beam in the temperature range from 60 to 300°C. The maximum G values of the organic acids were obtained at 140°C. The effect of addition of nitric oxide or nitrous oxide to the mixture on the G values of the products was also studied.

Systematic experiments on the bulk polymerization of styrene at high dose rate were begun in 1973 in this laboratory. It was found in the case of moderately dried styrene that radical and ionic polymers and oligomer were produced by the polymerization; when wet styrene (water content 3.5×10^{-2} mol/l) is used, super polymer of molecular weight about one

million was formed besides the three kinds of the above mentioned polymers. Formation of radical and ionic polymers has already been studied to a considerable extent. Oligomers and super polymers remain almost untouched, though they are interesting not only from fundamental but also from practical points of view. Some experimental results are reported in the present report on the content of the super polymer in percent of the total polymer. The highest value in the polymerization of wet styrene was about 10%. The super polymer is formed not only in the presence of water, but also in the presence of many additives. For example in the case of the addition of ethylene glycol and DPPH, the content of super polymer was 22% and 36%, respectively. It is expected that higher values will be obtained by further investigation.

Radiation-induced cationic telomerization has been studied on butadiene in the presence of several chlorine containing compounds (RX) as telogen to investigate average molecular weight, concentration of terminal group and structure of the telomer. The average molecular weight of the telomer decreased with increasing [RX]/[B], in which 1-chloro-2-butene was used as RX, but the number of terminal chlorine atoms per a telomer molecule was about 1.2 independent of [RX]/[B] ratio and the structure of the telomer was not much different from that obtained by usual catalytic solution telomerization. Similar experiments have been carried out using benzyl chloride, cumyl chloride, and epichloro hydrine as RX.

Studies on radiation-induced emulsion polymerization of styrene have been carried out using flow system at high dose rate, and the average diameter of the polymer particles was found to be 50 $\sim$ 70 nm which are significantly smaller than that obtained at lower dose rate.

In an attempt to obtain polyethylene (PE) filament having thermal stability, the graft polymerization of acrylic acid onto PE filament has been studied by pre-irradiation method using electron beam. The PE fiber of lower degree of grafting than that of previously obtained by γ-ray irradiation showed good thermal stability and improved mechanical properties at

high temperature.

Preliminary experiments to prepare strongly acidic cationic ion exchange resin for general purposes have been carried out by radiation-induced grafting. Under certain reaction conditions in the presence of swelling agent, vinyl monomers having sulfonic group can be successfully grafted onto powder of vinyl acetate-vinyl chloride-copolymer. Exchange capacity of the resin against cupric or lithic ion was about 40% of that commercially obtained, but the rate of exchange of the former exceeds the latter.

Administrative changes were made in the Laboratory on June 1, 1981. Dr. Yunosuke Oshima moved to Takasaki Radiation Chemistry Research Establishment as head of the Pilot Scale Research Station and Dr. Isamu Kuriyama was appointed head of the Laboratory. Professor I. Sakurada who directed the research activities as the head since 1958 and as an advisor since 1975 retired on March 31, 1981, to whom we are very much indebted for his direction and encouragement of our research.

Dr. Isamu Kuriyama, Head
Osaka Laboratory for Radiation Chemistry
Japan Atomic Energy Research Institute

II. RECENT RESEARCH ACTIVITIES

[1] Radiation-Induced Reactions of Carbon Monoxide, Hydrogen, and Methane

1. Irradiation of Circulating Mixtures of Carbon Monoxide and Hydrogen under Elevated Pressure

-- Effects of Temperature and Pressure on the Amounts of Products

In the former annual reports[1,2], we reported the effects of pressure and temperature on the amounts of products at elevated pressure, in which some abnormal phenomena were noticed: e.g., G value of acetaldehyde formation increased, reached a maximum, and then decreased with increasing pressure. These phenomena are considered to be related to the problem that the efficiency of trapping condensable products by the cold traps included in the gas circulation system becomes poorer with increasing gas pressure. The temperature in the irradiation zone was also difficult to maintain at a desired value at higher gas pressure above 5000 Torr during circulation.

In order to remove these difficulties, studies have been carried out to find the pressure and temperature dependence of the G values of the products using a modified gas circulation system in which the pre-cooling coil and pre-heating coil were additionally installed before and after the cold traps, and the results were compared with the former experimental results (JAERI-M 8569, 9214).

Irradiations were performed by electron beams from the HDRA (0.6 MeV, 1 mA) for 100 seconds on the mixture of CO and H_2 (CO 55 mole%) at 10°C. The dose rate measured by N_2O dosimetry was 3.42×10^{-4} eV·N_2O molecule^{-1}·sec^{-1}.

The method of analysis of the irradiation products were the same as that reported previously[1]. After the irradiation, the reactants and products in the reaction vessel were pumped

out through cold traps in which condensable products were collected. The collected products were subjected to gas chromatography and mass spectrometry.

The G values of the products from the reactant containing 55 mole% CO are plotted against pressure of the reactant in Fig. 1. The conversion of feed gas to products were approximately 0.3%. The G (HCHO) value increases with increasing pressure. The G(CH_3CHO) increases more steeply with increasing pressure but seems to level off above 5000 Torr. The G(C_2H_5CHO) shows similar tendency, although the values are smaller than those of CH_3CHO. The G(CH_3OH) increases with pressure but above 5000 Torr, the G value decreases with pressure. The G (CH_4) and G(TOX) seem to decrease with increasing pressure. Difference of some experimental conditions from those in the

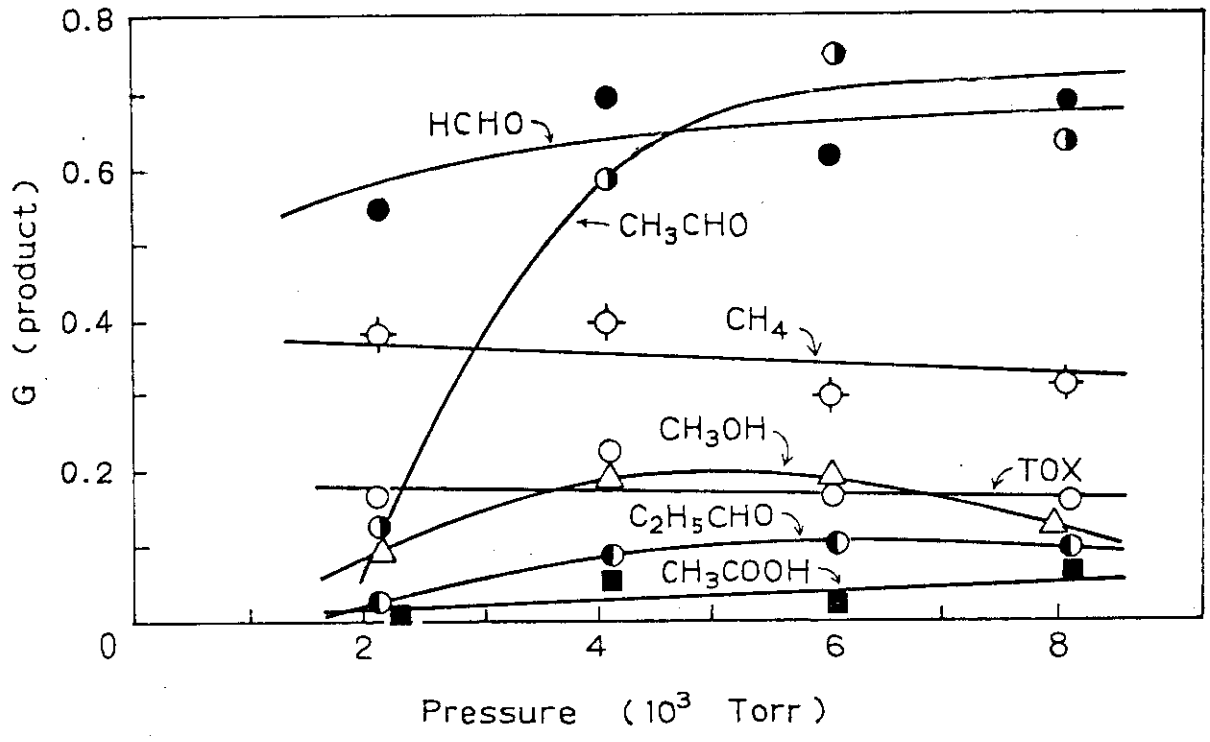

Fig. 1. Effects of pressure of the reactant on the G values of the products: CO content, 55 mole%; Electron beam, 0.6 MeV, 1 mA; Irradiation time, 100 sec; Dose, 1.3×10^{-2} eV·molec^{-1} (8.0 Mrad); Temperature, 10°C.

previous experiment makes it difficult to compare directly the data with those previously obtained, but with help of known dependence of G value on several parameters including CO content, temperature, or dose, the following remarks can be made.

The most remarkable difference is that $G(CH_3CHO)$ does not decrease with increasing pressure but increases to 0.7 above 5000 Torr whereas it decreased with increasing pressure above 5000 Torr in the previous report.

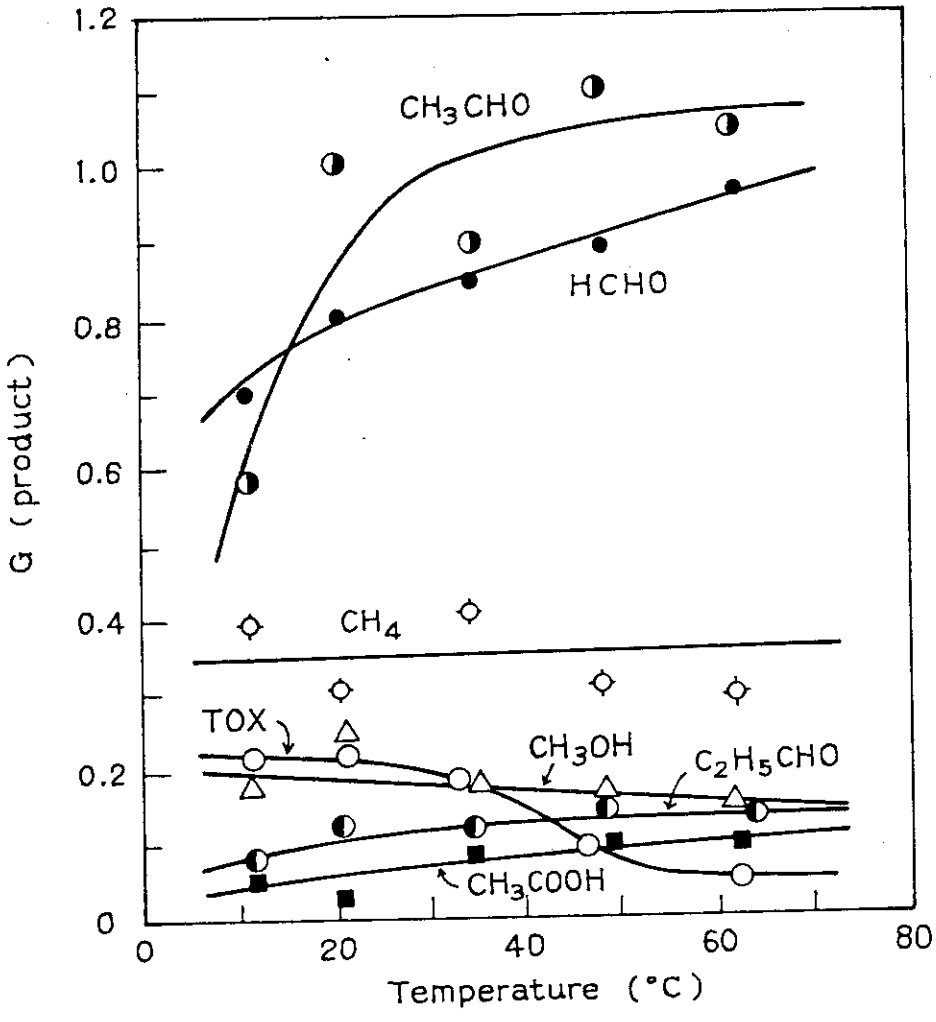

Fig. 2. Effects of temperature on G values of the products: CO content, 55 mole%; Pressure, 4000 Torr; Electron beam, 0.6 MeV, 1 mA; Irradiation time, 100 sec; Energy absorbed in the mixture, 1.8×10^{22} eV (Dose, 8.0 Mrad).

The pressure effects on the yields of other compounds are not much different from those reported previously.

In Fig. 2, the G values of main products are plotted as a function of temperature during irradiation. The results that the G(HCHO) and $G(CH_3CHO)$ continue to increase up to 60°C instead of the previous results where G(HCHO) and $G(CH_3CHO)$ decreased with increasing temperature above 40°C, may again come from the improved trap efficiency which is still high enough to remove the products from the circulating gas even at higher temperatures above 40°C. The G values of minor products except trioxane are also increased at higher temperature region. The G(TOX) decreases with increasing temperature as previously reported.

It is revealed that the decrease of the G(HCHO) and $G(CH_3CHO)$ with increasing pressure and temperature above certain values found in the previous experiments are not observed by improving the trap efficiency in the circulation system, but we can not mention whether the G value with increasing pressure and temperature would be increased more by further improvement of the trap efficiency, nor could we pursue this problem further.

(S. Sugimoto and M. Nishii)

1) S. Sugimoto and M. Nishii, JAERI-M 8569, 16 (1979).
2) Ibid., JAERI-M 9214, 5 (1980).

2. The Radiation Chemical Reactions of the Ternary Mixture of CO, H_2, and CH_4

In a preliminary experiment, it was found that the $G(CH_3CHO)$ increased with the addition of a small amount of methane.[1] Arai et al.[2], reported that acetic and propionic acids were produced with high G values of 1.6 and 1.2, respectively, from $CO-CH_4$ mixture by electron irradiation. In the present study, the ternary mixture of $CO-H_2-CH_4$ was irradiated to see whether acetic acid and acetaldehyde can be obtained with high G values.

The methods of irradiation and analysis of the products are the same as those previously described. The irradiation were carried out using electrons (0.6 MeV, 1 mA) for 200 sec and energies absorbed by mixtures in the irradiation vessel were $1.7 \times 10^{22} \sim 2.8 \times 10^{22}$ eV depending on the gas composition. The gas pressure was 4000 Torr.

In Figs. 1 and 2, the G values of the main products are plotted as a function of CH_4 content in mole %, where the molar ratio of CO to H_2 are kept constant at 15/85. The irradiation temperature is 25°C. The $G(CH_3CHO)$ (Fig. 1), $G(CH_3COOH)$

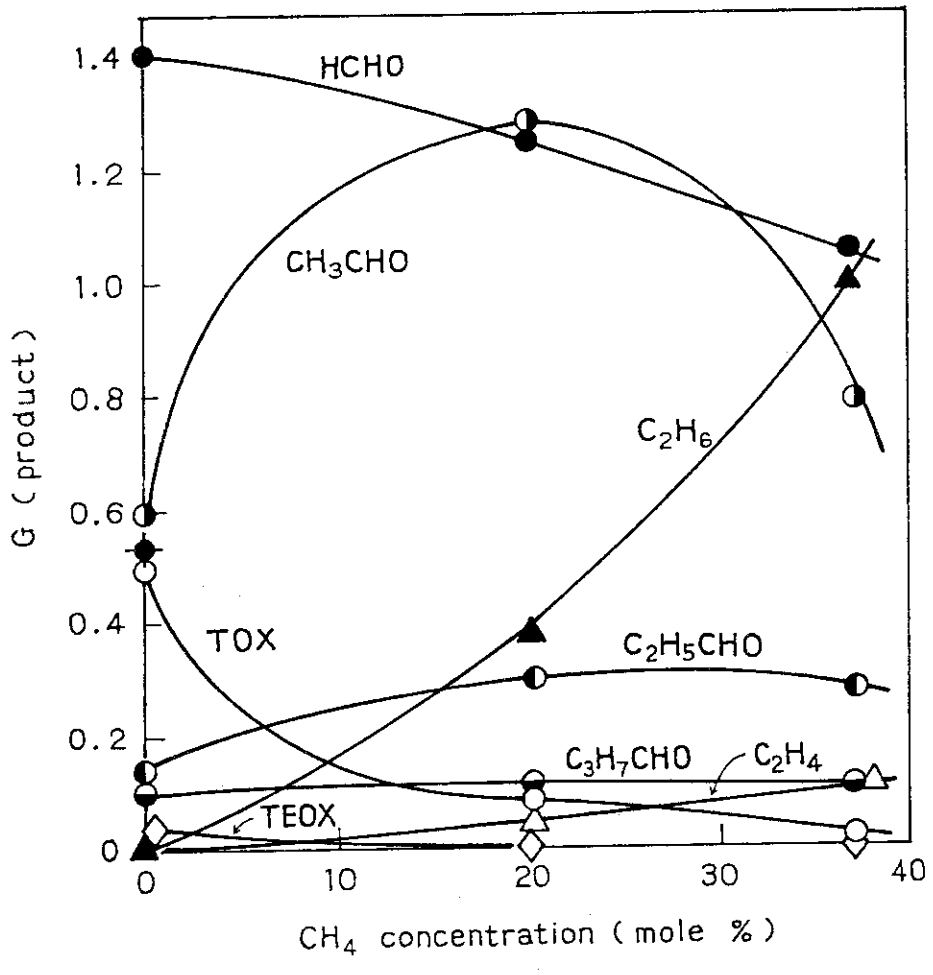

Fig. 1. The G values of aldehydes, cyclic ethers, and hydrocarbons as a function of CH_4 concentration: CO/H_2, 15/85; Pressure, 4000 Torr; Temperature, 25°C; Energy absorbed by the mixture in the irradiation vessel (plots from left to right), 1.7, 2.2, and 2.8×10^{22} eV.

(Fig. 2), and G(HCOOH) (Fig. 2) increase with the addition of CH_4 (20 mole%), reach maxima, but then decrease with further addition of CH_4. The G(HCHO), G(trioxane), G(tetraoxane), G(CH_3OH), G(C_2H_5OH), and G(CO_2) decrease with increasing CH_4 concentration. Other compounds which contain C-C bond carbons increase with increasing CH_4 concentration.

Figure 3 shows the effects of CO concentration on the G values of aldehydes and hydrocarbons produced from the ternary

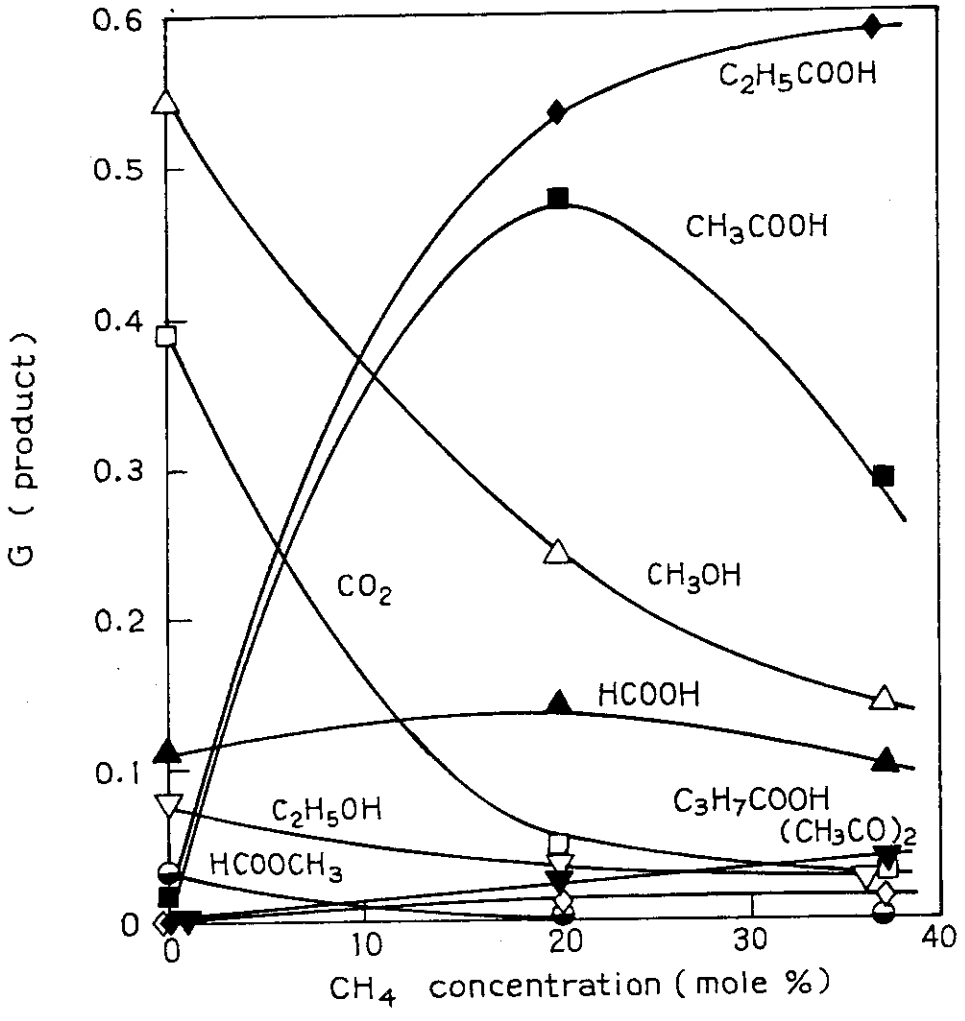

Fig. 2. The G values of alcohols, acids, methyl formate, biacetyl, and carbon dioxide as a function of CH_4 concentration: CO/H_2, 15/85; Pressure, 4000 Torr; Irradiation, 0.6 MeV, 1 mA, 200 sec; Temperature, 25°C.

mixture of CO, H_2, and CH_4 where CH_4 content was kept constant at 20 mole%. Data obtained from CO-H_2 mixture without CH_4 are also included in the figure for comparison. The same plots are shown in Fig. 4 for acids, alcohols, and biacetyl.

Since the G values of CH_3CHO, HCHO, C_2H_6 and C_3H_7CHO obtained without CH_4 lie on the plots obtained with the presence of CH_4 as shown in Fig. 3, the presence of CH_4 does not have much effect on the reactions producing these compounds. However, the presence of CH_4 seems to be important for CH_3CHO,

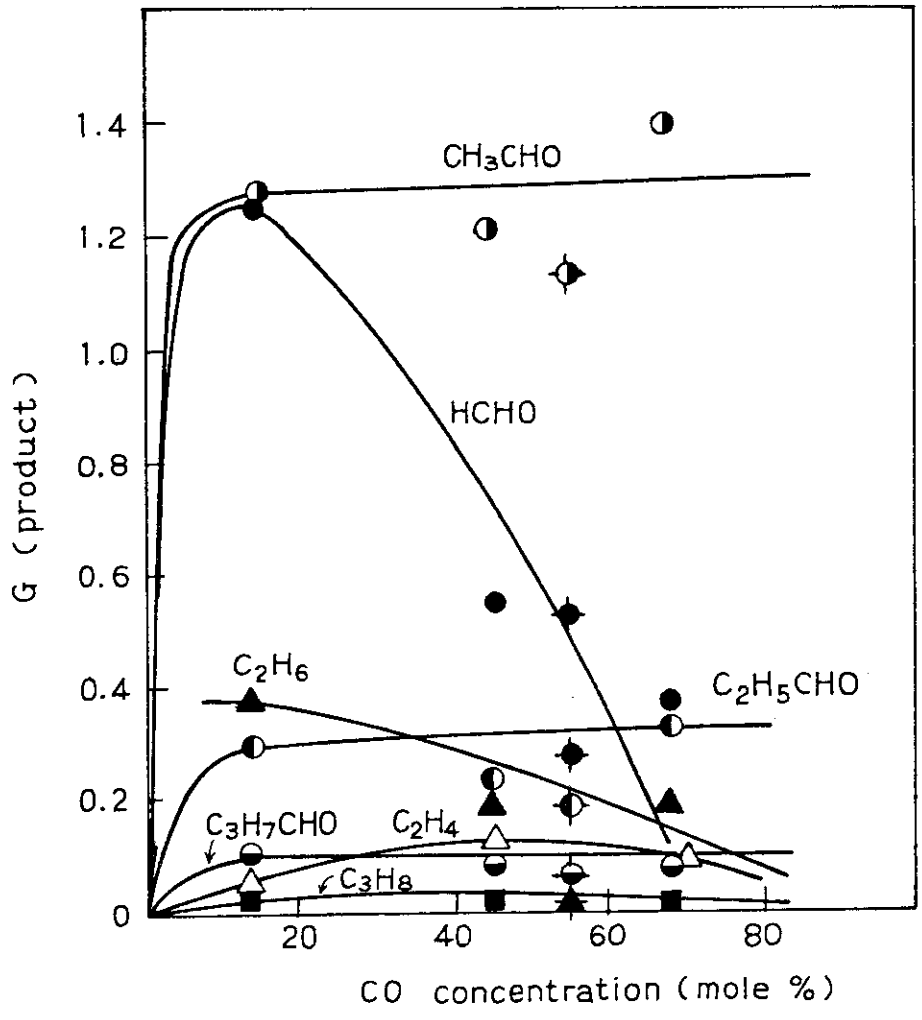

Fig. 3. The G values of aldehydes and hydrocarbons as a function of CO concentration: CH_4 content, 20 mole%; Irradiation, 0.6 MeV, 1 mA, 200 sec; Temperature, 30°C. Symbols superimposed with + denote the values obtained in the mixture without CH_4.

C_2H_5CHO and C_3H_7CHO at lower CO concentration where the G values of these compounds are small when no CH_4 is present in the system (Fig. 6, JAERI-M 9214, p. 11). Since the G values of acid formation are reported to be small except for HCOOH for mixture without CH_4, CH_4 may have important role for the formation of these acids except HCOOH. These acids may be produced by a series of reactions involving CH_3^+ ion as proposed by Arai et al.[2] Methane has negative effect on the formation of alcohols.

Through the above experiments, the products which are

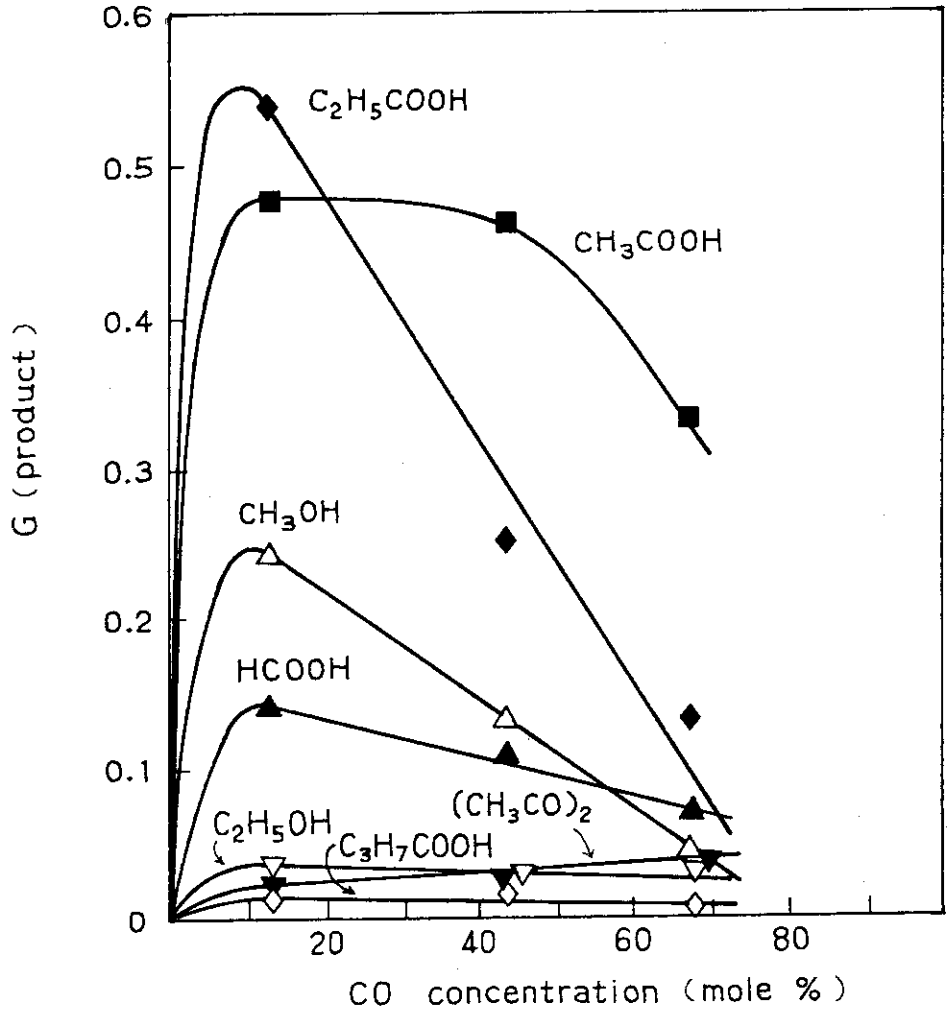

Fig. 4. G values of acids and alcohols as a function of CO concentration: Experimental conditions are given in the caption of Figure 3.

favored by the addition of methane and their maximum G values (in parentheses) are: CH_3COOH (0.48), C_2H_5COOH (0.6), CH_3CHO (1.25), C_2H_5CHO (0.35), and C_3H_7CHO (0.1).

(S. Sugimoto and M. Nishii)

1) S. Sugimoto and M. Nishii, JAERI-M 7899 (1978).
2) H. Arai, S. Nagai, and M. Hatada, Radiat. Phys. Chem., 17, 211 (1981).

3. The Radiation-Induced Reactions of Acetaldehyde in the $CO-H_2$ Mixture by Electron Irradiation

During the course of the study[1] on radiation chemistry of $CO-H_2$ mixture, acetaldehyde was found to be produced as a C_2 compound, which contains carbon-carbon bond in a molecule, with rather good yield. According to our past studies, amount of acetaldehyde increased with dose, pressure, and temperature, but it seemed to level-off or decreased above certain values of these parameters. One or both of the following two cases may be considered as the cause of the above undesired results: one is that acetaldehyde once produced is converted to other compounds by successive reactions induced by further irradiation when acetaldehyde is recycled in the irradiation zone, and the other is that some compounds formed during irradiation inhibit or retard the formation of acetaldehyde. The results of the previous study[2] in which the amount of acetaldehyde increased by improved trap efficiency indicate the possibility of the former case as the cause of the leveling-off the amount of the product with increasing dose.

In this study, the products from $CO-H_2$ mixture containing various amounts of acetaldehyde were analyzed in order to know the reaction scheme of acetaldehyde in $CO-H_2$ mixture by radiation. Radiation chemical products from $CO-H_2$ mixture of different CO contents containing small amounts of CH_3CHO and from $CO-D_2$ mixture with or without the presence of CH_3CHO were also investigated for the same purpose.

Experimental method and technique are the same as those described in the previous study[1] except that the known amount of acetaldehyde was added to the mixture. The gas pressure was kept constant at 4000 Torr. The CO content was 55 mole% while the acetaldehyde content was varied from 0 to 0.15 mole%. In another series of experiment, the CO content was varied while the acetaldehyde content was ca. 0.095 mole%. The irradiations were carried out using electron beams of 0.6 MeV and 1 mA at room temperature (ca. 25°C) for 100 ∿ 400 sec.

Table 1 shows the amounts of products obtained by 16 Mrad irradiation of $CO-H_2$ mixtures containing different amounts of acetaldehyde. The concentration of acetaldehyde after the irradiation increases with increasing amount of the initial concentration of acetaldehyde. The values in the parentheses indicate the amount of acetaldehyde consumed during irradiation which is calculated on the assumption that the amount of acetaldehyde produced from $CO-H_2$ mixture by irradiation is independent of the initial amount of acetaldehyde and is equal to the amount of acetaldehyde produced from $CO-H_2$ which did not initially contain acetaldehyde. According to the above assumption, the formation and loss of acetaldehyde can be expressed by

$$CO + H_2 \longrightarrow CH_3CHO \qquad [1]$$

$$CH_3CHO + X^* \xrightarrow{k_2} -CH_3CHO \qquad [2]$$

where X* denotes active species produced from CO or H_2 by irradiation. Therefore, the concentration of acetaldehyde becomes

$$\frac{d}{dt}[CH_3CHO] = v_1 - k_2[CH_3CHO][X^*] \qquad (1)$$

where [X*] is assumed to be constant, and v_1 is the rate of acetaldehyde formation by reaction [1]. The integration of eq. (1) with initial concentration of acetaldehyde, $[CH_3CHO]_0$ gives the following equation:

Table 1. The Amounts of Products in μmole from CH-H_2 Mixture Containing Different Amount of CH_3CHO

CH_3CHO content (mole%)	0	0.04	0.07	0.078	0.13
$[CH_3CHO]_0$ (μmole)	0	1077.3	1774.4	2027.6	3802.5
CH_4	180.9	182.9	180.7	191.8	210.6
$C_2H_4 + C_2H_2$	4.47	13.4	14.36	19.95	43.0
C_2H_6	4.68	9.27	6.72	7.39	9.52
X	32.12	11.51	50.28	23.91	64.83
C_3H_8	0.96	0.	0.	-	0.08
HCHO	453.4	547.9	731.3	522.6	902.0
CH_3CHO	365.7	725.9	1106.	1635.	2685.
$(-CH_3CHO)$		(717.1)	(1034.1)	(757.8)	(1483.2)
C_2H_5CHO	51.29	25.44	12.83	16.53	49.13
CH_3OH	118.5	110.6	76.67	151.7	77.40
C_2H_5OH	3.40	9.62	2.39	5.91	13.36
$n-C_3H_7OH$	0.	0.54	1.57	3.44	3.44
HCOOH	6.24	28.10	31.11	25.46	57.47
CH_3COOH	24.71	173.9	83.29	128.1	244.2
C_2H_5COOH	0.39	25.18	24.57	31.84	84.33
$n-C_3H_7COOH$	0.25	3.17	2.66	1.59	3.38
$HCOOCH_3$	42.90	7.52	3.63	2.36	4.14
$(CH_3CO)_2$	1.20	2.26	0.	2.30	1.47
Trioxane	44.45	13.72	10.84	6.89	8.31
Tetraoxane	7.18	3.05	2.33	2.20	0.90
H_2O	554.5	707.8	899.1	616.0	692.7
CO_2	375.6	417.6	559.9	279.5	296.8
$G(+CH_3CHO)$	0.61	-1.20	-1.77	-1.27	-2.31

CO content, ca. 55 mole%; Dose, 16 Mrad

$$\ln \frac{v_1 - k'[CH_3CHO]}{v_1 - k'[CH_3CHO]_0} = -k_1 t \qquad (2)$$

where k' is $k_2[X^*]$. At a certain time, t_1, the $[CH_3CHO]$ can be expressed as a function of $[CH_3CHO]_0$ by the following equation.

$$[CH_3CHO] = C_1 + C_2[CH_3CHO]_0 \qquad (3)$$

where C_1 and C_2 are constants. The linear plot of $[CH_3CHO]$ against $[CH_3CHO]_0$ in Fig. 1 seems to fit eq. (3) supporting the above consideration.

The G value of acetaldehyde consumption is plotted in Fig. 2 as a function of $[CH_3CHO]_0$. The G values of other products are also plotted as a function of $[CH_3CHO]_0$ in Figs. 3 and 4. It is noted that the G values of HCHO, HCOOH, CH_3COOH, and C_2H_5COOH and C_2H_4 increase, while those of trioxane,

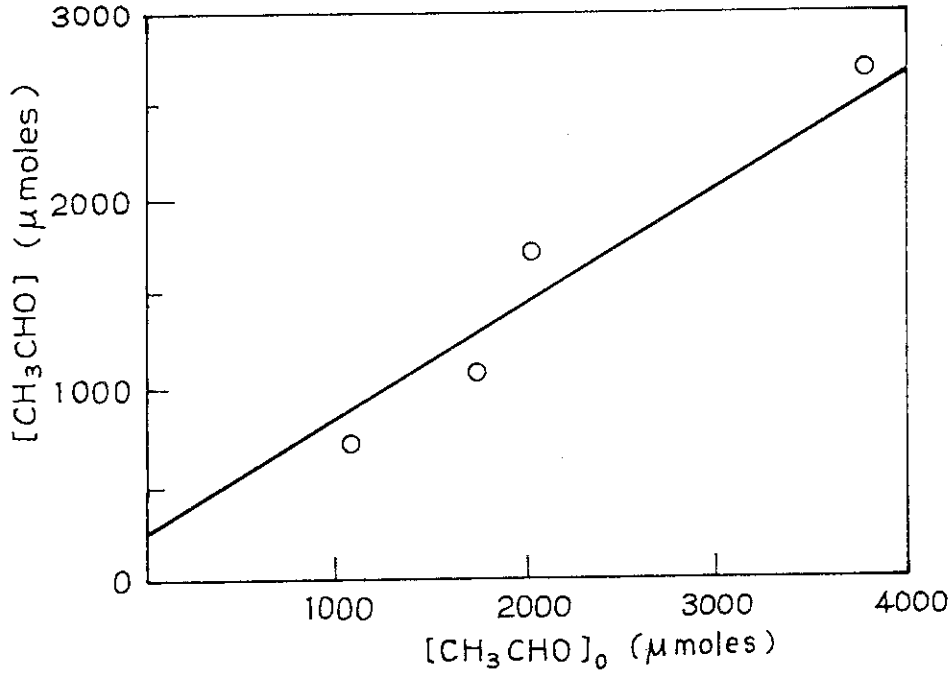

Fig. 1. The effect of initial amount of CH_3CHO in CO-H_2 mixture on the amount of CH_3CHO at 16 Mrad irradiation: CO content, 55 mole%.

$HCOOCH_3$, and CH_3OH decrease with increasing amount of $[CH_3CHO]_0$. The acetaldehyde consumed may change to compounds whose G values increase with increasing $[CH_3CHO]_0$, but definite quantitative relation between the amounts of acetaldehyde consumed and the increased amounts of products supposedly come from the consumed acetaldehyde has not obtained.

In order to know which of the reactants CO or H_2 is more important in reaction [2], the $G(CH_3CHO)$ was obtained for CO-H_2 mixture containing 0.095 mole% CH_3CHO as a function of CO mole% in the mixture.

The result is given in Fig. 5, where the result obtained for CO-H_2 mixture which did not contain initially acetaldehyde (given by $G^0(CH_3CHO)$ in the figure). The $G(-CH_3CHO)$ plot shows a concave down-ward curve, indicating that both active species produced from H_2 and those from CO react to destruct

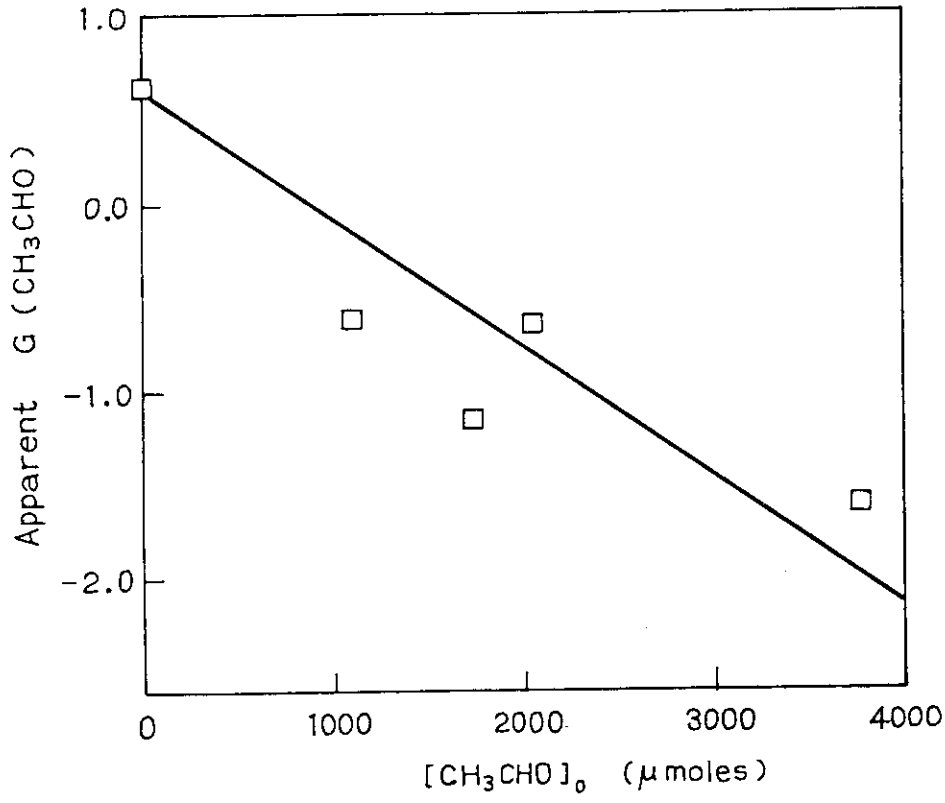

Fig. 2. Apparent $G(CH_3CHO)$ as a function of initial concentration of acetaldehyde: Dose 16 Mrad; CO content, 55 mole%.

acetaldehyde. Since acetaldehyde is produced from CO-H_2 mixture, the net G(-CH_3CHO) is given by the sum of G(-CH_3CHO) + $G^0(CH_3CHO)$, which is also shown by a broken line in Fig. 5. The net G(-CH_3CHO) plot also gives a concave down-ward curve, but the minimum point appeared at 30 mole% CO. The decrease of net G(-CH_3CHO) may be come from that active species from H_2 and those from CO are consumed to react to form products with CO

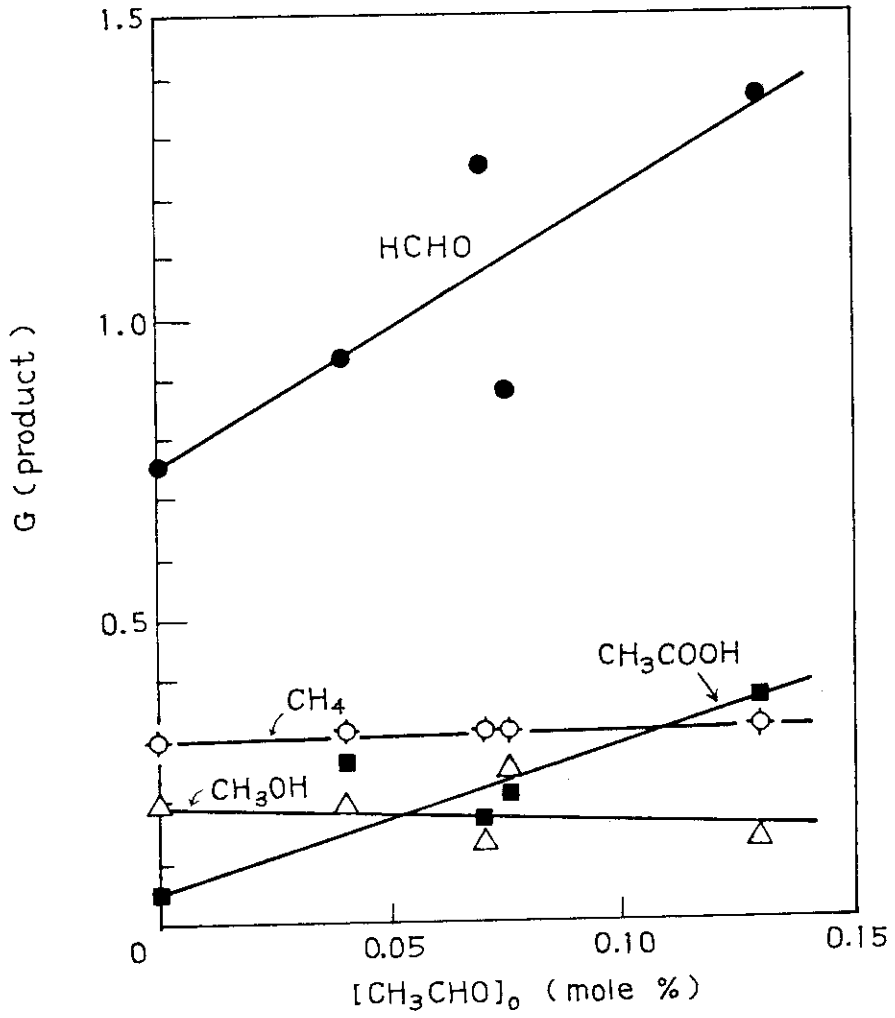

Fig. 3. The effect of acetaldehyde concentration on G values of the products from CO-H_2 mixture: CO content, 55 mole%; Pressure, 4000 Torr; Irradiation conditions, 0.6 MeV, 1 mA, 300 sec; Energy absorbed by the mixture in the irradiation vessel, 3.5×10^{22} eV (Dose, 16 Mrad); Temperature, 25°C.

and H_2, respectively. (Reaction [7] and [8] and thus these reactions compete with the reaction destructing acetaldehyde (reaction [5] and [6]).)

$$CO \xrightarrow{\sim\sim} CO' \qquad [3]$$

$$H_2 \xrightarrow{\sim\sim} H_2' \qquad [4]$$

$$H_2' + CH_3CHO \longrightarrow -CH_3CHO \qquad [5]$$

$$CO' + CH_3CHO \longrightarrow -CH_3CHO \qquad [6]$$

$$CO' + H_2 \longrightarrow CH_3CHO \qquad [7]$$

$$H_2' + CO \longrightarrow CH_3CHO \qquad [8]$$

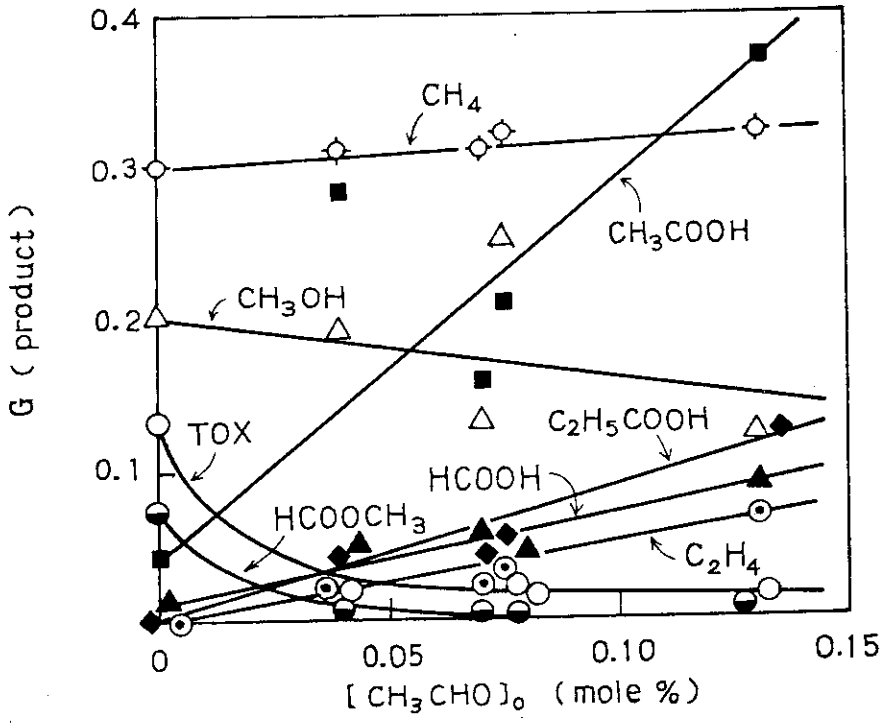

Fig. 4. The effect of acetaldehyde concentration on the G values of the products from CO-H_2 mixture: The experimental conditions are given in the caption of Fig. 3.

Here, H_2' and CO' denote active species produced from H_2 and CO, respectively, by irradiation. The G values of other compounds are plotted in Figs. 6 and 7 as a function of CO content. The G value of HCHO formation (Fig. 6) shows maximum value at ca. 20 mole% CO which is not much different from the CO content (15 mole%) where $G_{max}(HCHO)$ appears in the CO-H_2 mixture without CH_3CHO. The large values of $G(CH_4)$ at low CO content region (Fig. 6) prove that CH_4 is a radiolytic product of CH_3CHO in H_2 atmosphere. The G values of C_2H_5CHO, $(CH_3CO)_2$,

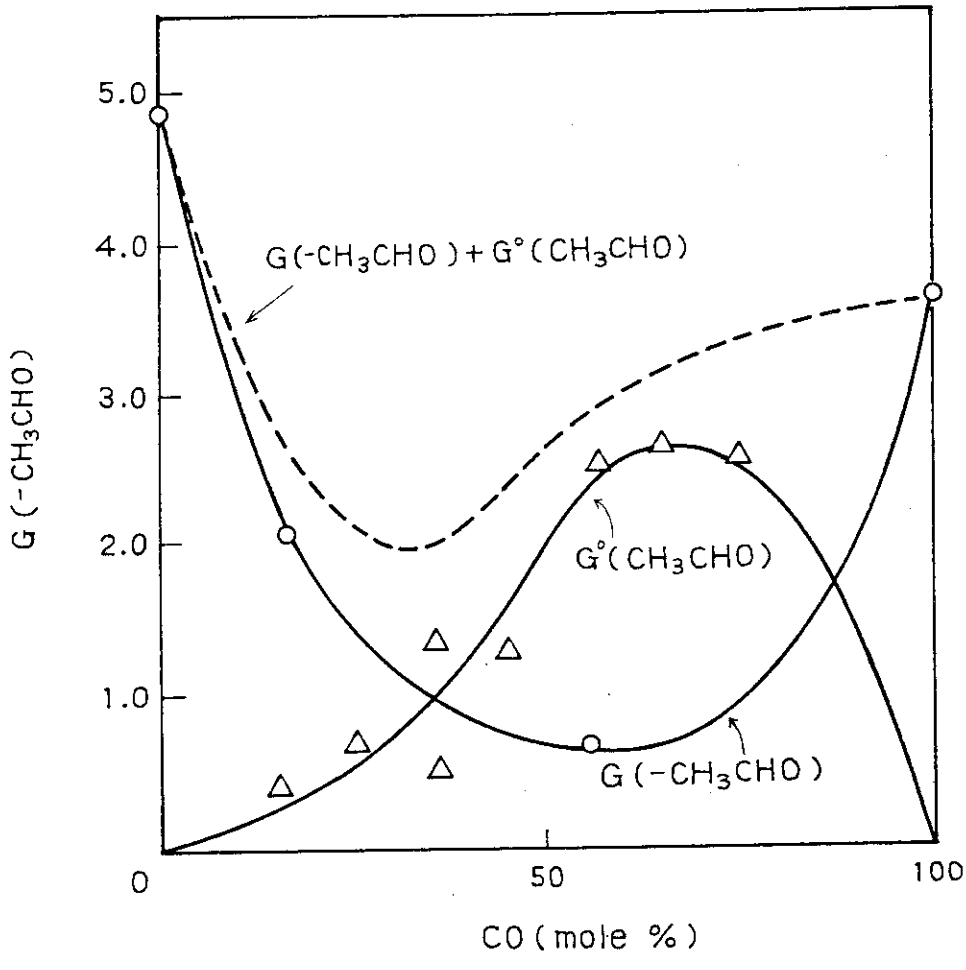

Fig. 5. G values of acetaldehyde formation and disappearance as a function of CO concentration in the mixture: Experimental conditions are given in caption of Fig. 6.

HCOOH, CH_3COOH, and C_2H_5COOH (Fig. 7) are not zero at zero mole% CO, indicating that these compounds are resulted from CH_3CHO. Quantitative conclusion is not obtained at present, but considerable part of CH_3CHO disappeared by radiation seems to be converted to HCHO, CH_3COOH, and C_2H_5COOH.

The results from CO-D_2-CH_3CHO mixture were expected to elucidate the fate of CH_3CHO, distinguishing the products of CH_3CHO from those of CO-D_2 mixture, but unfortunately the results were complicated due to isotopic exchange reactions

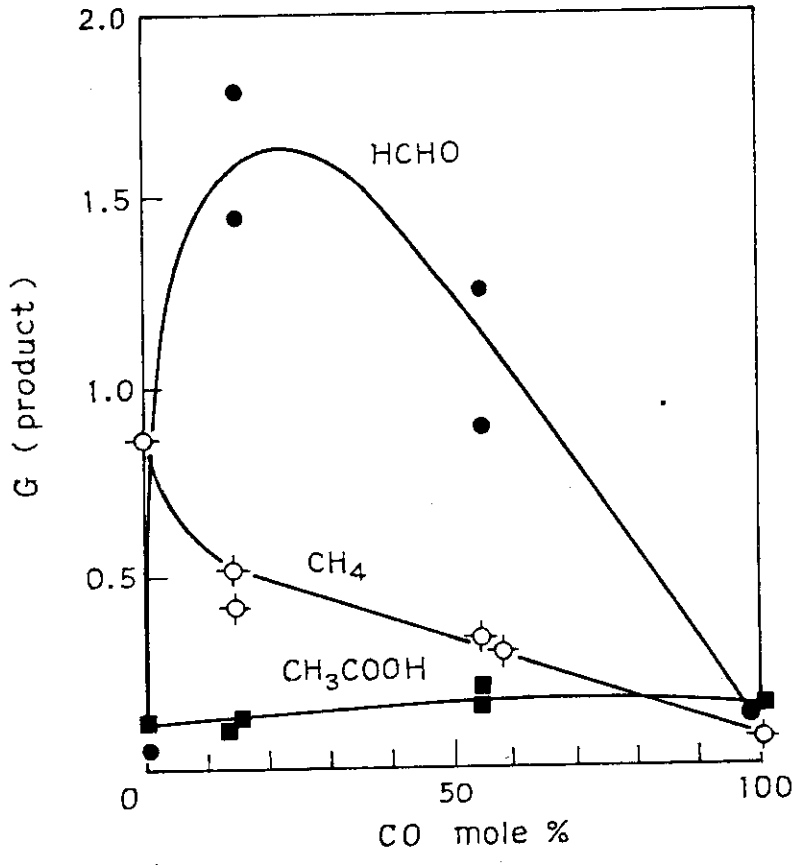

Fig. 6. The G values of HCHO, CH_3COOH and CH_4 from CO-H_2 mixture containing a small amount of acetaldehyde (0.07 ∿ 0.12 mole%) as a function of CO content: Pressure, 4000 Torr, CH_3CHO content, 0.095 mole%; Temperature, RT; Irradiation, 0.6 MeV, 1 mA; Irradiation time, 100 ∿ 400 sec; Dose, 16 ∿ 68 Mrad.

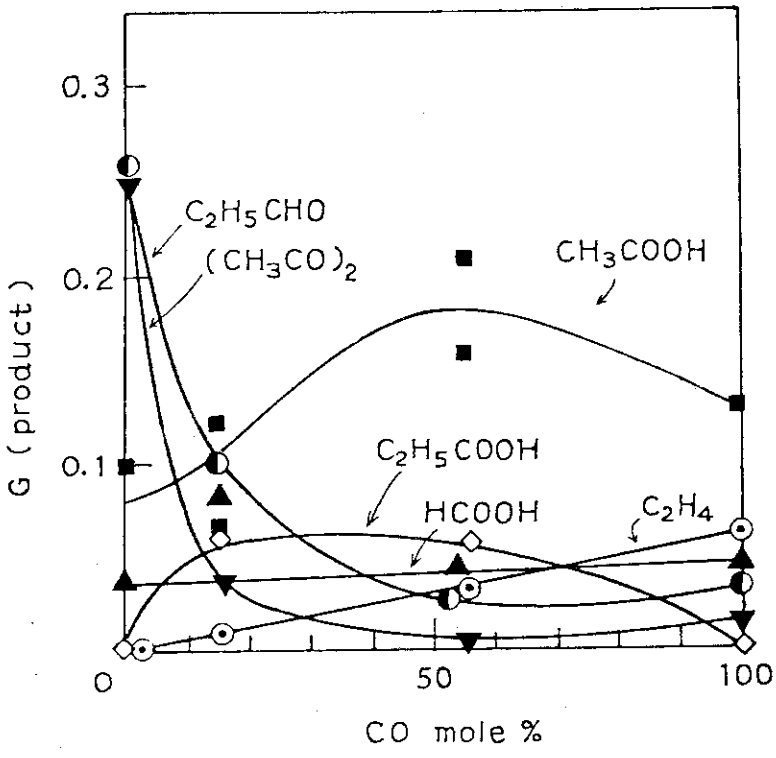

Fig. 7. G values of HCOOH, CH_3COOH, C_2H_5COOH, C_2H_5CHO, $(CH_3CO)_2$ and C_2H_4 as a function of CO content. Experimental condition is given in the caption of Fig. 6.

involving H_2O contaminated in the analysis system. Detailed analysis of the results remains for further studies.

(S. Sugimoto and N. Nishii)

1) S. Sugimoto and M. Nishii, JAERI-M 9214, 5, 13 (1980).
2) S. Sugimoto and M. Nishii, This report.

4. Further Studies on the Formation of Hydrocarbons by Irradiation of $CO-H_2$ Mixture over Silica Gel

Previous studies of radiation effects on $CO-H_2$ mixture in the presence of silica gel[1,2] reveal that silica gel exhibits catalytic activity for the formation of hydrocarbons and for the water-gas shift reaction under electron beam irradiation.

Concerning the hydrocarbon formation over silica gel, it has already been shown that most of the hydrocarbons are produced by the secondary reaction between H_2 and the carbonaceous solid deposited on silica gel by the radiolysis of CO. The present study was carried out to find the role of silica gel in the formation of hydrocarbons by studying the radiolysis of CO and the radiation-induced hydrogenolysis of the resulting solid over silica gel separately.

The flow reactor FIXCAT-II[1)] was used in this study. Radiolysis of CO was carried out in the absence of solid catalyst, and the presence of TiO_2 and silica gel at the flow rate of 50 ml/min at 300°C. Elemental analysis of the carbonaceous solid produced from CO was made using a Yanagimoto CHN Corder. The carbonaceous solid was irradiated under H_2 flow at the flow rate of 50 ml/min. Product analysis was carried out by gaschromatography.[1)]

Fig. 1 shows the concentration of CO_2 produced by radiolysis of CO in the absence of solid catalyst and in the presence of TiO_2 and of silica gel at 300°C as a function of time after initiating irradiation. It may be seen from Fig. 1 that the concentration of CO_2 produced over TiO_2 agrees well with that in the homogeneous radiolysis, indicating that TiO_2 which shows no activity for the hydrocarbon formation from CO-H_2 mixture under irradiation of electron beams[2)] exhibits apparently no effect on the radiolysis of CO. On the other hand, the CO_2 concentration is greatly enhanced by the presence of silica gel, especially in the early stage of irradiation.

The carbonaceous solid, the other product of CO radiolysis, remains deposited on the reactor walls, predominantly on the inside of the Ti foil window in the radiolysis of CO in the absence of solid catalyst and in the presence of TiO_2, while it deposited on silica gel surface in the radiolysis over silica gel. In separate experiments to study the nature of the carbonaceous solid, CO was irradiated both in the absence and presence of silica gel for 2 hrs. About 10 mg of the carbonaceous solid was obtained by the homogeneous radiolysis, while irradiation of CO over silica gel produced about 100 mg of the solid.

Therefore, it may be concluded that silica gel exhibits catalytic activity for the radiolysis of CO to produce CO_2 and the carbonaceous solid in good yields.

Elemental analysis of the carbonaceous solid indicates that the C/O atom ratio is approximately 1.5 for the solid produced by the homogeneous radiolysis of CO while it is around 5.0 for the solid produced over silica gel. This result implies that decarboxylation of the carbonaceous solid takes place over silica gel as will be described later.

The carbonaceous solid is decomposed to low molecular weight hydrocarbons by irradiation under H_2 flow. Fig. 2 (a)

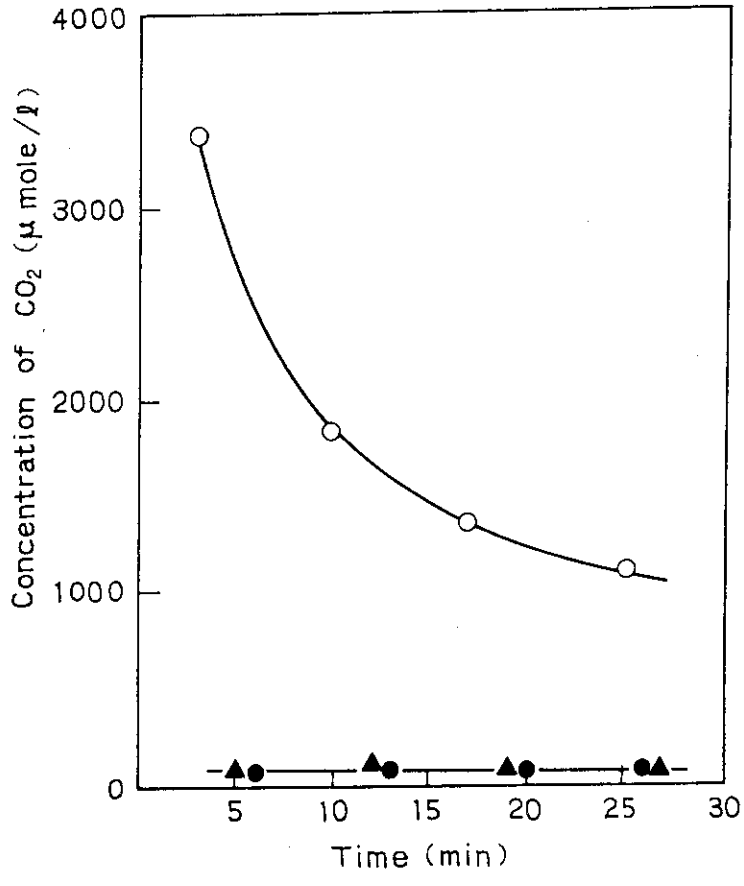

Fig. 1. Concentration of CO_2 produced by irradiation of CO at 300°C as a function of time after initiating irradiation: (●) homogeneous, (▲) over TiO_2, (○) over silica gel.

and (b) show the concentrations of hydrocarbons produced during irradiation of the carbonaceous solid over silica gel and the solid in the absence of solid catalyst at 300°C, respectively, as a function of irradiation time. It is apparent that the carbonaceous solid over silica gel may be rapidly converted to paraffins whereas the decomposition of the solid produced by

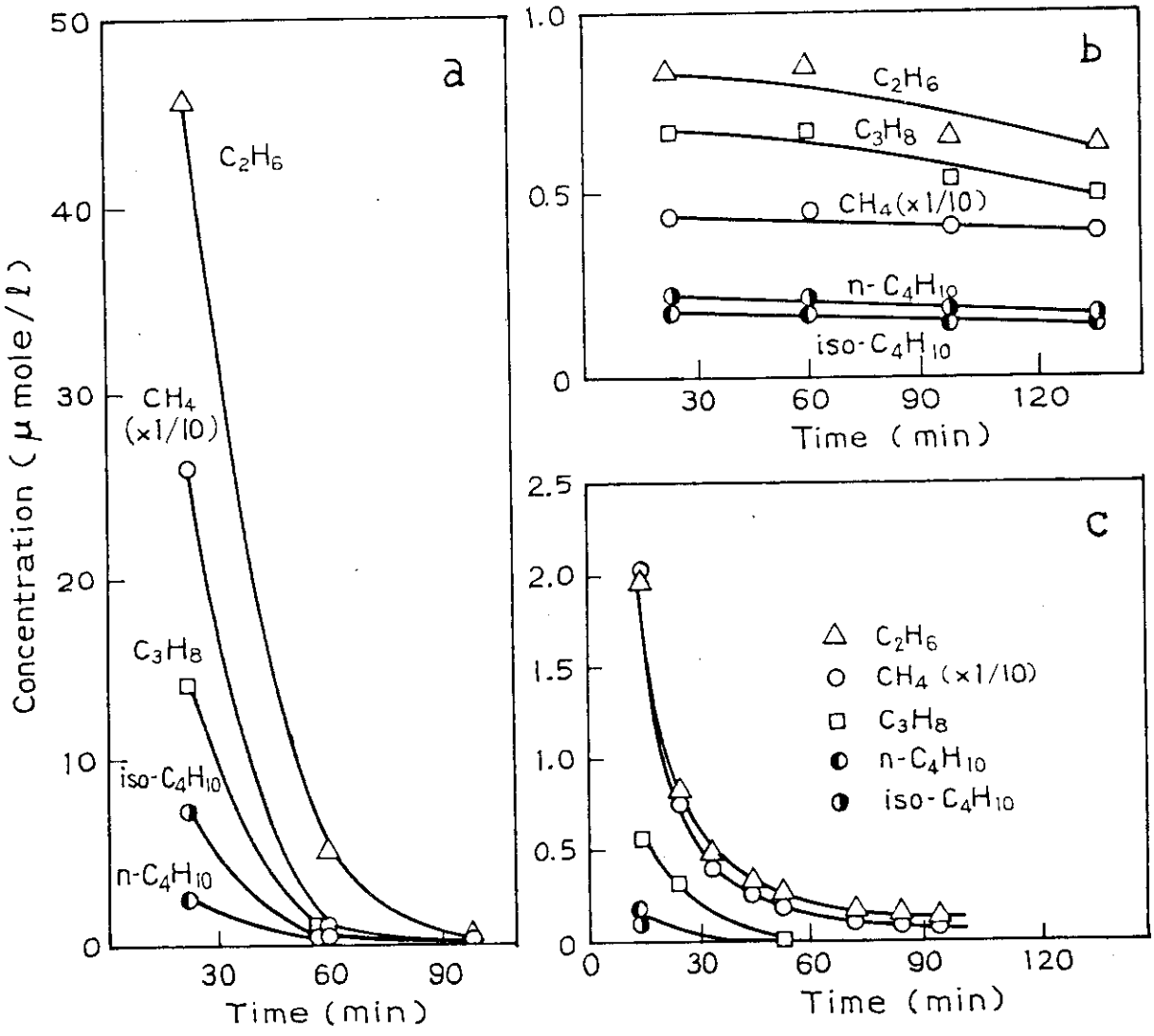

Fig. 2. Concentrations of hydrocarbons produced by irradiation under H_2 stream of (a) the carbonaceous solid deposited on silica gel after CO radiolysis, (b) the carbonaceous solid formed by homogeneous radiolysis of CO, and (c) the solid same as (b), dispersed on silica gel.

the homogeneous radiolysis of CO proceeds slowly. When the carbonaceous solid produced by the homogeneous radiolysis is dispersed on silica gel, it is decomposed as rapidly as the solid produced over silica gel as shown in Fig. 2 (c). These results indicate that silica gel promotes the radiation-induced hydrogenolysis of the carbonaceous solid produced not only over silica gel but also in the absence of solid catalyst, irrespective of the difference in the composition of the solid.

As stated already, the formation of carbon-rich carbo-

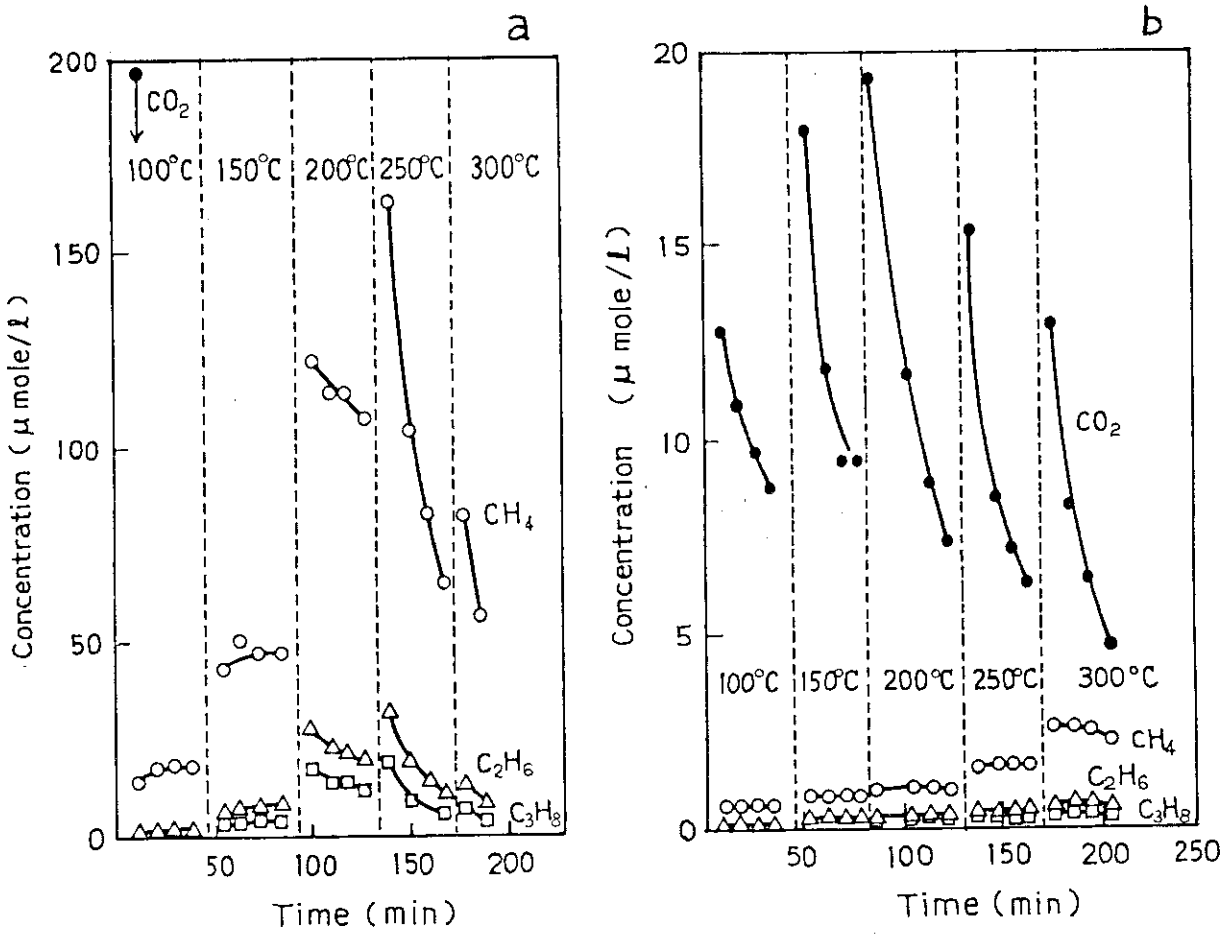

Fig. 3. Concentration of the products by radiation-induced hydrogenolysis of the carbonaceous solid formed by irradiation at 100°C of CO over silica gel (a) and by homogeneous radiation of CO (b): Electron beam current, 1 mA.

naceous solid by irradiation of CO over silica gel suggests that the decarboxylation of the solid takes place favorably over silica gel. In an attempt to confirm this suggestion, the hydrogenolysis of the carbonaceous solid was studied as a function of the reaction temperature. Fig. 3 shows the results of the experiment in which the carbonaceous solid produced by the radiolysis of CO in the presence of silica gel and in the absence of solid catalyst at 100°C was irradiated under H_2 flow at various temperatures. As shown in Fig. 3 (a), the dominant products from the carbonaceous solid over silica gel are low molecular weight paraffins and the formation of CO_2 is detected only in the initial stage of irradiation at the lowest temperature studied, 100°C at which the carbonaceous solid had been produced. In contrast, the hydrogenolysis of the carbonaceous solid by the homogeneous radiolysis (Fig. 3 (b)) produces CO_2 in the concentration higher than that of low molecular weight paraffins at each reaction temperature.

In summary, silica gel promotes the radiolysis of CO to produce CO_2 and the carbonaceous solid in high yields. The carbonaceous solid is richer in C atom than the solid produced by the homogeneous radiolysis of CO, which results from the decarboxylation of the solid by the presence of silica gel. Silica gel also promotes the radiation-induced hydrogenolysis of the carbonaceous solid. The sensitization of these two reactions, the radiolysis of CO and the radiation-induced hydrogenolysis of the resultant solid, may explain the fact that hydrocarbons are produced over silica gel in high yield.

(S. Nagai, H. Arai and M. Hatada)

1) S. Nagai, H. Arai and M. Hatada, Radiat. Phys. Chem., 16, 175 (1980).
2) S. Nagai, H. Arai and M. Hatada, Radiat. Phys. Chem., in press.

5. Radiation-Induced Reaction of Carbon Monoxide with Water Adsorbed on Silica Gel

Previous studies of radiation effects on CO-H_2 mixture over silica gel suggest that silica gel may exhibit catalytic activity for the water-gas shift reaction (1) under electron beam irradiation.[1)]

$$CO + H_2O \longrightarrow CO_2 + H_2 \qquad (1)$$

The reaction (1) finds extensive use in industry to produce hydrogen and ammonia synthesis gas and is currently carried out using iron oxide-chromium oxide and zinc oxide-copper oxide catalysts. In the field of radiation chemistry, however, there have been no studies on the reaction (1) in spite of the importance both in the fundamental and applied points of view. The present report describes for the first time the radiation-induced water-gas shift reaction between CO and water adsorbed on silica gel.

Silica gel employed in the present study was obtained from a commercial source, Mallinckrodt, 100 mesh. The silica gel was used as received, which is referred to as hydrated silica gel. The water content of the hydrated silica gel was determined to be 19.2% from thermogravimetric analysis. The silica gel placed in the flow reactor FIXCAT-II was irradiated with electron beams of 600 keV under flowing of Ar for 70 min and of CO subsequently. Product analysis was carried out in the same manner as described already.[2)] For comparison, similar experiments were carried out for the dehydrated silica gel which was obtained by outgassing the hydrated silica gel at 450°C for several hrs.

Fig. 1 shows the concentrations of H_2 and CO_2 produced by irradiation of the hydrated and dehydrated silica gel under Ar and/or CO flow, as a function of irradiation time. It may be seen from Fig. 1 (a) that by irradiation of the hydrated silica gel under Ar flow, the concentration of H_2 evolved from adsorbed water decreases gradually to reach the steady-state value of

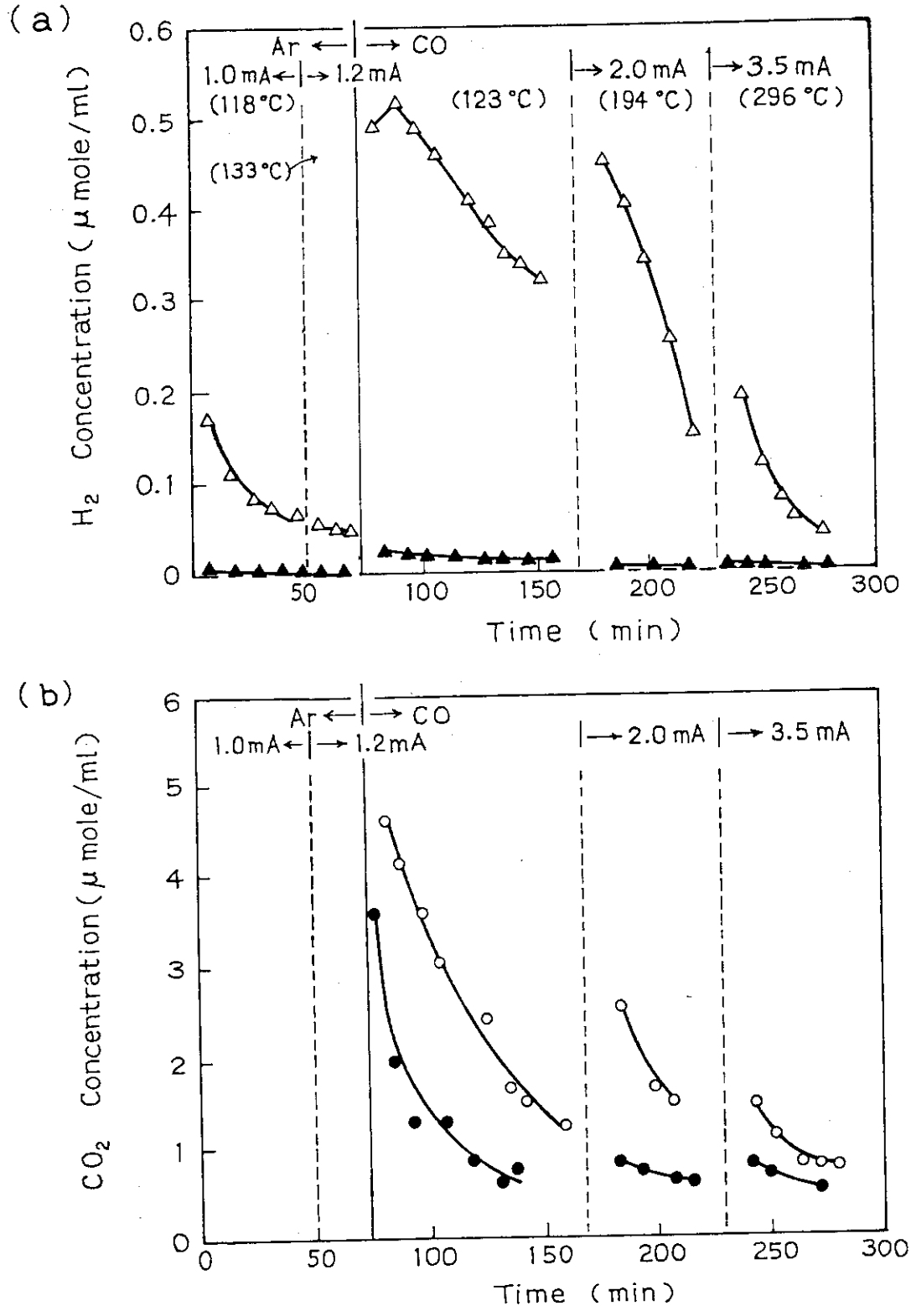

Fig. 1. Concentration of H_2 (a) and CO_2 (b) produced by irradiation of hydrated (open symbols), and dehydrated (closed symbols) under Ar and/or CO flow at the flow rate of 50 ml/min.

ca. 0.05 μmole/ml which corresponds to nearly 0.1 mole% of the effluent gas. When the gas flow was changed from Ar to CO while irradiation was being continued, the H_2 concentration suddenly increases by one order of magnitude in the initial stage and decreases gradually with irradiation time. It is noted that a similar result was also obtained for the dehydrated silica gel although the H_2 concentration observed under Ar or CO flow is much lower than that from the hydrated silica gel. These results clearly indicate that the water-gas shift reaction (1) takes place over silica gel under electron beam irradiation. Increase in the electron beam current which produces temperature rise as shown in Fig. 1 (a) results in a temporary increase in the H_2 concentration. In a separate experiment, it was found that no such increase in the H_2 concentration was observed at all under Ar flow by irradiation of the hydrated silica gel even with higher electron beam currents. Therefore, most of the H_2 evolved under CO flow must have been produced by the reaction (1).

As may be seen from Fig. 1 (b), the concentration of CO_2 produced during irradiation under CO flow is greater over the hydrated than dehydrated silica gel at all electron beam currents studied, which supports that CO indeed reacts with adsorbed water to produce CO_2 over silica gel. The decrease in the CO_2 concentration with irradiation time may be ascribed to the poisoning of silica gel surface by the deposition of carbonaceous solid produced from CO.

In addition to H_2 and CO_2, low-molecular weight paraffins were also produced by irradiation of the hydrated silica gel under CO flow, as shown in Fig. 2. The concentration of methane which is the dominant hydrocarbon produced increases markedly in the initial stages of irradiation at higher electron beam currents but decreases with irradiation time. The concentrations of ethane and propane show similar behavior to methane. These changes in the hydrocarbon concentration with electron beam current and irradiation time agree qualitatively with those obtained in the experiment where the carbonaceous solid produced from CO was irradiated under H_2 flow at various

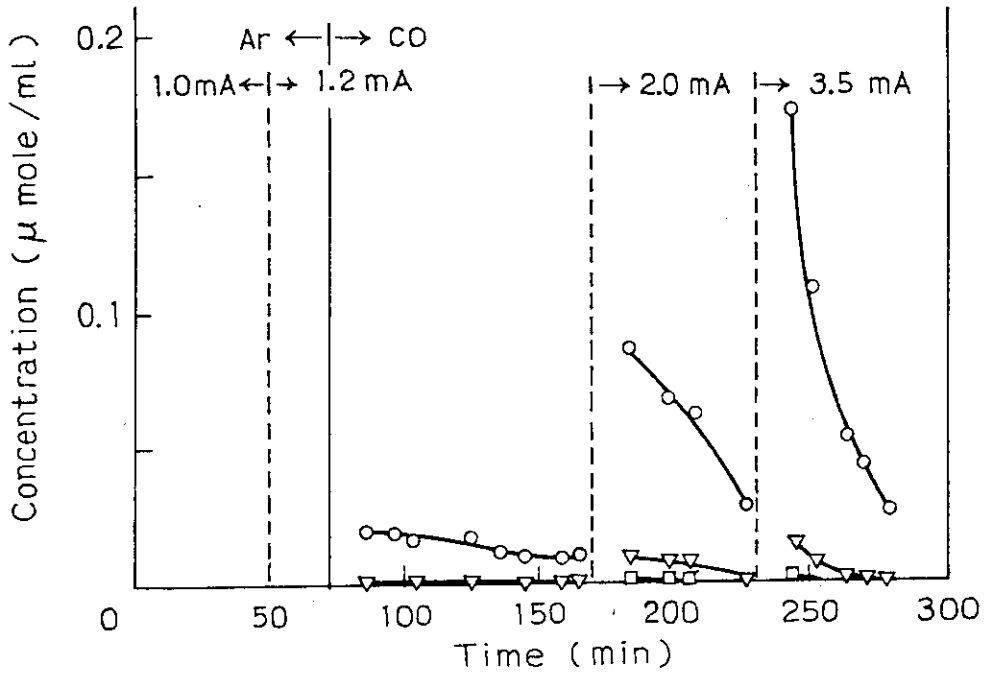

Fig. 2. Concentration of hydrocarbons produced by irradiation of hydrated silica gel under CO flow at 50 ml/min: CH_4 (○), C_2H_6 (▽), C_3H_8 (□).

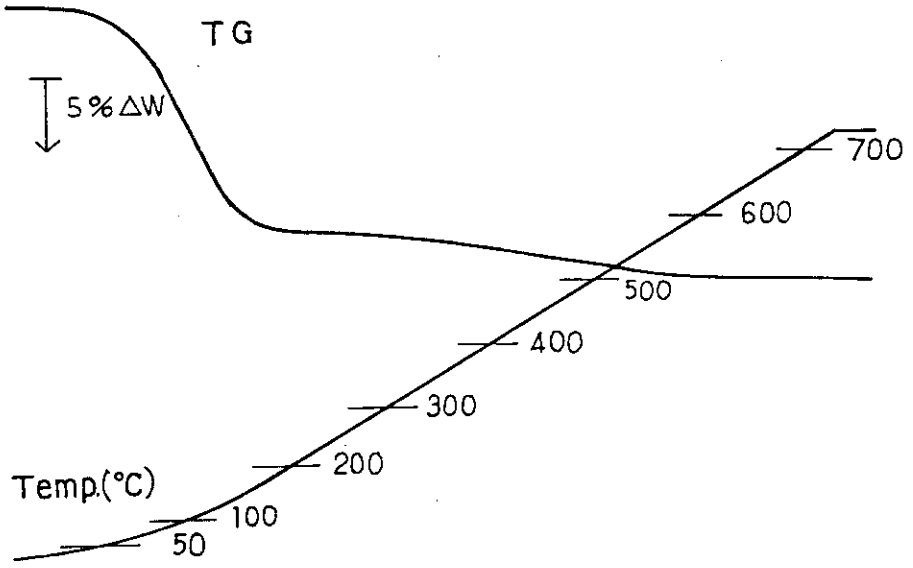

Fig. 3. Thermogravimetric curve for hydrated silica gel: Heating rate, 10°C/min; Atmosphere, in air.

temperatures.[3] Therefore, the formation of hydrocarbons found here may be ascribed to the radiation-induced reaction between the carbonaceous solid and hydrogen which was produced by reaction (1) and by radiolysis of adsorbed water.

The thermogravimetric curve for the hydrated silica gel is shown in Fig. 3 which indicates that the dominant weight loss takes place in the temperature range from 45°C to 200°C. By assuming that the weight loss observed is due to the desorption of water from the silica gel surface, the water content including surface OH groups may be estimated to be 19.2% by weight and about 80% of the water to be desorbed at relatively low temperatures, below 200°C. The latter result suggests that the water content of the hydrated silica gel decreases gradually during irradiation under Ar and CO flow since the reaction temperature is higher than 100°C as shown in Fig. 1 (a). Accordingly the decrease in the water content may be responsible for the decrease in the H_2 concentration with time of irradiation under Ar and CO flow. In the case of irradiation under CO flow, the surface poisoning due to the deposition of the carbonaceous solid may also contribute to the decrease in the H_2 concentration to some extent.

(S. Nagai, Y. Shimizu and M. Hatada)

1) JAERI-M 9214, 21 (1980).
2) S. Nagai, H. Arai and M. Hatada, Radiat. Phys. Chem., 16, 175 (1980).
3) This report.

6. Irradiation of Methane at High Temperature

We reported that the G values of the products from methane increased with increasing temperature between 150° and 300°.[1] It is interesting to know the radiation effects on methane at temperatures above 300°C, where thermal reaction of methane may also take place. This report describes the experimental results on the radiation-induced reactions of methane and

thermal reactions without radiation.

A cylindrical irradiation vessel of flow-without-circulation type was made of stainless steel (SUS 304) and used instead of that used in the previous studies (FIXCAT II). The vessel has an irradiation window (stainless steel, 10 μm thick, 20 mmø) at the top and the electron beam penetrates into the vessel through the window. The dose rate was estimated to be 0.96×10^{20} eV(10% reactant at 25°C)$^{-1}\cdot s^{-1}$ for the electron beams of 0.6 MeV and 0.1 mA from the amount of ethane produced by irradiation at 117°C using the G value of ethane formation (2.5) obtained in the previous study at the same temperature. The vessel was heated in the electric furnace up to 750°C and methane to be irradiated was fed from the bottom of the reactor after removal of a trace amount of oxygen by passing over magnesium ribbon at 230°C followed by preheating through a pre-heating coil at the irradiation temperature.

The method of analysis of the products were previously described.[1)]

The results are summarized in Table 1. No detectable products were formed up to 300°C in the blank without irradiation, but above 400°C, hydrogen, ethane and ethylene were formed. The radiation chemical products also increased with increasing temperature. The amounts of the products when exposed to radiation always exceeds those without radiation up to 420°C, but at 550°C the amounts of hydrogen decreased by the irradiation. Since the amount of hydrogen produced at 550°C, independent of the employment of irradiation, is large excess to that expected from stoichiometric relation (1) as a counter

$$nCH_4 \longrightarrow C_nH_{2n+2} + (n-1)\ H_2 \qquad (1)$$

part of the formation of hydrocarbons detected in the experiment, considerable amount of carbon may be produced by reaction (2):

$$CH_4 \longrightarrow 2H_2 + C \qquad (2)$$

Table 1. Yields of the Products from Methane by Electron Irradiation at High Temperatures (117 ∿ 760°C)
(Yield in μmole/10ℓ, 28°C, 1 atm Reactor)

Sampling Time	16:02	16:30	16:52	17:12	17:40	18:04	18:23	18:49	19:08	19:50	20:21	20:43
Temp. (°C)	117	215	305	420	550	580	580	550	550	420	750	760
Electron Beam	Yes	Yes	Yes	Yes	Yes	Yes	No	Yes	No	Yes	Yes	No
H_2	60	73	72	90	1350	3150	5000	1600	2200	130	80900	61000
C_2H_2	0.1	0.15	0.31	0.13	0.06	0.	0.	0.	0.	0.	0.	0.
C_2H_4	2.2	5.3	6.3	6.0	8.7	7.2	0.	5.7	0.03	4.7	161.	185.
C_2H_6	23.	29.	32.	32.	34.	35.	6.3	31.	2.5	30.	104.	87.
C_3H_6	0.1	0.51	1.3	2.8	2.2	2.9	0.	3.3	0.	2.9	3.3	4.5
C_3H_8	2.6	0.81	0.75	0.35	0.09	0.06	0.	0.08	0.	0.42	0.	0.

Table 2. G values of the Products from Methane at High Temperature

Sampling Time	16:02	16:30	16:52	17:12	19:50	17:40	18:49	18:04	20:21
Temp. (°C)	117	215	305	420	420	550	550	580	750
H_2	6.6	13.12	15.32	22.96	33.2	-258.6	-182.5	-583.3	7491.
C_2H_2	0.01	0.03	0.07	0.03	0.	0.02	0.	0.	0.
C_2H_4	0.24	0.95	1.34	1.53	1.20	2.64	1.72	2.27	-9.03
C_2H_6	2.53	5.21	6.81	8.16	7.66	9.58	8.67	9.05	6.40
C_3H_6	0.01	0.09	0.28	0.71	0.74	0.67	1.00	0.91	-0.45
C_3H_8	0.29	0.15	0.16	0.09	0.11	0.03	0.02	0.02	0.

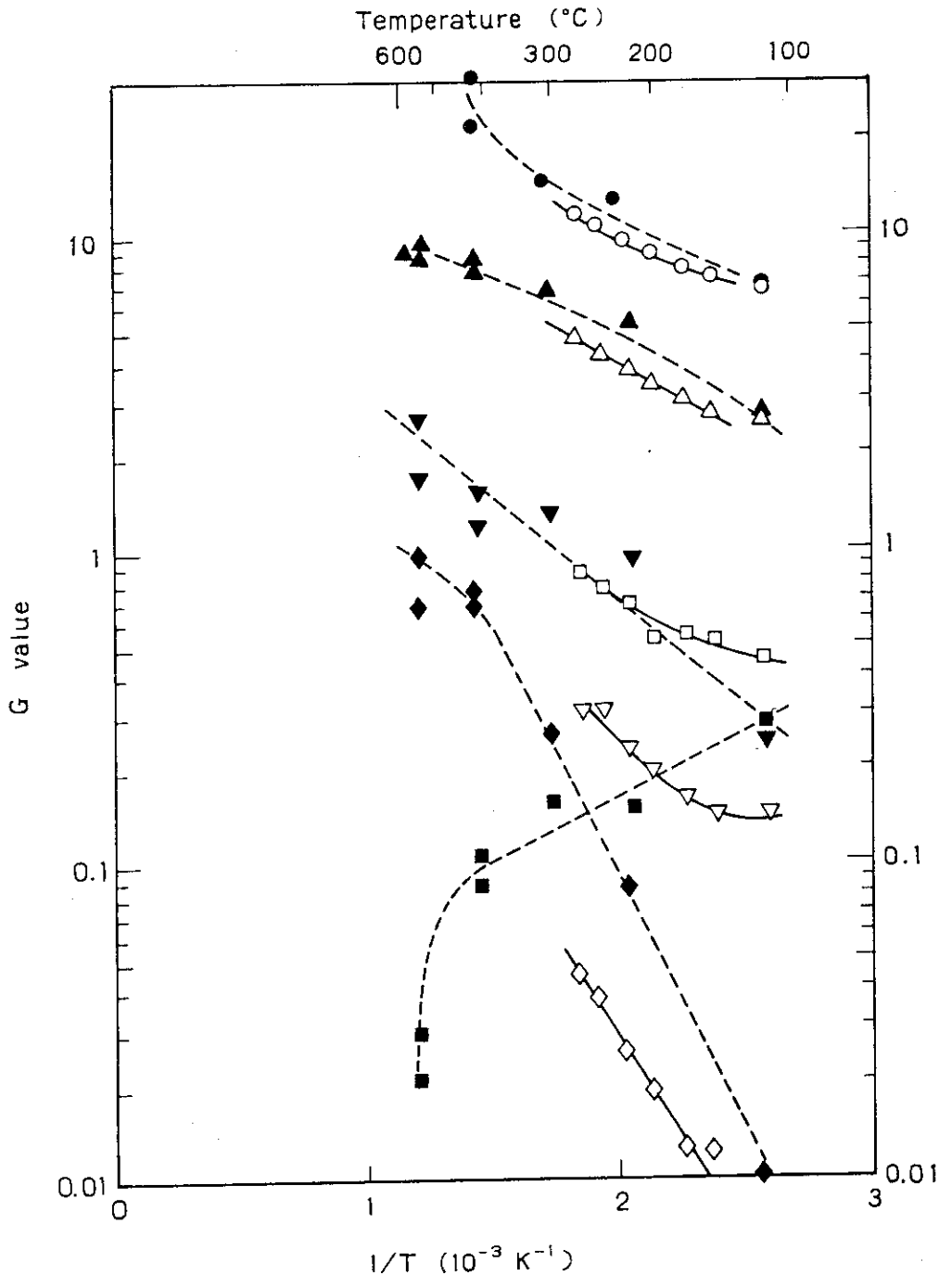

Fig. 1. G values of the products as a function of 1/T: (●) H_2; (▲) C_2H_6; (▼) C_2H_4; (■) C_3H_8; (◆) C_3H_6; Blank figures denote data obtained in the previous study.

The decrease of hydrogen production by irradiation at 550°C possibly indicates that radiation favors the reaction of H and C to reproduce methane or to convert to higher hydrocarbons.

The G values in Table 2 were calculated based on the amount of the product from which the amount of the thermal reaction product at the same temperature was subtracted.

In Fig. 1, the G values of the products were plotted as a function of 1/T. The G values of hydrogen ethane, ethylene, and propylene increase with increasing temperature but the plots came above those obtained previously. However, the G value of propane decreases with increasing temperature contrary

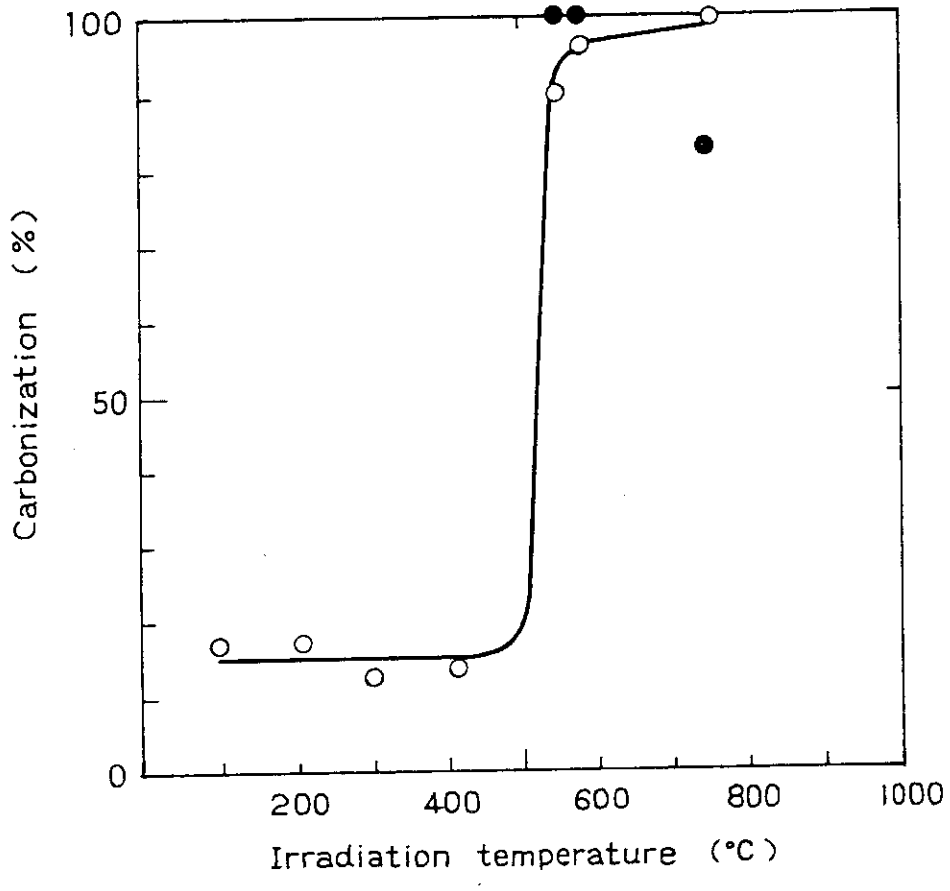

Fig. 2. Selectivity to carbon formation as a function of temperature: (o) under irradiation; (•) blank experiment without irradiation.

to the previous result.

The scattered points above 560°C possibly due to the catalytic reactions on the wall which make it difficult to go into details further.

It is possible to calculate the selectivity of the reaction to form carbon and hydrogen, when one considers the following stoichiometric relations:

$$CH_4 = 2H_2 + C$$

$$2CH_4 = H_2 + C_2H_6$$

$$2CH_4 = 2H_2 + C_2H_4$$

$$3CH_4 = 2H_2 + C_3H_8$$

$$3CH_4 = 3H_2 + C_3H_6$$

The selectivity of the reaction to give carbon, F, is given by:

$$F = \frac{\frac{1}{2}(Y_{H_2}) \times \frac{1}{2} \times 100}{\frac{1}{2}(Y_{H_2}) + 2(Y_{C_2H_6}) + 2(Y_{C_2H_4}) + 3(Y_{C_3H_8}) + 3(Y_{C_3H_6})}$$

where Y's are the amounts of the products indicated by subscripts. The calculated selectivity is shown in Fig. 2 where it is evident that the carbon formation proceeds selectively above 550 ∿ 580°C.

(H. Arai, S. Nagai, and M. Hatada)

1) H. Arai, S. Nagai, K. Matsuda, and M. Hatada, Radiat. Phys. Chem., 17, 151-157 (1981).

7. The Molecular Weight Distribution of Hydrocarbon Products from Methane by Electron Irradiation

In the last annual report, it was reported[1] that hydrocarbons having various number of carbon atoms were produced when methane was irradiated with electron beams. The results of gaschromatographic analysis, GPC, infrared spectroscopic analysis, and molecular refractometry indicated that these hydrocarbons were highly branched saturated hydrocarbons having molecular weight distribution ranging from 30 to 5200 or higher which were roughly fractionated into three fractions; gas, condensable liquid, and non-volatile liquid. The broad distribution of molecular weight may be combined results of many reactions, i.e., consecutive growth of hydrocarbon chain as discussed previously[1], scission of the chain, abstraction reaction of an H atom by radicals, and combination reactions of radicals.

This report describes a discussion on the amount of the product as a function of carbon number in the product. The amount of the products having carbon atoms up to 5 can be determined with less ambiguity by gaschromatographic analysis as described in the previous report[1]. The condensable liquid was separated into many peaks by gachromatographic analysis. The molecular weight of these peaks are estimated using a known relation between molecular weight and retention time assuming the width of retention time due to the presence of branched isomers. The molecular weight distribution of the non-volatile fraction was tentatively obtained from GPC curves using a calibration curve prepared for polystyrene of known molecular weight.

In Table 1, the amounts of products are listed as a function of carbon number for the products obtained by three different doses.

The amounts of products in m mole per 10 ℓ reactant at NTP were plotted in Figs. 1 and 2 (A) through (C) as a function of carbon number in the product molecule for the products containing carbons less than 6 and 380, respectively. The plots seem

Table 1. The Amounts of Hydrocarbons in Methane after Irradiation of Large Dose

Run No.	Gas			Condensable liquid			Non-volatile liquid			Sum		
Carbon No.	SS-1	SS-2	SS-3	SS-1	SS-2	SS-3	SS-1	SS-2	SS-3	SS-1	SS-2	SS-3
1	4400.	2112.	1238.4							4400.	2112.0	1238.4
2	1028.2	949.7	740.2							1028.2	949.7	740.2
2	264.4	277.2	224.8							264.4	277.2	244.8
4	133.4	156.6	156.6							133.4	156.6	156.6
5	61.9	62.6	88.6	2.91	7.48	42.10				64.81	70.08	130.7
6				9.43	27.13	49.01				9.43	27.13	49.01
7	[5887.9]	[3558.1]	[2448.6]	13.98	24.63	66.02				13.98	24.63	66.02
8				12.69	31.33	65.34				12.69	31.33	65.34
9				13.33	21.93	81.50	5.20	6.1	14.9	18.53	28.03	96.4
10				28.28	42.37	153.25	(5.80)	(8.5)	(21.8)	34.08	50.87	175.05
11				24.89	25.92	113.17	6.40	10.9	28.6	31.29	36.82	141.77
12				20.72	17.30	63.66	4.80	21.9	43.5	25.52	39.20	107.16
13				14.71	9.97	26.69	(7.00)	(28.0)	(54.4)	21.71	37.97	81.09
14				5.66	5.98	9.43	9.20	34.1	65.3	14.86	40.08	74.73
15				2.26	1.99	0.0	(14.4)	(42.35)	(78.5)	16.66	44.34	78.50
16							19.6	50.6	91.7	19.6	50.6	91.7
17				[149.0]	[216.0]	[656.0]	(25.0)	(59.2)	(100.9)	25.0	59.2	100.9
18							30.4	67.7	110.0	30.4	67.7	110.0
19							39.6	81.1	115.0	39.6	81.1	115.0
20							(42.2)	(85.7)	105.0	42.2	85.7	105.0
21							44.8	90.3	55.0	44.8	90.3	55.0
24							25.5	50.0	50.3	25.1	50.0	50.3
27							23.1	46.1	23.8	23.1	46.1	23.8
31							10.5	21.0	18.1	10.5	21.0	18.1
37							7.41	15.3	12.7	7.41	15.3	12.7
45							5.54	10.3	2.40	5.54	10.3	2.40
64							0.956	2.2	2.01	0.956	2.2	2.01
100							0.663	1.72	1.56	0.663	1.72	1.56
136							0.449	1.31	0.894	0.449	1.31	0.894
171							0.273	0.893	0.559	0.273	0.893	0.559
207							0.156	0.536	0.279	0.156	0.536	0.279
243							0.078	0.297	0.167	0.078	0.297	0.167
279							0.039	0.119	0.0372	0.039	0.119	0.0372
371							0.0065	0.198	0.0186	0.0065	0.0198	0.0186
							[723.0]	[1576.0]	[2072.0]	[6760.0]	[5350.1]	[5176.6]

The amount in milligram per 10% reactant.

The values in parentheses are extrapolated values. The values in brackets indicate sum.

Doses for Run No. SS-1, SS-2, and SS-3 are given in Table 2.

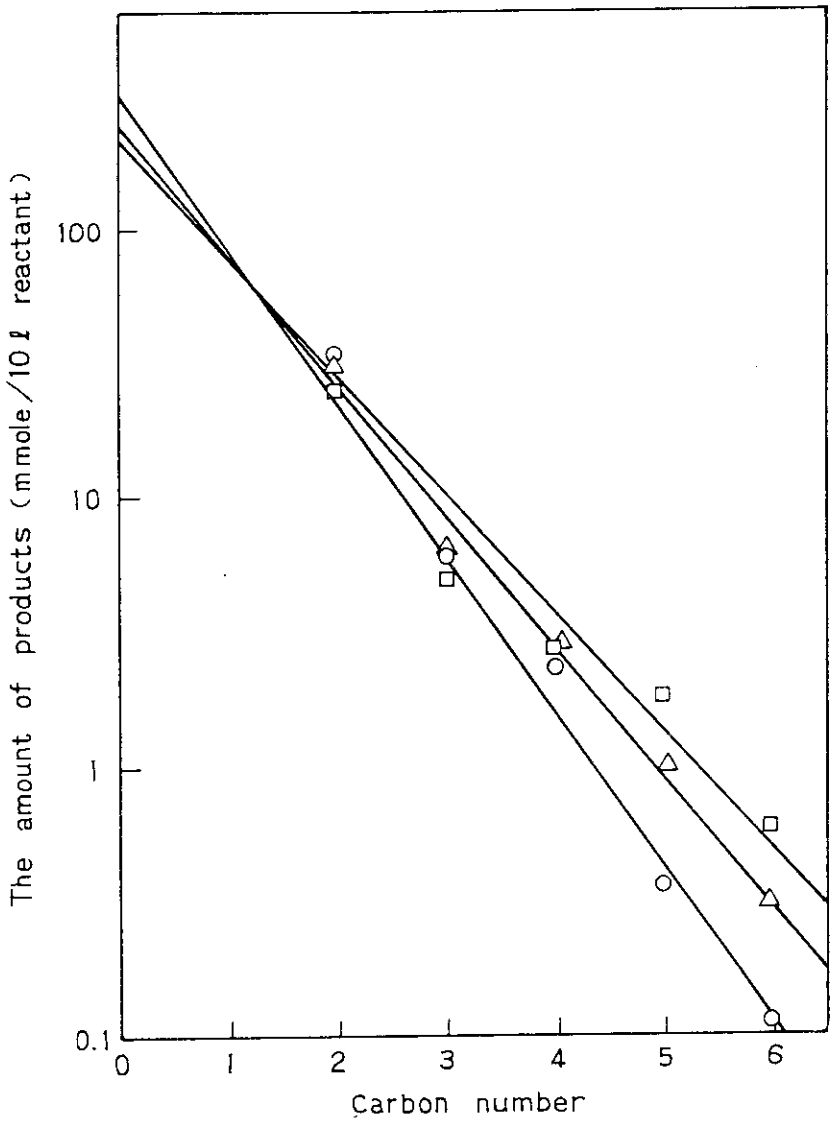

Fig. 1. The amount of products in m mole/10ℓ reactant as a function of carbon number: Dose (o) 3.6 x 10^3 Mrad, (Δ) 7.2 x 10^3 Mrad, and (□) 14.5 x 10^3 Mrad.

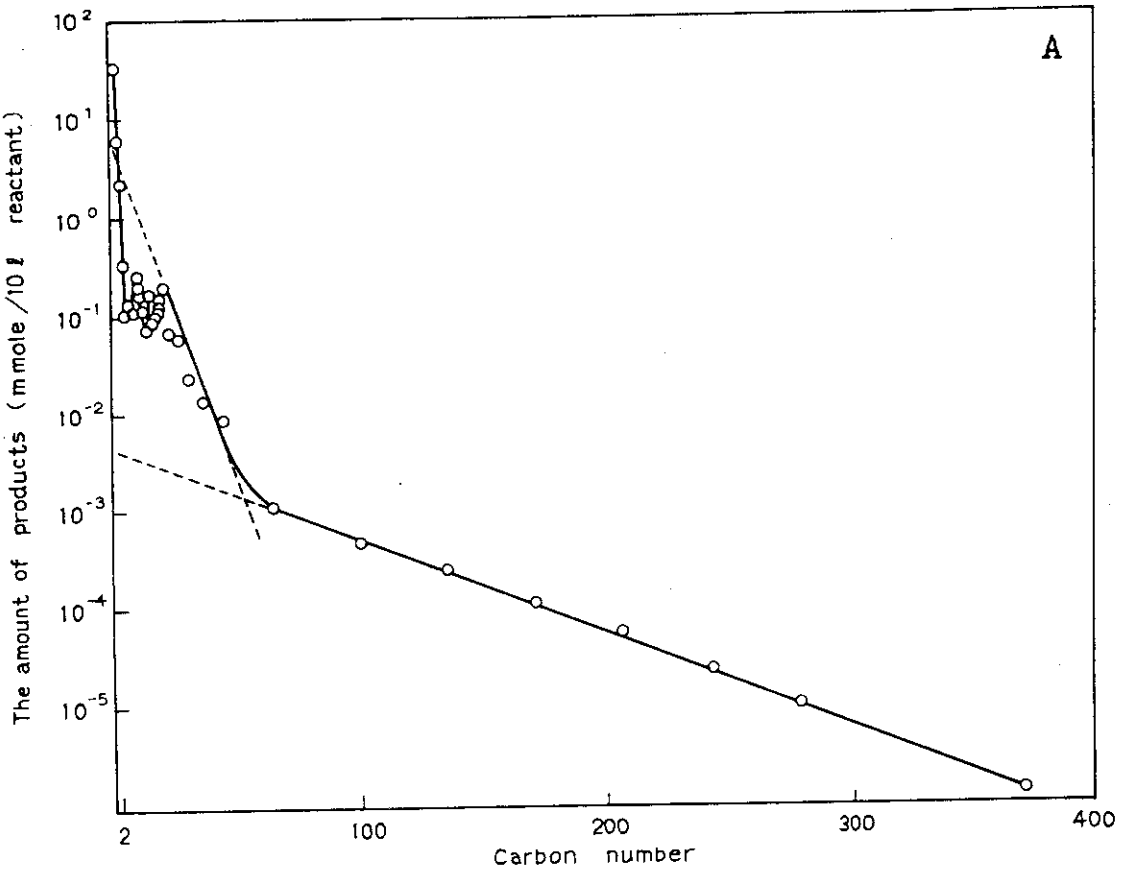
A
The amount of products (mmole/10ℓ reactant)
10^{2}
10^{1}
10^{0}
10^{-1}
10^{-2}
10^{-3}
10^{-4}
10^{-5}
2
100
200
300
400
Carbon number

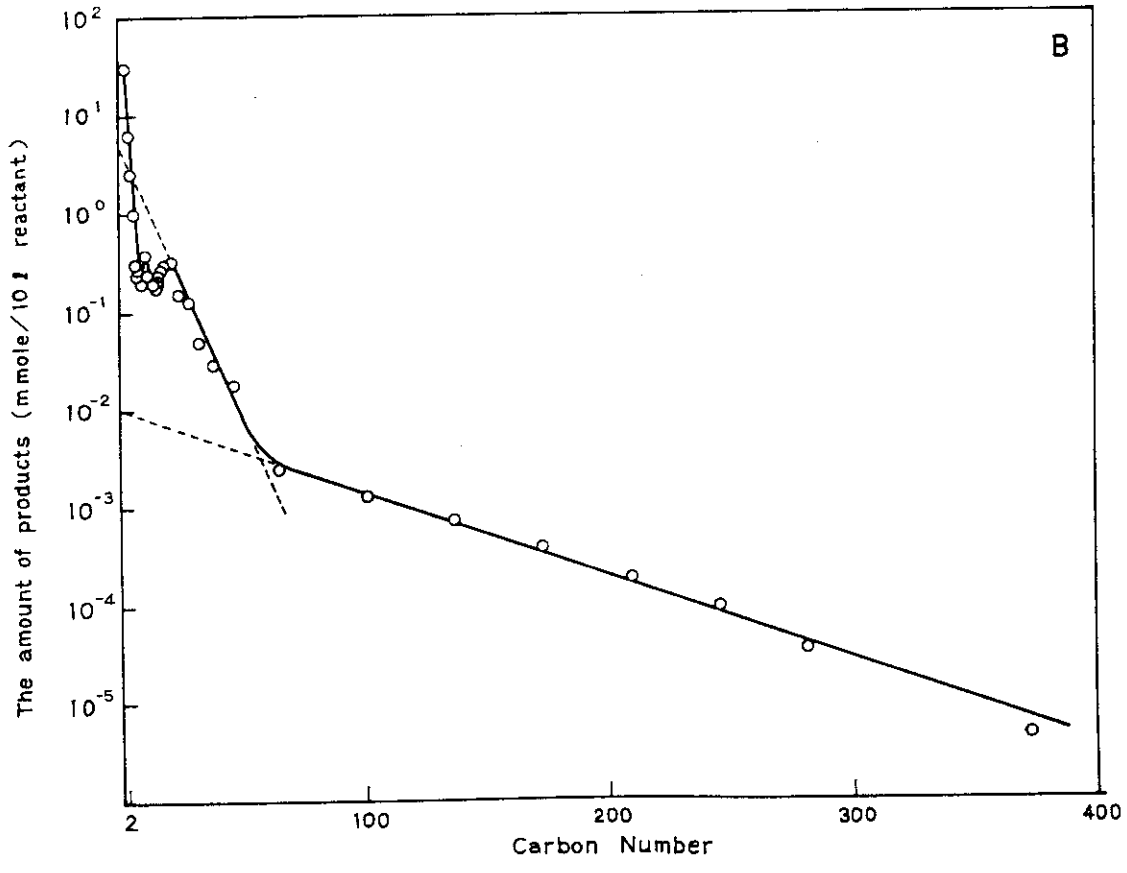
B
The amount of products (mmole/10ℓ reactant)
10^{2}
10^{1}
10^{0}
10^{-1}
10^{-2}
10^{-3}
10^{-4}
10^{-5}
2
100
200
300
400
Carbon Number

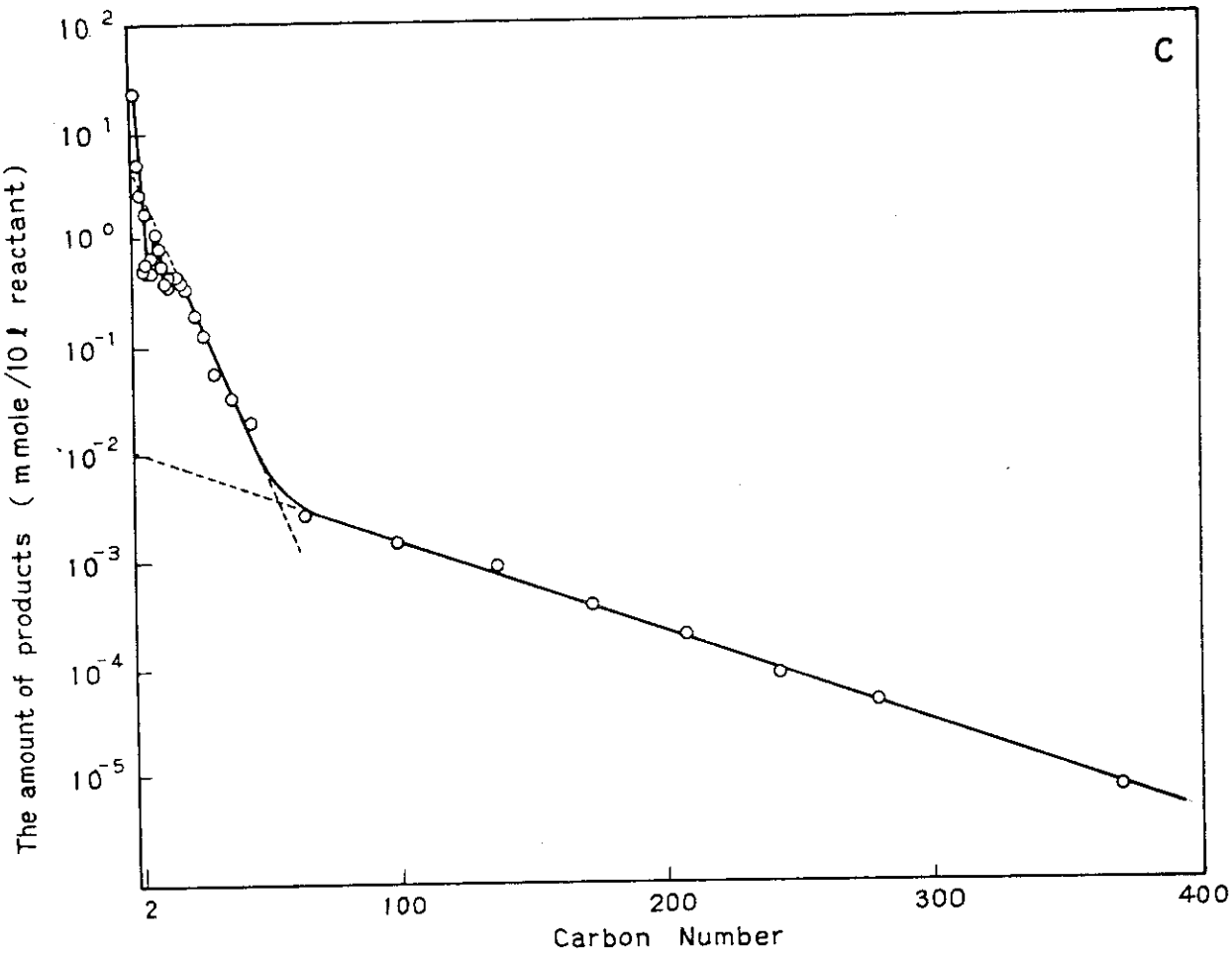

Fig. 2. The amounts of products as a function of carbon number:
A, 3.6 x 10^{3} Mrad; B, 7.2 x 10^{3} Mrad; and
C, 14.5 x 10^{3} Mrad.

to lie on a monotonous line except two irregular parts; one appears at the carbon numbers corresponding to the overlapping area of the three fractions at carbon number from 6 to 20, and the other at 60. These irregular part of the former is possibly resulted from that the collection of the compounds of this molecular weight region was not satisfactory. Another reason for these irregular parts may be that the assumption made on the molecular weight determination from GPC curve was not reasonable enough to estimate correct molecular weight.

The amount of products in m mole per 10 ℓ reactant, Y_P, plotted on the ordinate is proportional to the weight fraction of the products divided by carbon number, P, by eq. (1),

$$m_P/P = Y_P \cdot MW_{-CH_2-} / \sum_{P=2} M_P \qquad (1)$$

where m_P and M_P are weight fraction and weight in g of the hydrocarbons having P carbon atoms, respectively, and MW_{-CH_2-} is the molecular weight of CH_2 unit, which is 14. The three linear parts of the curves can be fitted by eq. (2),

$$\log(m_P/P) = A + BP \qquad (2)$$

where A and B are constants. One may notice that the type of this equation is that of known as Schulz's "Einheitliche Kopplung" equation (3).

$$\log(m_P/P) = \log(\ell n^2 \alpha) + P \log\alpha \qquad (3)$$

The irregularities found in the present study were also reported by two authors in the Schulz plots for hydrocarbons obtained in the Fischer-Tropsch syntheses and are explained by thermodynamical equilibrium among n-hydrocarbons.

The Schulz' equation is applicable only to the case where chain grows linearly and terminates by a single mechanism, and not to the present case where complex chain growth and termination occur, but one may calculate formally α-values from the intercept, Y_0, and slope, B. The results are given in Table 2.

Table 2. Calculation of α-values

	SS-1		SS-2		SS-3	
Dose (x 10^3 Mrad)	3.6		7.2		14.5	
$\sum_{P=2} M_P$ (mg)	2360		3238		3938	
α-values from Intercept (Y_0)	Y_0	α	Y_0	α	Y_0	α
$C_2 - C_6$	316	0.254	251	0.352	224	0.373
$C_{20} - C_{60}$	5.62	0.833	3.98	0.877	3.98	0.888
$C_{60} - C_{280}$	0.0045	0.995	0.0112	0.993	0.0100	0.994
α-values from Slope (B)	-B	α	-B	α	-B	α
$C_2 - C_6$	0.575	0.266	0.487	0.326	0.440	0.363
$C_{20} - C_{60}$	7.12×10^{-2}	0.849	5.67×10^{-2}	0.878	6.0×10^{-2}	0.871
$C_{60} - C_{280}$	9.5×10^{-3}	0.978	8.7×10^{-3}	0.980	8.6×10^{-3}	0.980

Table 3. The Amount of Hydrocarbons

Dose (10^3 Mrad)	$-CH_4$(m) (mole)	H_2(h) (mole)	x (mole)	n	14·n·x (g)
3.6	0.171	0.144	0.027	6.33	2.39
7.2	0.314	0.225	0.089	3.52	4.38
14.5	0.369	0.335	0.034	10.85	5.16
25.	0.405	0.395	0.01	40.5	5.7

$[CH_4]_0$ = 0.446 mole

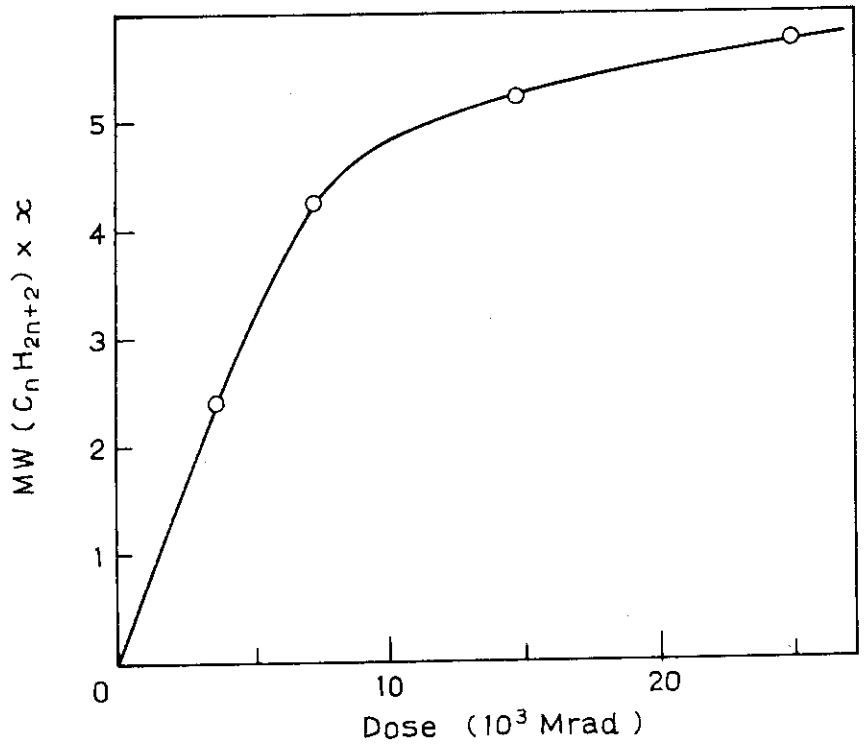

Fig. 3. The weight of hydrocarbons as a function of dose.

The stoichiometric relation of the reaction producing hydrocarbons and hydrogen from methane is written as

$$m\ CH_4 = x\ C_n\ H_{2n+2} + h\ H_2 \quad ,$$

where x and n can be calculated using following relations and experimentally obtained values of m and h, which are the amount of methane consumed and that of hydrogen produced, respectively.

$$x = m - h$$

$$n = m/(m - h)$$

The results are given in Table 3. The weight of hydrocarbon is given by $14 \cdot n \cdot x$ and this quantity is plotted against dose in Fig. 3, where it is evident that the amount of hydrocarbon increases but levels off of certain value with increasing dose. The average number of carbons in hydrocarbon also increases with increasing dose except the accidentally small point obtained at 7.2 Mrad. These consideration lead to a conclusion that methane is converted to higher hydrocarbons by continued irradiation.

(M. Hatada, H. Arai, and S. Nagai)

1) M. Hatada, H. Arai, S. Nagai, and K. Matsuda, JAERI-M 9214, 42 (1980).
2) C. W. Montgomery, J. Chem. Phys., 16, 424 (1948).
3) G. Henrici-Olive and S. Olive, Augew. Chem., 88, 144 (1976).

8. The Effect of Temperature on Radiation-Induced Reactions of $CO-CH_4$ Mixture

The studies[1] were carried out on the radiation chemical reactions of $CO-CH_4$ mixture induced by electron irradiation in a whole range of gas composition, and it was reported that the maximum G values of acetic acid and propionic acid were 1.6 and 1.2 at 15 mole% and 90 mole% of CO, respectively, and the G value of ethylene formation reached the maximum value of 0.14 at 40 mole% of CO. The studies have been carried out this year on the temperature dependence of the G values of the products from $CO-CH_4$ mixture.

The method of experiment was of flow type without circulation and the same as those described previously[1]. The

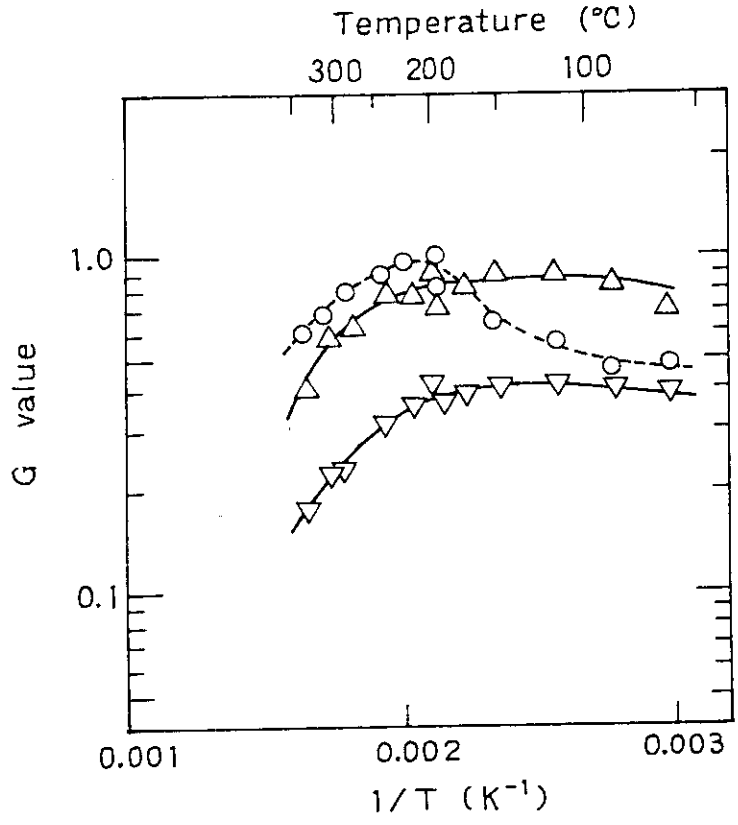

Fig. 1. G values of acetic acid (o), propionic acid (Δ) and acetaldehyde (∇) as a function of 1/T: Dose, 7.3 Mrad; CO content, 90 mole%.

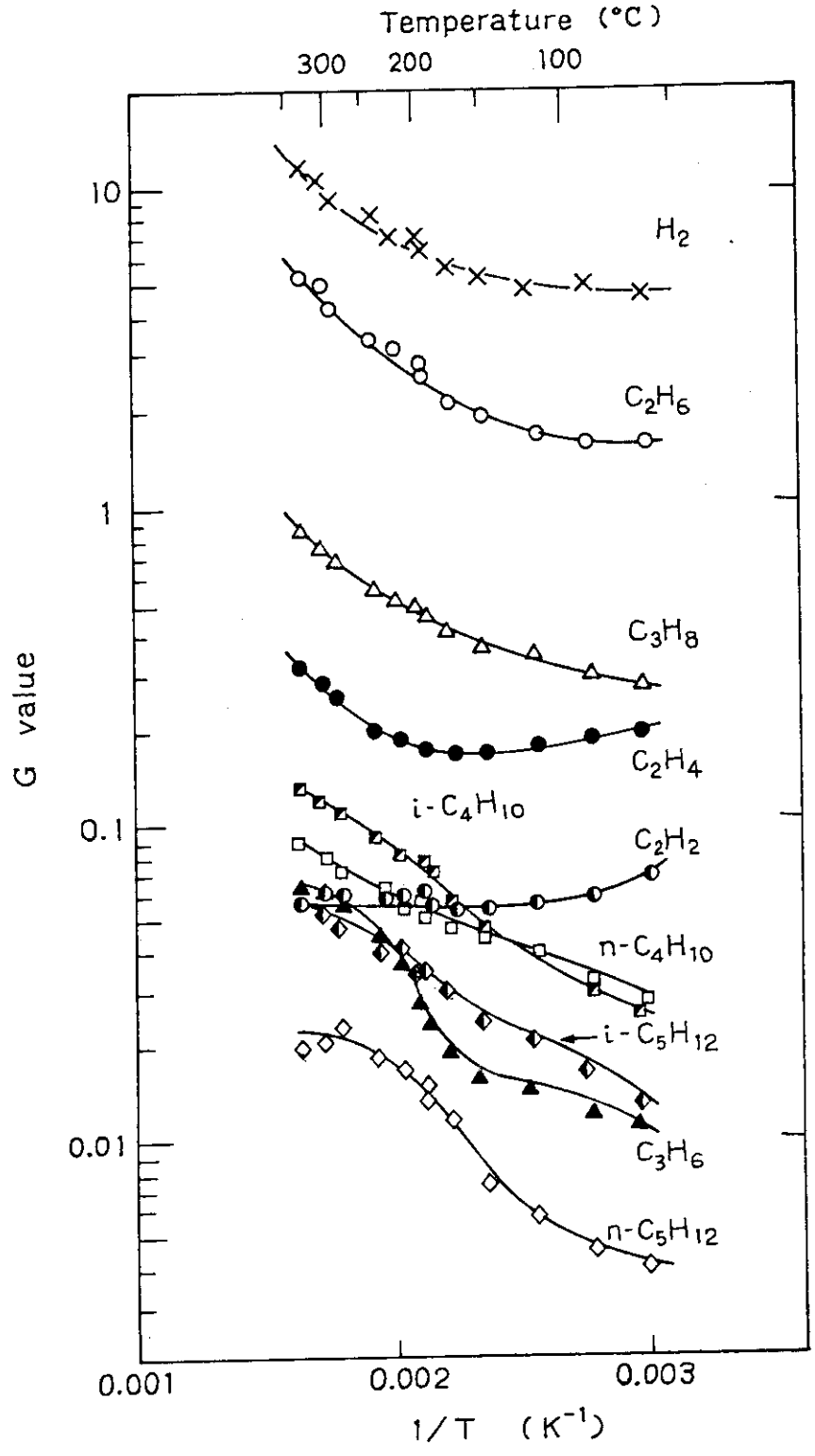

Fig. 2. G values of hydrogen and hydrocarbons as a function of 1/T: Dose, 7.3 Mrad; CO content, 90 mole%.

temperature during irradiation was changed from 60° to 350°C by adjusting the current of electric heater installed under the reaction zone. The CO content and the flow rate of the mixture were kept constant at 90 mole% and 100 ml/min, respectively. The irradiation was carried out with electron beam (0.6 MeV, 1 mA, scanning width 30 cm) and the dose absorbed by gas at this condition was 7.3 Mrad.

In Fig. 1, the G values of acetic acid, propionic acid, and acetaldehyde were plotted against 1/T. The G value of acetic acid increased with increasing temperature up to 200°C, reached a maximum of 1.0 at 200°C and then decreased with increasing temperature. The G values of propionic acid and acetaldehyde were independent of temperature up to 200°C, but above this temperature, they decreased with increasing temperature. The apparent activation energies of acetic acid, propionic acid, and acetaldehyde formations above 200°C were calculated to be -4.6, -5.6, and -4.6 kcal/mole, respectively. The decrease of these oxygen containing products above 200°C may be come from that the thermal decomposition of these compounds or precursors of them occurs above this temperature. The small apparent activation energies may indicate that the decomposition reactions are catalyzed by the vessel wall.

The temperature dependences of G values of hydrogen and hydrocarbons are shown in Fig. 2. The G values of most products except ethylene and acetylene increase with increasing temperature. The shapes of the curves are qualitatively the same as those obtained for methane without carbon monoxide[2]. The G values of ethylene and acetylene decrease with increasing temperature up to 180°C. The decrease may be possibly resulted from that hydrogen addition to the unsaturated compounds increases effectively with increasing temperature.

(H. Arai, S. Nagai, and M. Hatada)

1) H. Arai, et al., JAERI-M 9214, 56 (1980).
2) H. Arai, et al., JAERI-M 9214, 34 (1980).

9. Effects of Nitric and Nitrous Oxides Addition on Radiation Chemical Reaction of Methane-Carbon Monoxide Mixture

It was reported[1] that organic acids were produced in addition to hydrogen and hydrocarbon products from CH_4-CO mixture by electron irradiation. In an attempt to obtain some insight into the reaction mechanism, scavenger studies have been carried out using nitric and nitrous oxides which are known as radical scavenger and positive charge acceptor, and electron scavenger, respectively, according to the following reactions:

$$R\cdot + NO \longrightarrow RNO \quad (1)$$

$$R^+ + NO \longrightarrow R + NO^+ \quad (2)$$

$$e + N_2O \longrightarrow N_2O^- \longrightarrow N_2 + O^- \quad (3)$$

The methods of experiment were the same as those reported in the previous studies in that a flow reactor (FIXCAT-II) without circulation of irradiated gas was used. The reaction temperature was mostly 120°C except some experiments which were carried out at 150°C. The flow rate of CH_4-CO mixture (molar ratio, 9 : 1) was kept constant at 100 ml/min and flow rates of nitric oxide and nitrous oxide were changed from 0.004 to 10 ml/min, and from 0.09 to 7 ml/min, respectively.

In Fig. 1 through Fig. 3, and in Table 1, the G values of the products from CH_4-CO mixture containing NO are shown as a function of NO content. As shown in Fig. 1, the $G(CH_3COOH)$ decreased markedly with the addition of a small amount of NO, and becomes almost zero at NO content of 0.2 mole%. The $G(C_2H_5COOH)$ seems to decrease with the addition of NO, but the value was obscured by the formation of an unidentified product, X, the peak of which appeared on the gas chromatogram at the retention time which is very close to that of C_2H_5COOH. The decrease of $G(CH_3COOH)$ by the addition of NO may be explained

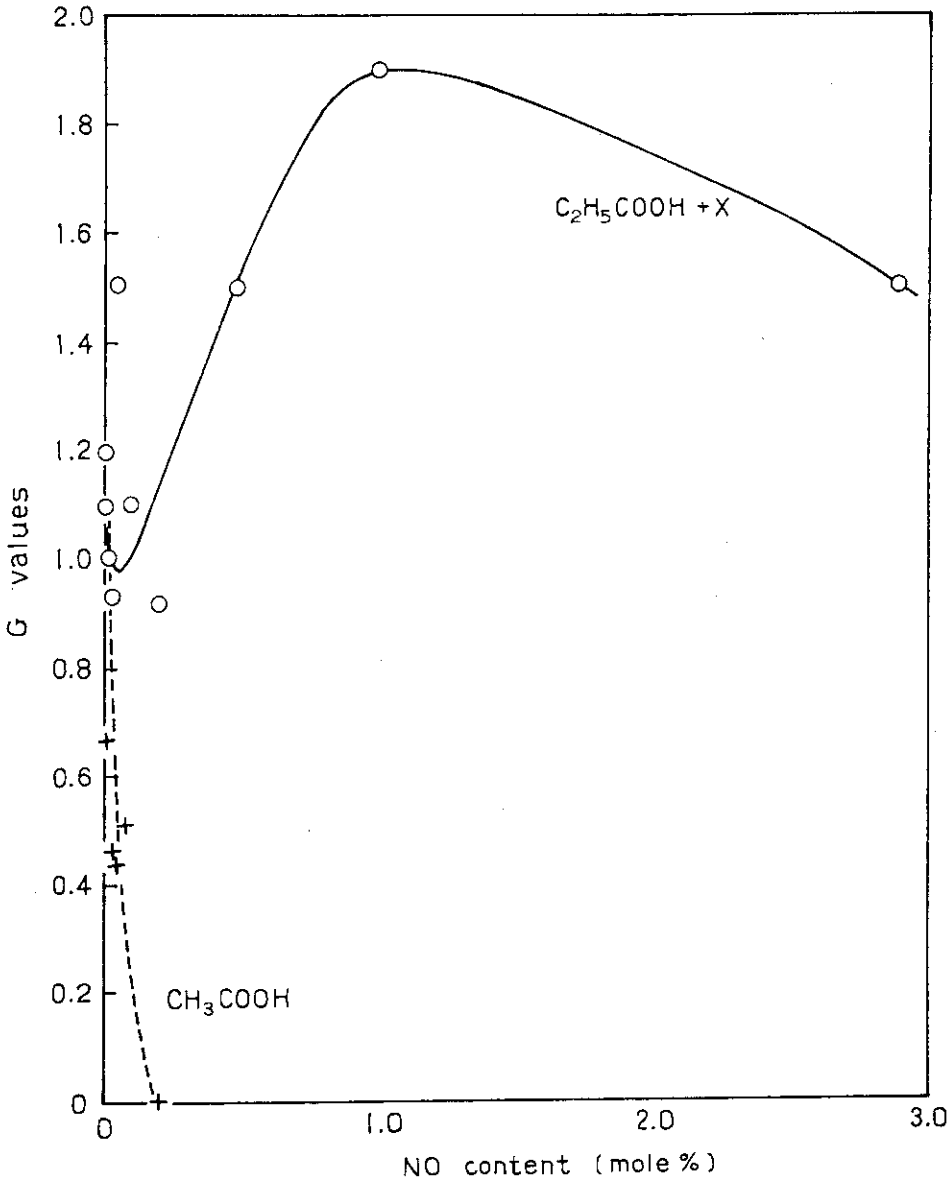

Fig. 1. Effect of addition of nitric oxide on $G(CH_3COOH)$ and $G(C_2H_5COOH)$.
× denotes an unidentified product.

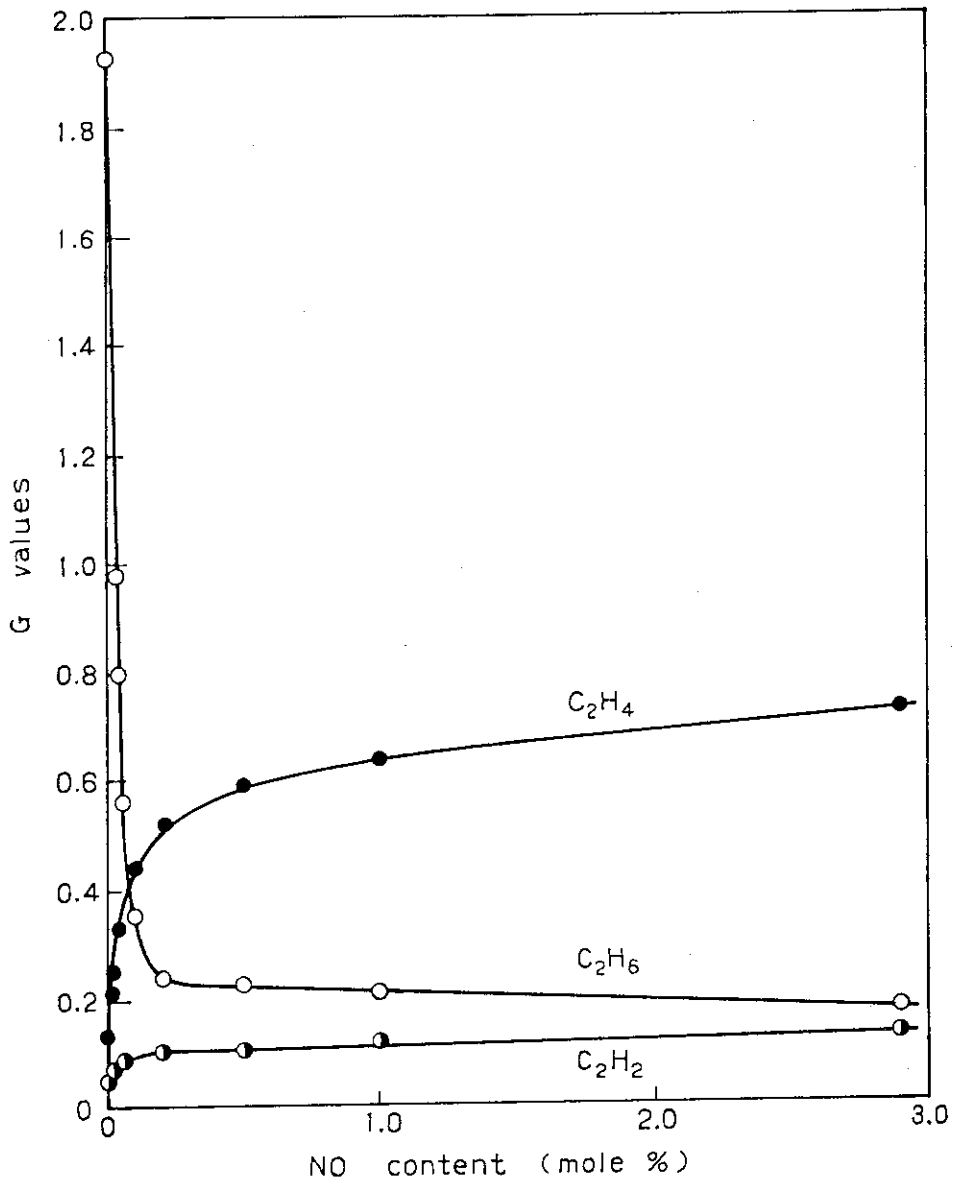

Fig. 2. Effect of addition of nitric oxide on $G(C_2H_2)$, $G(C_2H_4)$ and $G(C_2H_6)$.

by reaction (4) which competes with reaction (5) producing the ionic precursor of CH_3COOH.

$$CH_3^+ + NO \longrightarrow \dot{C}H_3 + NO^+ \quad (4)$$

$$CH_3^+ + CO \longrightarrow CH_3CO^+ \xrightarrow{H_2O} CH_3COOH \quad (5)$$

With increasing content of NO, $G(C_2H_4)$ increased, while $G(C_2H_6)$ decreased, indicating that NO reacts with H atoms by reaction (6), which escaped from being scavenged by CO and otherwise add to the double bond of C_2H_4 producing C_2H_6.

$$H + NO \longrightarrow HNO \quad (6)$$

$$H + C_2H_4 \longrightarrow \dot{C}_2H_5 \longrightarrow C_2H_6 \quad (7)$$

The $G(C_2H_2)$ also increased with increasing NO content (Fig. 2). Similar phenomenon that the unsaturated hydrocarbon increased

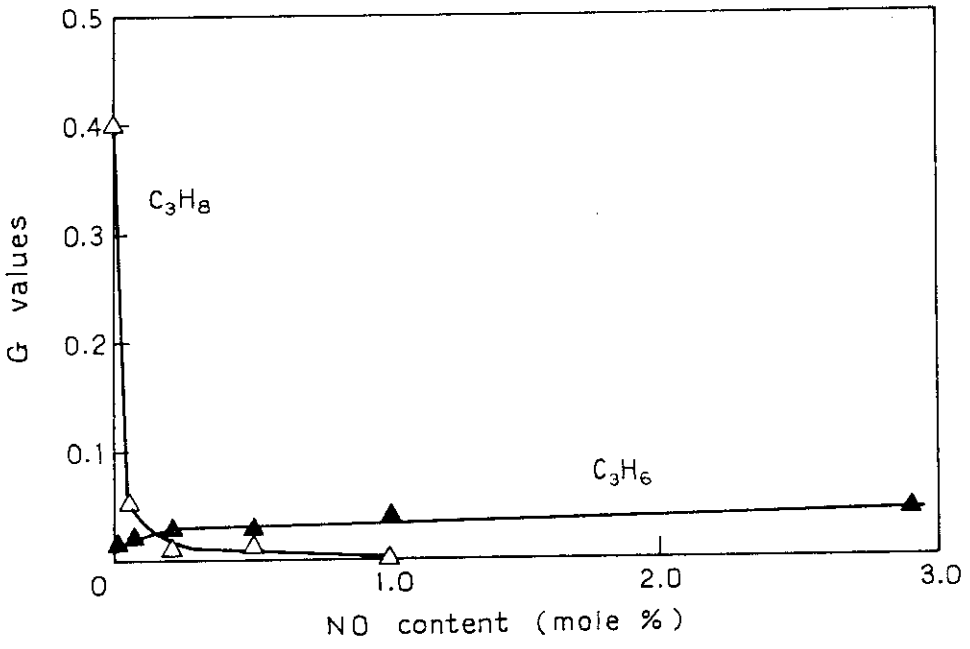

Fig. 3. Effect of addition of nitric oxide on $G(C_3H_6)$ and $G(C_3H_8)$.

with increasing NO content in sacrifice of the saturated compound was found for C_3 hydrocarbons (Fig. 3).

In Fig. 4, the G values of inorganic products were plotted against NO content. With increasing NO content, the $G(H_2)$ decreased while $G(H_2O)$ and $G(N_2O)$ increased. The $G(CO_2)$ decreased slightly by addition of NO. These results may suggest that nitric oxide decomposes to form N_2O and O, the latter of which further reacts with hydrogen atoms, which are produced from CH_4 and escaped from being scavenged by CO and olefins, to form H_2O, and CO to form CO_2.

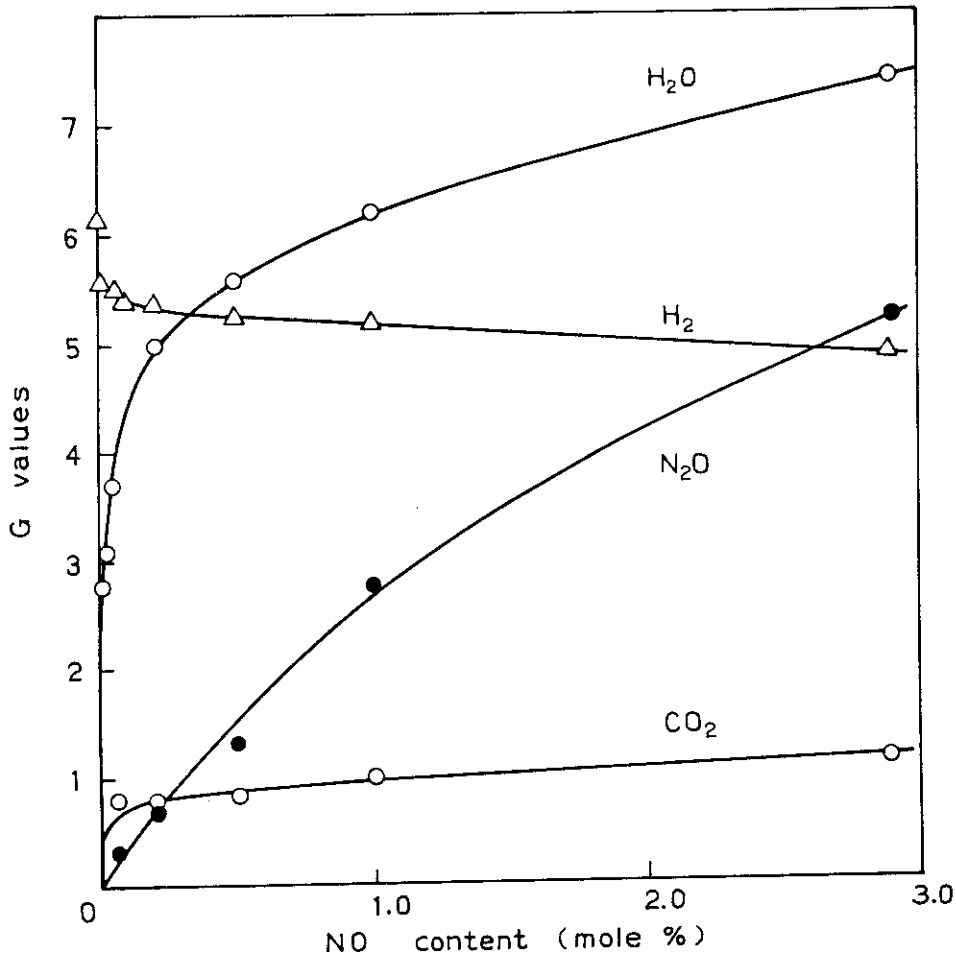

Fig. 4. Effect of addition of nitric oxide on G values of inorganic products.

Table 1. Electron Beam Irradiation of Methane-Carbon Monoxide Mixtures in the Presence of Nitric Oxide

Electron beam, 0.6 MeV, 1 mA; Scanning width, 30 cm; Flow rate, CH_4 90 ml/min, CO 10 ml/min

11 21 79

Exp. No.	11:12	11:55	12:40	13:23	14:05	14:58	15:33	16:20
Beam Current (mA)	1	1	1	1	1	1	1	1
Flow-rate (CH_4)	90	90	90	90	90	90	90	90
(ml/min) CO	10	10	10	10	10	10	10	10
NO	0	0	0.004	0.004	0.014	0.024	0.054	0.094
Irrad. Temp. (°C)	119	119	119	119	119	119	119	119
Yield in μmole/10ℓ reactant gas at 25°C, 1 atm, (G-value)								
H_2	560 (6.2)	560 (6.2)	550 (6.1)	510 (5.7)	510 (5.6)	500 (5.6)	490 (5.5)	490 (5.4)
C_2H_2	4.0 (0.044)	3.1 (0.035)	3.6 (0.039)	4.2 (0.047)	5.2 (0.057)	5.9 (0.065)	7.0 (0.077)	7.8 (0.086)
C_2H_4	12 (0.13)	12 (0.14)	13 (0.14)	16 (0.17)	19 (0.21)	23 (0.25)	30 (0.33)	40 (0.44)
C_2H_6	173 (1.92)	173 (1.92)	154 (1.71)	114 (1.27)	87.7 (0.974)	71.5 (0.793)	50.5 (0.561)	31 (0.35
C_3H_6	1.0 (0.011)	9.98(0.011)	0.86(0.010)	0.90(0.010)	0.84(0.009)	1.0 (0.011)	1.3 (0.015)	1.9 (0.21)
C_3H_8	36.3 (0.403)	36.3 (0.403)	29.9 (0.332)	22.0 (0.245)	15.1 (0.167)	10.7 (0.119)	4.6 (0.051)	0.83(0.009)
$i\text{-}C_4H_{10}$	5.0 (0.055)	5.2 (0.058)	3.3 (0.037)	1.8 (0.019)	1.0 (0.012)	0.73(0.008)	0.59(0.007)	0.21(0.002)
$1\text{-}C_4H_8$	0.08(0.0009)	0.09(0.001)	0.07(0.007)	0.08(0.009)	≈0	≈0	≈0	≈0
$n\text{-}C_4H_{10}$	5.1 (0.057)	5.3 (0.059)	3.7 (0.041)	2.1 (0.023)	1.2 (0.013)	0.88(0.010)	—	—
$neo\text{-}C_5H_{12}$	0.9 (0.01)	1.1 (0.013)	0.8 (0.009)	0.5 (0.006)	0.1 (0.001)	0.2 (0.002)	≈0	≈0
$i\text{-}C_5H_{12}$	3.4 (0.037)	3.8 (0.042)	1.8 (0.020)	0.92(0.010)	1.1 (0.012)	1.2 (0.014)	1.4 (0.015)	1.9 (0.021)
$n\text{-}C_5H_{12}$	0.55(0.006)	0.63(0.007)	0.30(0.003)	0.17(0.002)	≈0	≈0	≈0	≈0
HCHO	—	14 (0.16)	4.7 (0.052)	0	0	0	0	0
CH_3OH	1.0 (0.01)	2 (0.02)	2 (0.02)	8 (0.09)	7.0 (0.077)	6.5 (0.072)	13 (0.14)	4.4 (0.049)
CH_3CHO	27 (0.30)	26 (0.29)	28 (0.31)	18 (0.20)	11 (0.12)	4.7 (0.052)	7.3 (0.081)	3.7 (0.041)
C_2H_5OH								
CH_3COCH_3	6.3 (0.07)	6.8 (0.075)	5.7 (0.064)	6.3 (0.070)	1.4 (0.015)	2.6 (0.029)	1.4 (0.015)	0.38(0.004)
CH_3COOH	60 (0.66)	91 (1.0)	56 (0.62)	41 (0.46)	42 (0.46)	39 (0.44)	50 (0.51)	0
C_2H_5COOH	100 (1.1)	110 (1.2)	92 (1.0)	76 (0.85)	91 (1.0)	84 (0.93)	140 (1.5)	100 (1.1)
CO_2	—	13 (0.15)	24 (0.26)	43 (0.48)	62 (0.68)	73 (0.81)	73 (0.81)	67 (0.75)
H_2O	≈0	≈0	28 (0.32)	97 (1.1)	250 (2.8)	280 (3.1)	340 (3.7)	370 (4.1)
N_2O	0	0	4.1 (0.045)	15 (0.17)	22 (0.24)	27 (0.30)	33 (0.37)	40 (0.44)
Absorbed energy in Mrad	12.4	12.4	12.4	12.4	12.4	12.4	12.4	12.4
in eV/g	7.74×10^{20}	7.74×10^{20}	7.74×10^{20}	7.74×10^{20}	7.74×10^{20}	7.74×10^{20}	7.74×10^{20}	7.74×10^{20}
in eV/10ℓ gas	5.43×10^{21}	5.43×10^{21}	5.43×10^{21}	5.43×10^{21}	5.43×10^{21}	5.43×10^{21}	5.43×10^{21}	5.43×10^{21}
Time after Initiating Irradiation (min)	30	73	37	80	40	50	42	43

Table 1. Electron Beam Irradiation of Methane-Carbon Monoxide Mixtures in the Presence of Nitric Oxide (continued)

11 21 79							11 22 79	
Exp. No.	17:03	17:47	18:30	19:15	19:57	10:48	11:42	
Beam Current (mA)	1	1	1	1	1	1	1	
Flow-rate (ml/min) CH_4	90	90	90	90	90	90	90	
CO	10	10	10	10	10	10		
NO	0.20	0.50	1.0	3.0	10.0	1.0	1.0	
Irrad. Temp. (°C)	119	119	119	119	119	149	149	
Yield in μmole/10ℓ reactant gas at 25°C, 1 atm, (G-value)								
H_2	480 (5.4)	480 (5.3)	460 (5.2)	430 (4.9)	360 (4.2)	460 (5.6)	460 (5.6)	
C_2H_2	8.4 (0.093)	8.7 (0.096)	9.7 (0.11)	10 (0.12)	8.9 (0.11)	10 (0.12)	10 (0.12)	
C_2H_4	47 (0.52)	53 (0.59)	57 (0.64)	64 (0.72)	56 (0.66)	57 (0.69)	60 (0.73)	
C_2H_6	20 (0.23)	20 (0.22)	17 (0.20)	15 (0.17)	11 (0.13)	15 (0.19)	15 (0.19)	
C_3H_6	2.3 (0.026)	2.6 (0.028)	3.4 (0.038)	3.7 (0.042)	3.7 (0.043)	3.9 (0.047)	3.9 (0.048)	
C_3H_8	0.1 (0.001)	0.05(0.0006)	≈0	≈0	≈0	0.07(0.0008)	0.11(0.001)	
$i\text{-}C_4H_{10}$	0.44(0.004)	0.49(0.004)	0.46(0.005)	0.19(0.002)	0.25(0.003)	0.25(0.003)	0.21(0.002)	
$1\text{-}C_4H_8$	0	0	0	0	0	0	0	
$n\text{-}C_4H_{10}$	≈0	0	0	0	0	0	0	
$neo\text{-}C_5H_{12}$	0	0	0	0	0	0	0	
$i\text{-}C_5H_{12}$	1.5 (0.017)	1.8 (0.020)	≈0	2.2 (0.025)	1.3 (0.016)	1.8 (0.022)	1.4 (0.017)	
$n\text{-}C_5H_{12}$	0	0	0	0	0	0	0	
HCHO	0	0	0	0	0	0	0	
CH_3OH	3.2 (0.035)	4.1 (0.046)	3.9 (0.044)	3.3 (0.037)	3.5 (0.041)	3.4 (0.041)	3.4 (0.041)	
CH_3CHO	1.9 (0.022)	2.7 (0.030)	2.5 (0.028)	3.8 (0.043)	7.6 (0.089)	3.8 (0.046)	3.3 (0.040)	
C_2H_5OH								
CH_3COCH_3	0.48(0.005)	0.31(0.003)	0.38(0.004)	—	0.56(0.007)	0.32(0.004)	0.2 (0.002)	
CH_3COOH	≈0	≈0	0	0	0	0	0	
C_2H_5COOH	83 (0.92)	140 (1.5)	170 (1.9)	132 (1.5)	68 (0.80)	86 (1.0)	81 (0.98)	
CO_2	73 (0.81)	76 (0.84)	90 (1.0)	98 (1.1)	110 (1.3)	66 (0.80)	66 (0.80)	
H_2O	450 (5.0)	500 (5.6)	550 (6.2)	650 (7.4)	800 (9.5)	520 (6.3)	510 (6.2)	
N_2O	63 (0.70)	120 (1.3)	250 (2.8)	460 (5.2)	550 (6.5)	180 (2.2)	180 (2.2)	
Absorbed energy								
in Mrad	12.4	12.4	12.2	11.9	10.9	11.3	11.3	
in eV/g	7.74×10^{20}	7.74×10^{20}	7.63×10^{20}	7.43×10^{20}	6.80×10^{20}	7.07×10^{20}	7.07×10^{20}	
in eV/10ℓ gas	5.43×10^{21}	5.43×10^{21}	5.40×10^{21}	5.33×10^{21}	5.10×10^{21}	5.00×10^{21}	5.00x10	
Time after Initiating Irradiation (min)	41	40	40	40	40	30	64	

Table 2. Electron Beam Irradiation of Methane-Carbon Monoxide Gas Mixtures in the Presence of N_2O

Electron beam, 0.6 MeV, 1 mA; Scanning width, 30 cm; Temperature, 120°C; Flow rates, CH_4 90 ml/min, CO 10 ml/min

11 10 79

Exp. No.	10:00	10:50	11:35	12:20	13:08	13:55
Beam Current (mA)	1	1	1	1	1	1
Flow-rate CH_4	90	90	90	90	90	90
(ml/min) CO	10	10	10	10	10	10
N_2O	0	0.09	0.30	0.96	3.0	7.0
Yield in μmole/10ℓ reactant gas at 25°C, 1 atm, (G-value)						
H_2	570 (6.2)	550 (6.1)	520 (5.8)	540 (5.9)	490 (5.4)	460 (5.2)
C_2H_2	3.9 (0.043)	3.5 (0.039)	3.5 (0.039)	3.3 (0.037)	3.1 (0.034)	2.8 (0.031)
C_2H_4	9.2 (0.10)	11 (0.13)	9.2 (0.10)	12 (0.13)	12 (0.13)	12 (0.14)
C_2H_6	167 (1.86)	167 (1.86)	174 (1.94)	182 (2.00)	185 (2.05)	186 (2.08)
C_3H_6	1.2 (0.013)	1.1 (0.012)	0.98(0.011)	0.78(0.009)	0.59(0.007)	0.49(0.006)
C_3H_8	37.4 (0.415)	38.6 (0.429)	38.4 (0.426)	37.5 (0.412)	33.4 (0.371)	27 (0.301)
$i\text{-}C_4H_{10}$	5.0 (0.055)	4.0 (0.044)	4.1 (0.046)	3.6 (0.039)	2.8 (0.031)	1.8 (0.020)
$1\text{-}C_4H_8$	0.12(0.001)	0.08(0.0008)	0.09(0.0009)	0.07(0.0007)	0.04(0.0004)	0.04(0.0004)
$n\text{-}C_4H_{10}$	5.1 (0.057)	4.9 (0.055)	4.6 (0.051)	3.9 (0.043)	2.7 (0.030)	1.6 (0.018)
$neo\text{-}C_5H_{12}$	1.1 (0.013)	1.0 (0.012)	0.78(0.009)	0.52(0.006)	0.31(0.003)	≈0
$i\text{-}C_5H_{12}$	2.9 (0.32)	2.6 (0.029)	2.2 (0.024)	1.6 (0.018)	0.94(0.010)	0.45(0.005)
$n\text{-}C_5H_{12}$	0.74(0.008)	0.63(0.007)	0.54(0.006)	0.39(0.004)	0.17(0.002)	0.08(0.009)
HCHO	16 (0.18)	—	9.4 (0.10)	5.1 (0.057)	0	0
CH_3OH	2 (0.02)	4.6 (0.050)	2.8 (0.031)	3.1 (0.034)	3.5 (0.039)	5.3 (0.060)
CH_3CHO	30 (0.33)	30 (0.34)	31 (0.34)	32 (0.35)	33 (0.36)	29 (0.32)
C_2H_5OH CH_3COCH_3	7.9 (0.087)	8.2 (0.092)	9.2 (0.10)	8.5 (0.094)	8.2 (0.091)	7.7 (0.086)
CH_3COOH	96 (1.0)	96 (1.0)	74 (0.82)	96 (1.0)	96 (1.0)	84 (0.94)
C_2H_5COOH	110 (1.2)	120 (1.3)	110 (1.2)	110 (1.2)	100 (1.1)	100 (1.1)
CO_2	—		66 (0.74)	72 (0.85)	250 (2.7)	230 (2.5)
H_2O	≈0	20 (0.22)	31 (0.35))1.09	78 (0.87))1.7	160 (1.7))4.4	260 (2.9))5.4
N_2O	0	140 (1.5)	86 (0.95)	170 (1.8)	300 (3.3)	450 (5.1)
Absorbed energy in Mrad	12.4	12.4	12.4	12.2	11.8	11.2
in eV/g	7.72×10^{20}	7.72×10^{20}	7.72×10^{20}	7.60×10^{20}	7.37×10^{20}	6.97×10^{20}
in eV/10ℓ gas	5.42×10^{21}	5.42×10^{21}	5.42×10^{21}	5.42×10^{21}	5.41×10^{21}	5.39×10^{21}
Time after Initiating Irradiation (min)	48	42	42	40	42	42

In Table 2, the G values of products from CH_4-CO mixture containing various amounts of N_2O were shown with experimental conditions. In Fig. 5, the $G(N_2)$ and sum of the $G(H_2O)$ and $G(CO_2)$ are plotted as a function of N_2O content. It is noted that both plots come to closer, indicating that oxygen atoms produced by N_2O decomposition reacted to form CO_2 and H_2O, satisfying the following stoichiometry:

$$2N_2O + nCO + (2-n)H_2 = 2N_2 + nCO_2 + (2-n)H_2O$$

where $0 < n < 2$.
At a small content of N_2O below 5 mole%, the $G(CO_2)$ is larger than $G(H_2O)$, but above 5 mole%, this relation is reversed.

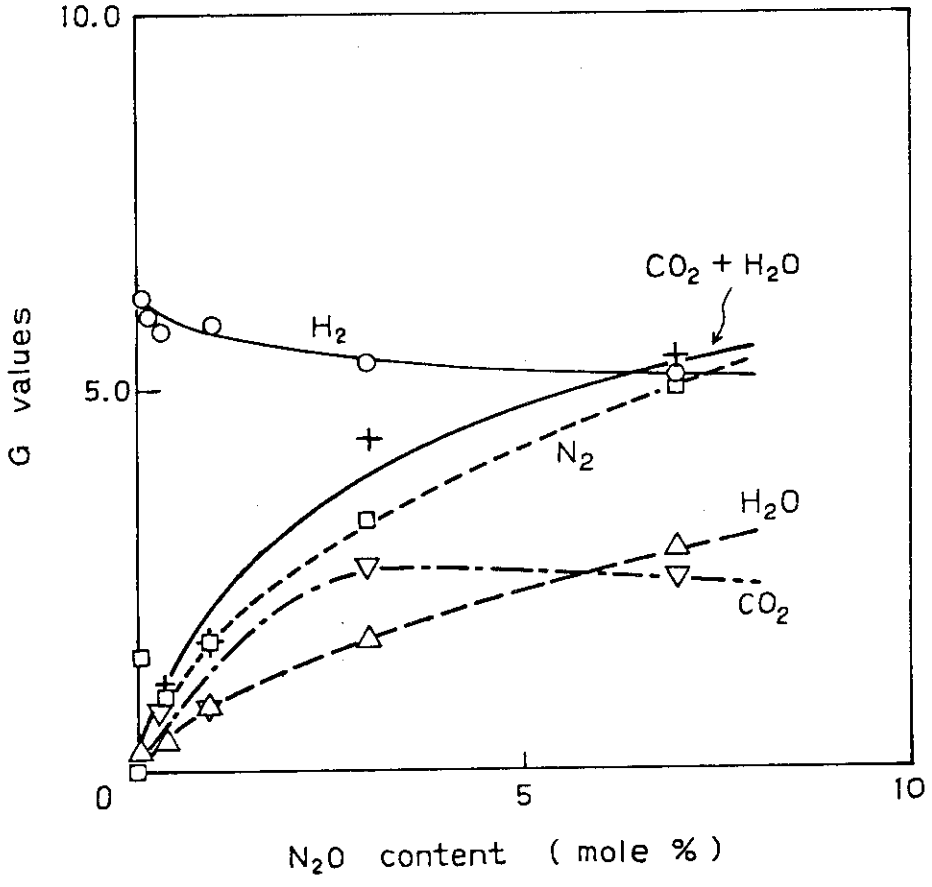

Fig. 5. Effect of addition of nitrous oxide on G values of inorganic products.

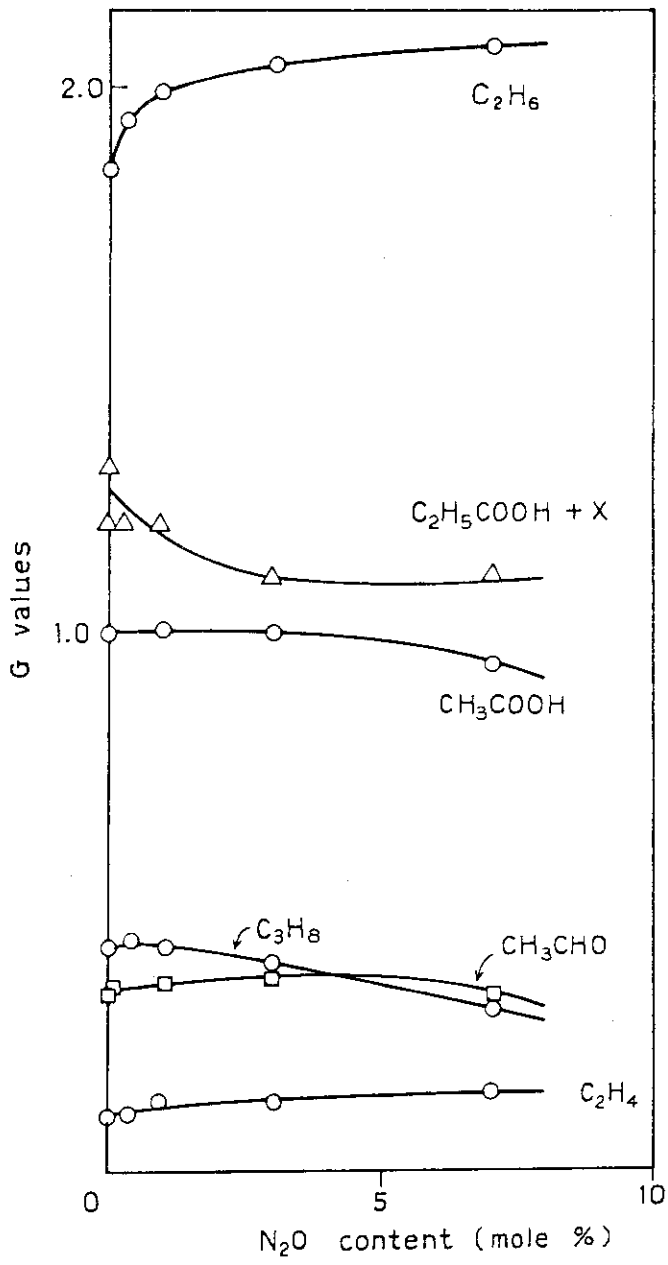

Fig. 6. Effect of addition of nitrous oxide on G values of C_2H_6, C_2H_4, C_3H_8, CH_3COOH, C_2H_5COOH, and CH_3CHO.

The $G(H_2)$ decreased with increasing N_2O content, indicating that the hydrogen atoms escaped from scavenging by CO are reacted with O^- formed from N_2O by reaction (3).

In Fig. 6, the G values of organic products are plotted as a function of N_2O content. The $G(C_2H_6)$ and $G(C_2H_4)$ increased with increasing N_2O content, but the G values of other compounds decreased with increasing N_2O content. However, these changes of G values caused by N_2O addition are small compared with those found for the CH_4-CO-NO mixture, possibly because N_2O reacts with electrons from the accelerator.

(H. Arai, S. Nagai, and M. Hatada)

1) H. Arai, S. Nagai, and M. Hatada, JAERI-M 9214, 56 (1980).

10. The G Values of Ethane and Ethylene in the Radiolysis of Methane at Small Doses

In the previous year, it was reported[1] that the G value of ethylene increased with decreasing dose and higher G value was obtained at higher dose rate, when compared at the same dose. The purpose of this study is to know the highest G value of ethylene obtained experimentally when the dose is so small as possible to allow quantitative determination of the products.

In order to give a small dose to the gas stream, a beam mask was placed on the irradiation vessel of the flow type to limit the irradiation zone. The slit width of the beam mask of 1, 3, and 10 cm decreases the irradiation time by 1/30, 1/10, and 1/3, respectively. The dose rate distributions along the gas stream as obtained by CTA dosimetry are shown in Fig. 1 for different slit width of the beam mask. The dose absorbed by methane was changed by changing the opening of the beam mask, flow rate, and beam current. The temperature of irradiation zone was not satisfactorily controlled by adjusting the flow rate of cooling water, and the temperature of the irradiation zone changed from 50°C to 200°C depending on beam current and

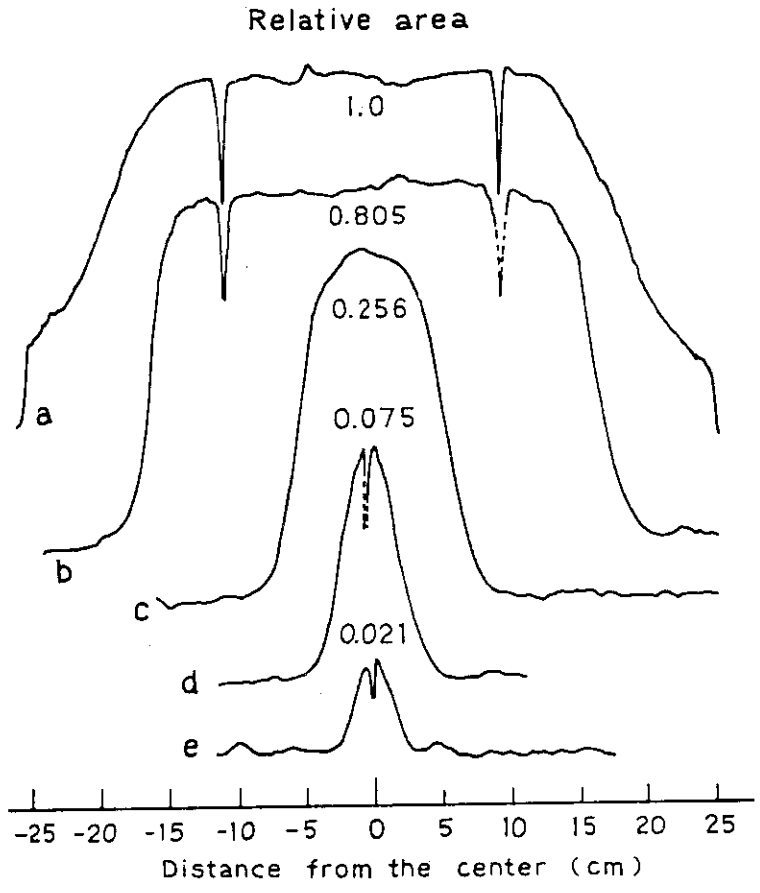

Fig. 1. Dose distribution curves as measured by CTA film dosimetry: Dose, 1 Mrad (0.6 MeV, 1 mA, 77 sec); No beam mask (a); With beam mask of openings of 30 cm (b), 10 cm (c), 3 cm (d) and 1 cm (e) gap.

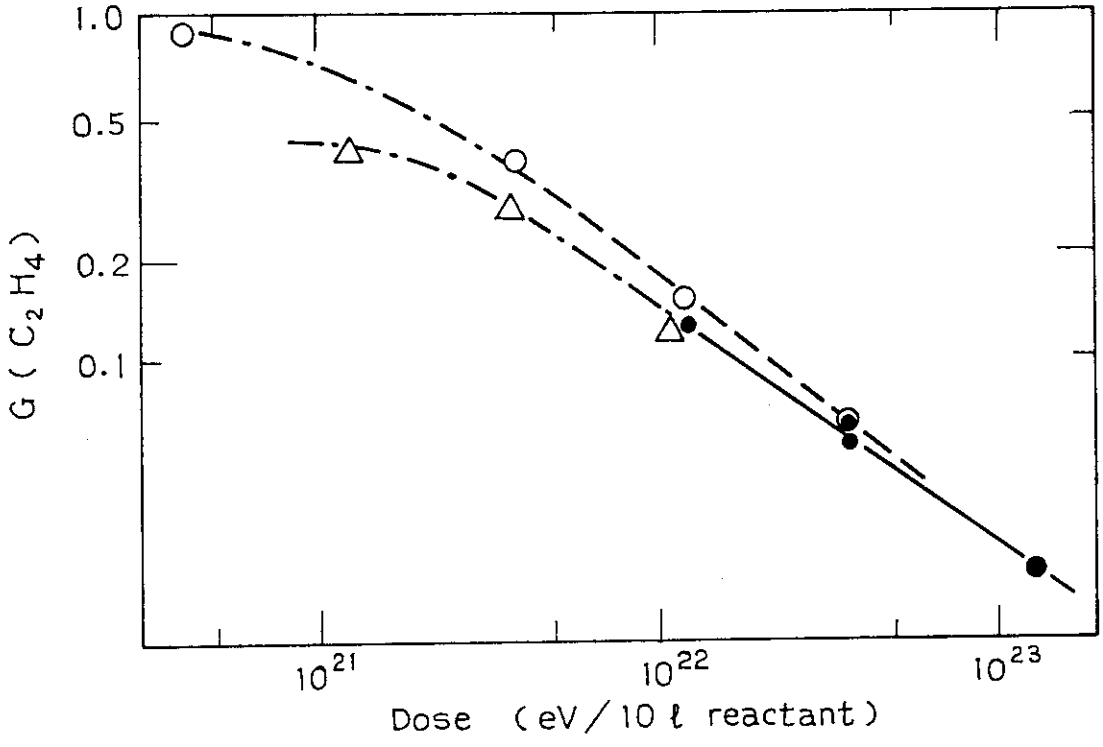

Fig. 2. $G(C_2H_4)$ as a function of dose: Beam current, 10 mA; Dose was changed by changing the gap of the beam mask; (o) 300 ml/min, (Δ) 100 ml/min, (●) no beam mask, at different flow rates (30 ∿ 300 ml/min), from H. Arai, et al.[1)]

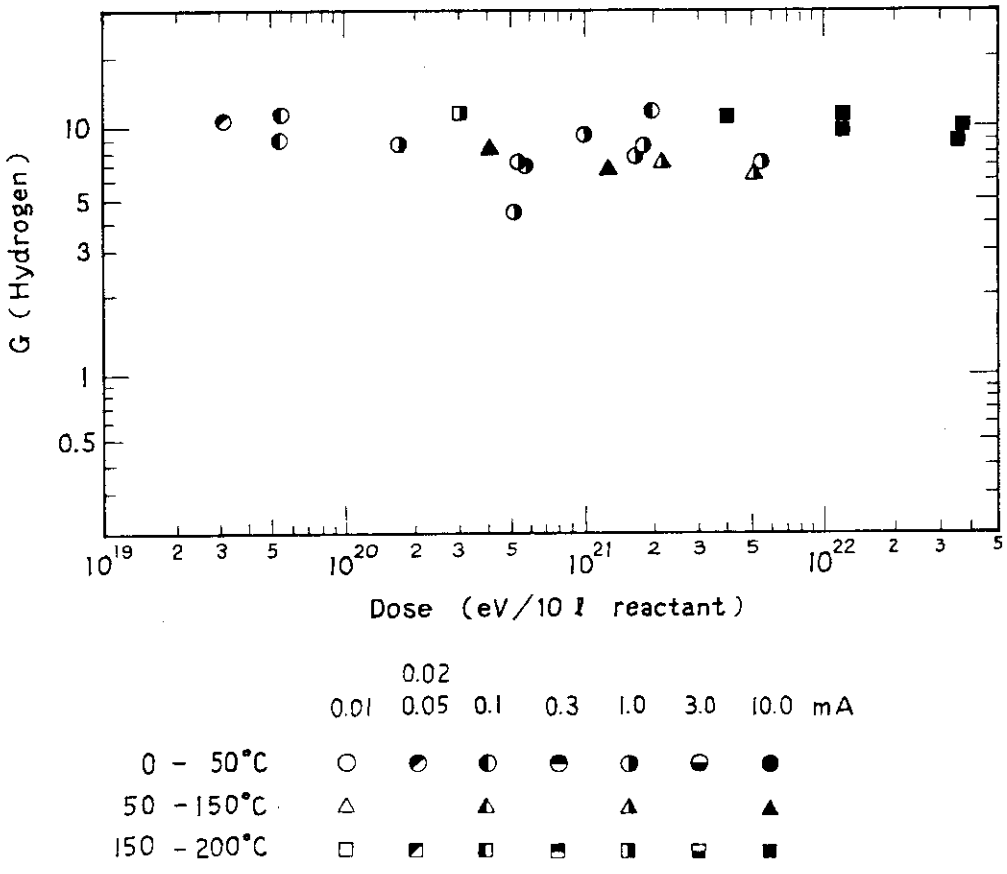

Fig. 3. G value of hydrogen formation as a function of dose.

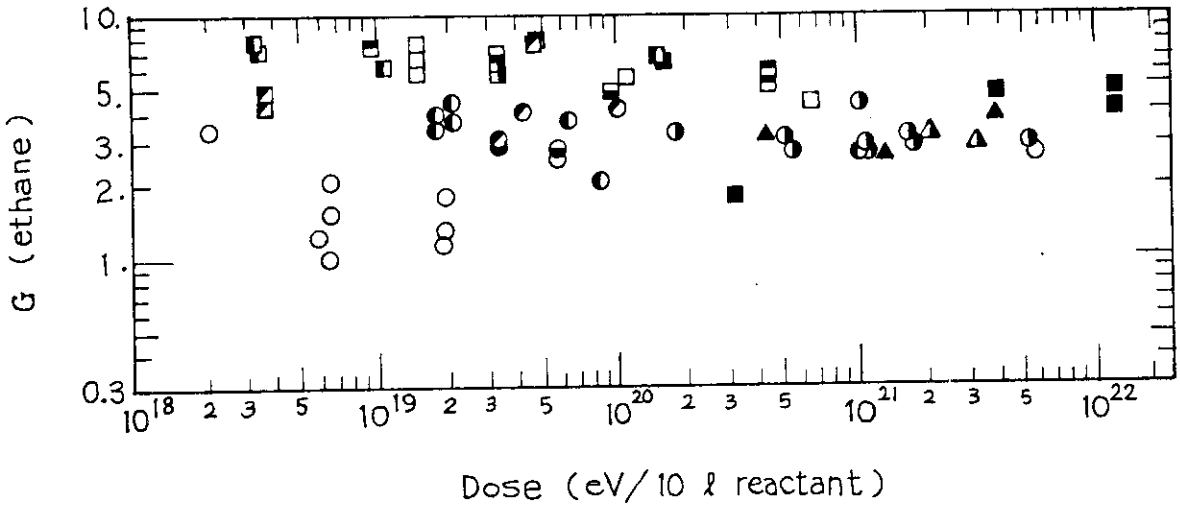

Fig. 4. G value of ethane as a function of dose.
For symbols, see the caption of Fig. 3.

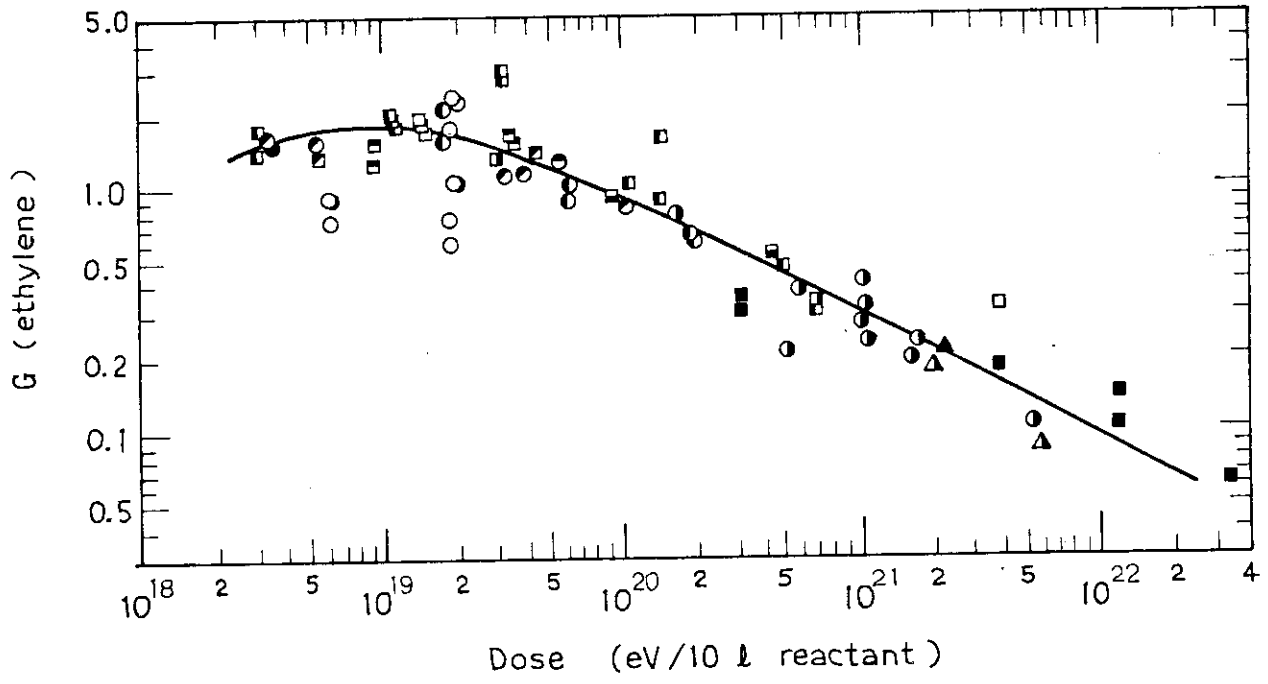

Fig. 5. G value of ethylene as a function of dose.
For symbols, see the caption of Fig. 3.

slit width.

Other methods of irradiation and analysis of the products were the same as those described previously.[1)]

In Fig. 2 the G value of ethylene is plotted as a function of dose which is changed by changing the slit width. The G values obtained at different slit widths were corrected to those at 200°C using known activation energies[2)] of reaction. The data obtained previously by changing flow rate are also included in the figure for comparison. Both plots agree well with each other, showing that both methods give the same results.

In Figs. 3, 4, and 5 the G values of hydrogen, ethane and ethylene are plotted as a function of dose. The correction of temperature to G values obtained at different temperature was not made. The points are scattered over a considerably wide range possibly because of the poor accuracy in determining small quantity of the products and partly because of the different temperatures at the irradiation zone. As shown in Fig. 3 through 5, the G values of hydrogen and ethane are independent of dose, while that of ethylene increases with decreasing dose, confirming the previous finding[1)]. However, the dose rate dependence of G value of ethylene, which was clearly observed in the previous study[1)], can not be detected in the present experiment due to large scattering of the data. The maximum G value of ethylene experimentally obtained is about 3.

(M. Hatada, S. Nagai, Y. Shimidzu, and K. Matsuda)

1) H. Arai, S. Nagai, K. Matsuda, and M. Hatada, JAERI-M 8569, 47 (1979).
2) H. Arai, S. Nagai, K. Matsuda, and M. Hatada, Radiat. Phys. Chem., 17, 151 (1981).

11. Effect of Pressure on the Amounts of Products from Methane by Electron Irradiation

It is well known that hydrogen and hydrocarbons are produced when methane is irradiated by ionizing radiation. The present study has been carried out to know the effect of pressure on the amounts of products from methane by electron irradiation.

The irradiation was carried out using a batch type irradiation vessel which was described in a former report with experimental procedure. The beam current and electron accelerating voltage were 1 mA and 600 keV, respectively, which allow 3.6×10^3 Mrad by 3 hr irradiation. The irradiation vessel was cooled by air stream during irradiation and the temperature of the gas was ca. 70°C as estimated from the pressure increment.

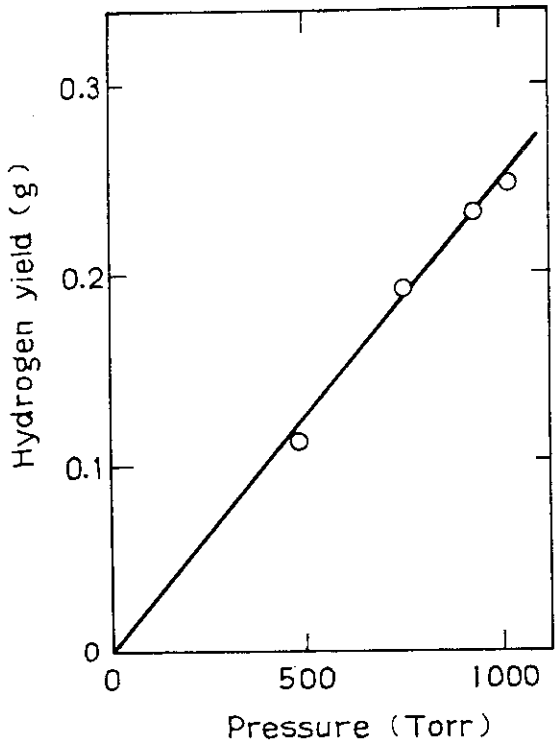

Fig. 1. The amount of hydrogen as a function of initial reactant pressure.

Table 1. The Amounts of Compounds after Irradiation under Different Pressures

Pressure (Torr)		501	760	981	1050
CH_4 (g)		3.06	4.83	6.00	6.72
Temp. (°C)		-	85.4	71.6	54.5
Absorbed dose in the gas (10^{23} eV)		6.9	10.8	13.5	15.2
Products (g)	H_2	0.111	0.194	0.237	0.249
	CH_4	1.74	2.77	3.87	4.18
	C_2H_4	0.003	0.002	0.001	0.003
	C_2H_6	0.424	0.700	0.841	0.942
	C_3	0.137	0.176	0.221	0.251
	C_4	0.079	0.090	0.102	0.123
	C_5	0.102	0.091	0.036	0.128
	C_6	0.034	0.022	0.011	0.024
	Liquid	0.201	0.486	0.521	0.646
Recovery (%)		91.0	93.4	97.3	96.2
$-CH_4$ (%)		37.6	38.1	36.3	35.1
H/C Balance		4.6	5.5	4.6	5.2

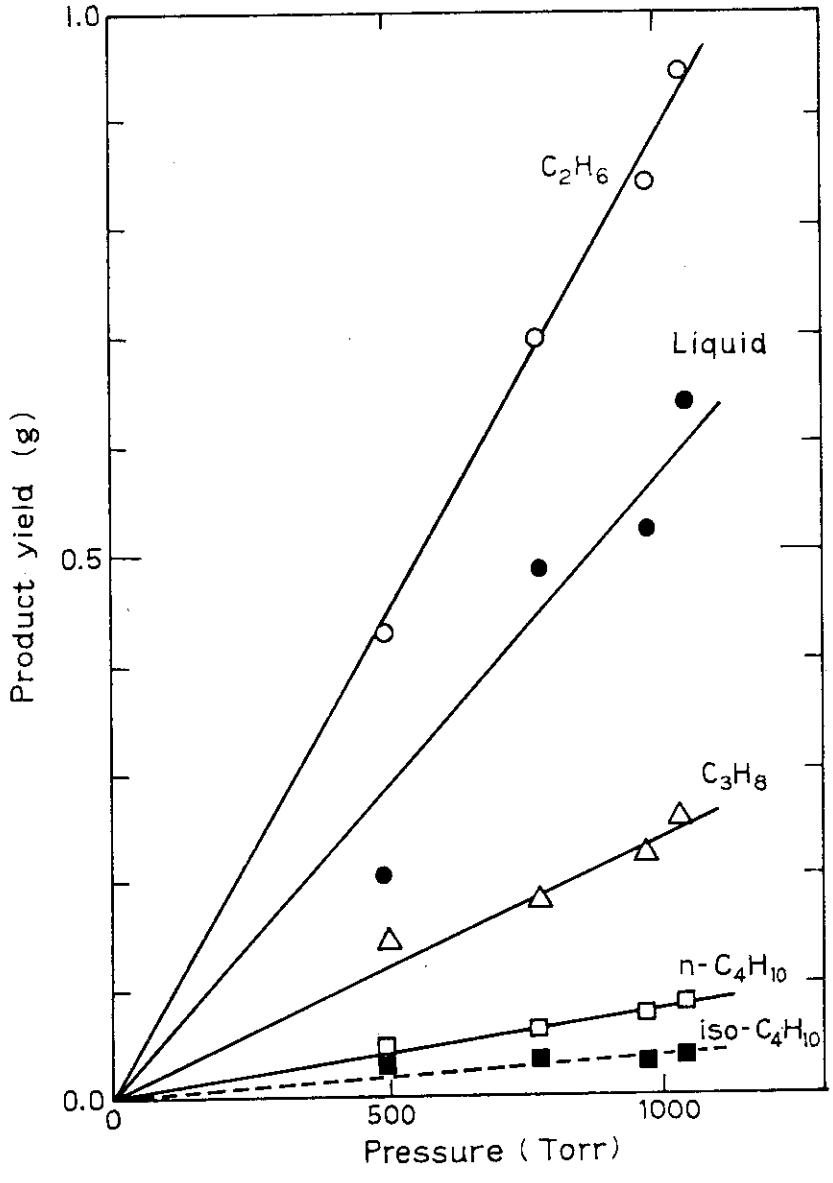

Fig. 2. The amounts of hydrocarbon products as a function of initial reactant pressure.

In Table 1, the experimental conditions were listed together with the amounts of products and methane found in the reaction vessel after 3.6×10^3 Mrad irradiation. The amounts of hydrogen and hydrocarbon products are plotted against the reactant pressure in Figs. 1 and 2, where it is shown that most products increased linearly with increasing initial reactant pressure.

In Fig. 3, the amount of consumed methane relative to the initial amount of methane, P, as defined by eq. (1) is plotted against initial reactant pressure.

$$P = \frac{\text{The residual methane (g)}}{\text{The weight of products (g)} + \text{The weight of residual methane (g)}} \times 100 \ (\%) \qquad (1)$$

It is clearly shown that the percent of consumed methane to the initial amount of methane is independent of the reactant pressure.

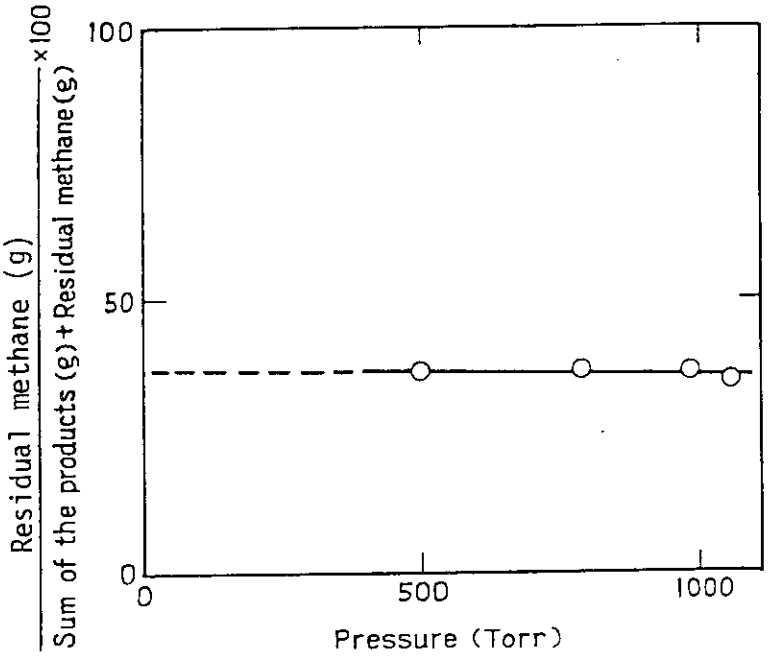

Fig. 3. The consumption ratio of methane as a function of reactant pressure: Dose, 3.6×10^3 Mrad.

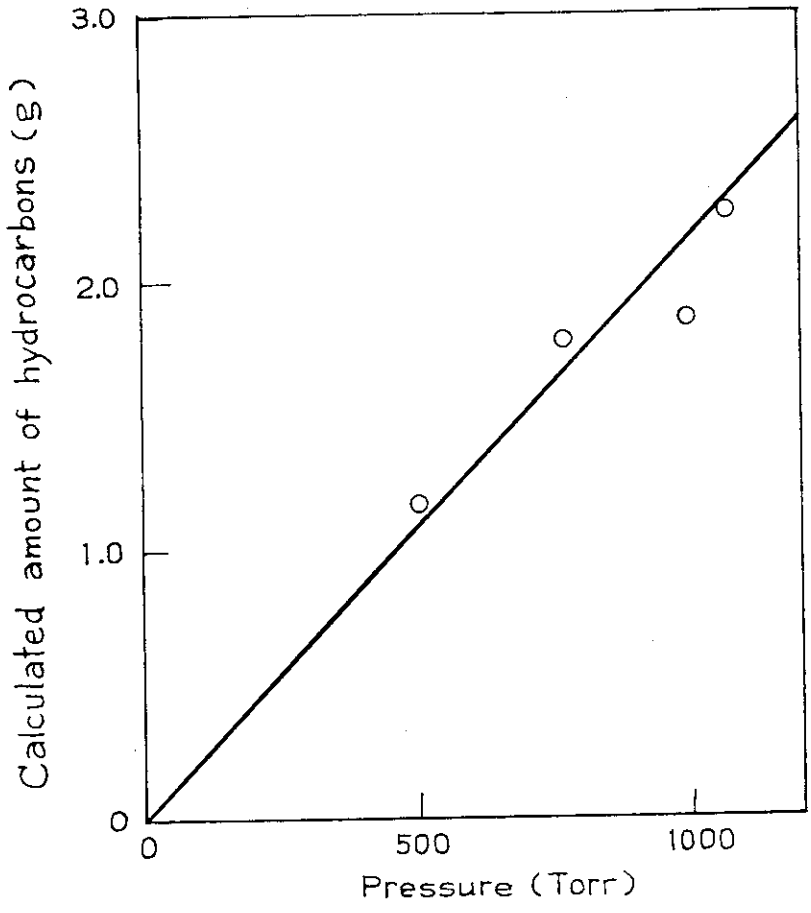

Fig. 4. The weight of hydrocarbon calculated from the mass balance as a function of reactant pressure.

The relation among the amounts of methane consumed, m, hydrogen produced, h, and hydrocarbons produced, x, can be expressed by eqs. (2), (3), and (4):

$$m\ CH_4 = x\ C_nH_{2n+2} + h\ H_2 \quad (2)$$

$$x = m - h \quad (3)$$

$$n = m / (m - h) \quad (4)$$

The amounts of methane and hydrogen were more accurately determined by gaschromatographic analysis than those of higher hydrocarbons. Therefore, the weight of hydrocarbon products

can be given by

$$MW(C_nH_{2n+2})\cdot x = (12n + 2n + 2)x = (14n + 2)x$$

where MW is an average molecular weight of C_nH_{2n+2}. The weight of hydrocarbon products thus calculated are plotted in Fig. 4 as a function of the initial reactant pressure. The plot indicates that the sum of the weights of hydrocarbons increases linearly with increasing initial reactant pressure.

(M. Hatada, H. Arai, and S. Nagai)

12. Selective Formation of Low Molecular Weight Hydrocarbons by Irradiation of Methane in the Presence of Molecular Sieves

Irradiation of methane produces hydrogen and a variety of hydrocarbons. For the purpose of synthesizing hydrocarbons from methane radiation chemically, it is important to find the route which leads to the desired product not only efficiently but also selectively. Recently some attempts have successfully been made on the selective catalytic synthesis of hydrocarbons from CO-H_2 mixture using the Fischer-Tropsch active metals such as Ru and Co supported by NaY-zeolite and alumina containing micro-pores of uniform dimensions.[1-2] It is of interest to examine if such selective synthesis of hydrocarbons would be feasible in the radiation chemical reaction of methane. In the present study, methane was irradiated in the presence of synthetic zeolites, molecular sieves 3A, 4A, 5A and 13X.

Takachiho research grade CH_4 (>99.95%) was used without further purification. The molecular sieves used in this study were of 3A, 4A, 5A and 13X types in powder form (200 mesh pass, Nishio Industry Co.). In the presence of the molecular sieves which had been outgassed at 500°C for several hrs, methane was irradiated with electron beams of 600 keV and 2 mA. The irradiated gas emerged out of the flow reactor FIXCAT-II was analyzed by gaschromatographs equipped with 3 m Porapak Q, 2 m

Porapak N and 2 m molecular sieve 5A columns. Most of the experiments were carried out at 300°C.

Blank experiments indicate that the four types of molecular sieves (MS) employed in the present study exhibit no catalytic activity for thermal reaction of methane up to 300°C without radiation.

Irradiation results in the production of hydrogen and low molecular weight hydrocarbons. Fig. 1 shows the yields of the products over the four types of MS's as a function of time

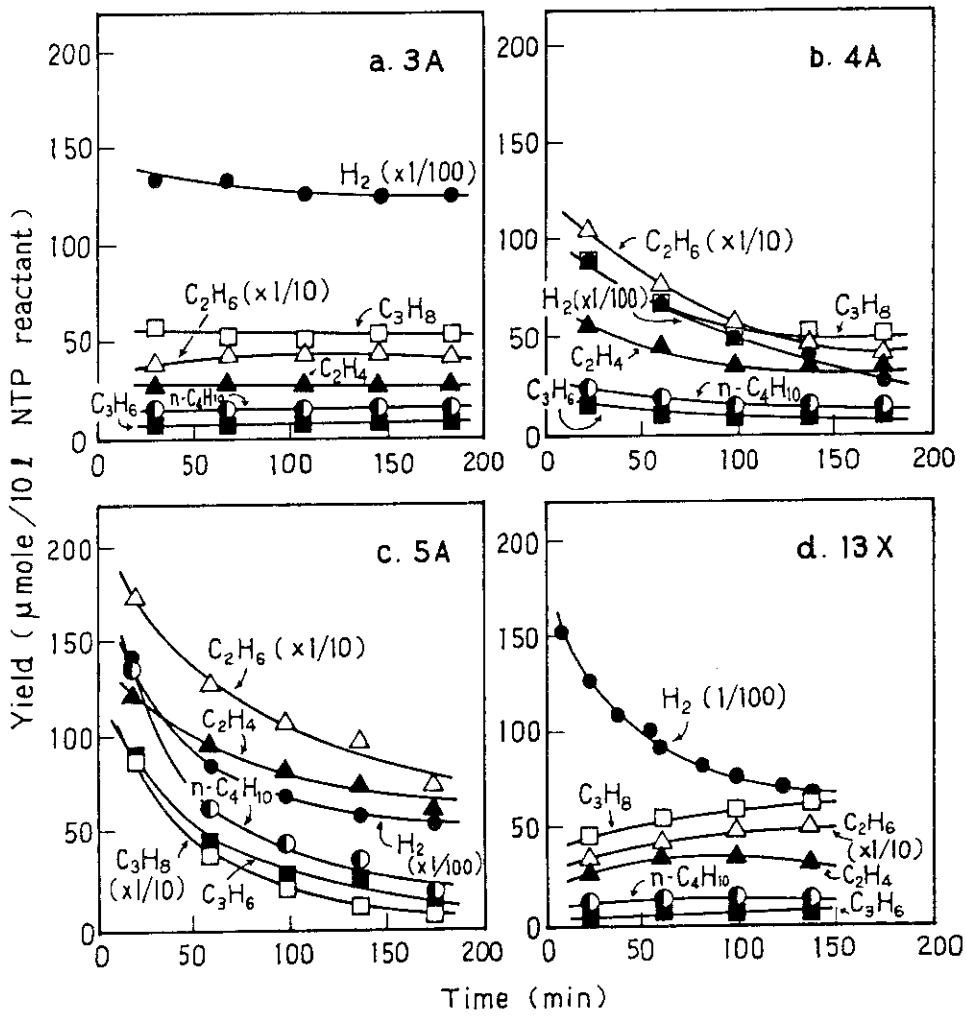

Fig. 1. Product yields vs. time after initiating irradiation of methane over various types of molecular sieves at 300°C: Electron beam, 0.6 MeV, 2 mA; CH_4, 100 ml/min; Solid, 2 gr.

after initiating irradiation. The yields of hydrocarbons over MS-3A and 13X do not differ significantly from those obtained by irradiation of methane in the homogeneous phase as will be described later. By contrast, MS-4A and 5A enhance the yields of hydrocabons as well as hydrogen especially in the initial stage of irradiation. The yield of each product over MS-4A and 5A, however, decreases with irradiation time and approaches gradually to the value obtained by the reaction in the absence of molecular sieves.

Table 1 compares the product yields after 22 min on stream by irradiation of methane in the absence and presence of molecular sieves. It may be seen that MS-3A has little effect on the radiation chemical reaction of methane whereas MS-4A enhances the yields of hydrogen and C_2 hydrocarbons and MS-5A the yields of hydrogen and C_2 - C_3 hydrocarbons. MS-13X increases the hydrogen yield but not the yields of hydrocarbons.

Table 1. Comparison of Product Yields

Solid	——	MS-3A	MS-4A	MS-5A	MS-13X
	Product yields (μmole/10ℓ NTP)				
H_2	1285	1334	8751	13738	12550
C_2H_4	18	29	56	125	30
C_2H_6	623	384	1056	1733	331
C_3H_6	7	9	16	90	7
C_3H_8	69	55	88	885	46
i-C_4H_{10}	20	17	24	63	8
n-C_4H_{10}	17	16	23	134	10
neo-C_5H_{12}	7	5	6	9	2
i-C_5H_{12}	13	12	13	31	5
n-C_5H_{12}	5	6	6	25	1

CH_4, 100 ml/min; Solid, 2 gr; Irradiation temperature, 300°C; Electron beam, 0.6 MeV, 2 mA.
Product yields are those determined 22 min. on stream.

The hydrocarbon distribution obtained with MS-4A and 5A is shown in Fig. 2, together with that obtained by irradiation of methane in the presence of silica gel. As may be seen from the figure, the yields of C_2 and C_3 hydrocarbons are 86% and 8% of the total hydrocarbon (C_2 - C_5) over MS-4A and 60% and 32% of that over MS-5A, respectively. On the other hand, the product distribution over silica gel extends over higher hydrocarbons.

The results obtained with MS-3A, 4A and 5A are well explained by taking into account the molecular diameters of methane and higher hydrocarbons and pore size of the MS's. That is, methane is not able to intrude into the pores of MS-3A, simply because the cross-sectional diameter of methane (4A) exceeds the pore-size of MS-3A. On the other hand, methane and C_2 hydrocarbons may pass through the pores of MS-4A and C_1 - C_3 hydrocarbons the pores of MS-5A. Therefore, the selective formation of C_2 and/or C_3 hydrocarbons over MS-4A and 5A suggests that they are produced inside the pores of the MS's.

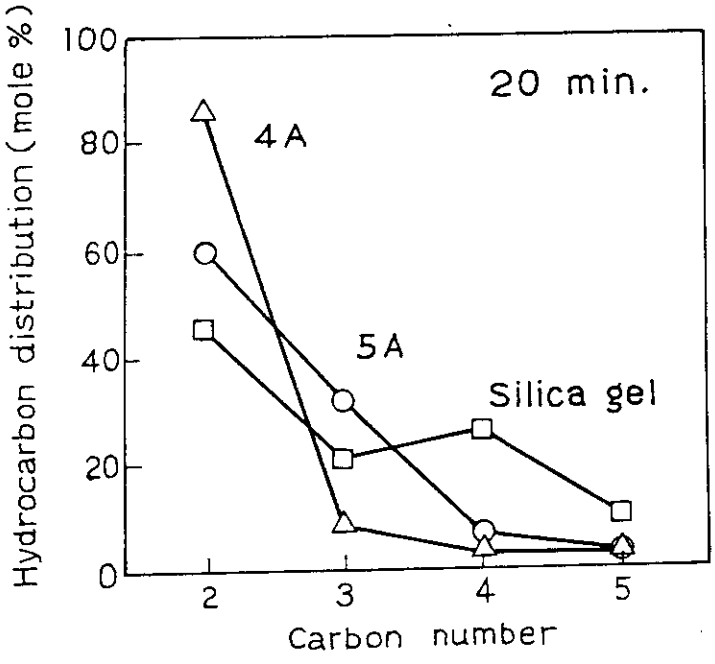

Fig. 2. Comparison of hydrocarbon distributions: Electron beam, 0.6 MeV, 2 mA; CH_4, 100 ml/min; Solid, 2 gr; Irradiation temperature, 300°C.

The reason why the yields of C_2 and C_3 hydrocarbons are enhanced by the MS's may be due to energy transfer from MS's to adsorbed methane, as in the case of the formation of hydrocarbons by irradiation of CO-H_2 mixture over silica gel.[3)]

It is curious that only hydrogen is favorably produced over MS-13X. One possibility may be that hydrocarbons, if formed, may not be allowed to desorb from MS-13X. To check the possibility, the concentrations of the products in the effluent of methane irradiated over MS-5A were determined before and after passing the effluent through MS-13X kept at 300°C. No significant difference, however, was detected in both cases.

(S. Nagai, Y. Shimizu, and M. Hatada)

1) H. H. Nijs, P. A. Jacobs and J. B. Uytterhoeven, J. Chem. Soc., Chem. Comm., 180, 1095 (1979).
2) D. Vanhove, P. Makambo and M. Blanchard, J. Chem. Soc. Chem. Comm., 605 (1979).
3) S. Nagai, H. Arai and M. Hatada, Radiat. Phys. Chem., 16, 175 (1980).

[2] Radiation-Induced Polymerization

1. Supplemental Experiments on the Formation of Super Polymer in the Radiation-Induced Polymerization of Water-Saturated Styrene

It has already been reported[1] that super polymer of molecular weight about 10^6 i.e. DP = 10.000 is formed when water-saturated styrene ($[H_2O] = 3.5 \times 10^{-2}$ mol/l) is irradiated at higher dose rates. The super polymer is distinguished as a clearly separated peak in the GPC molecular weight distribution curve of the polymerization product as shown in Fig. 1. It is noteworthy that no peak of the super polymer was observed by the irradiation of the moderately dried styrene ($[H_2O] = 3.2 \times 10^{-3}$ mol/l).

Water has practically no effect on the radical polymerization, but is an inhibitor of the ionic polymerization. In the case of the super-polymerization it is clear that water plays a roll in the reaction. Investigation by changing the water-

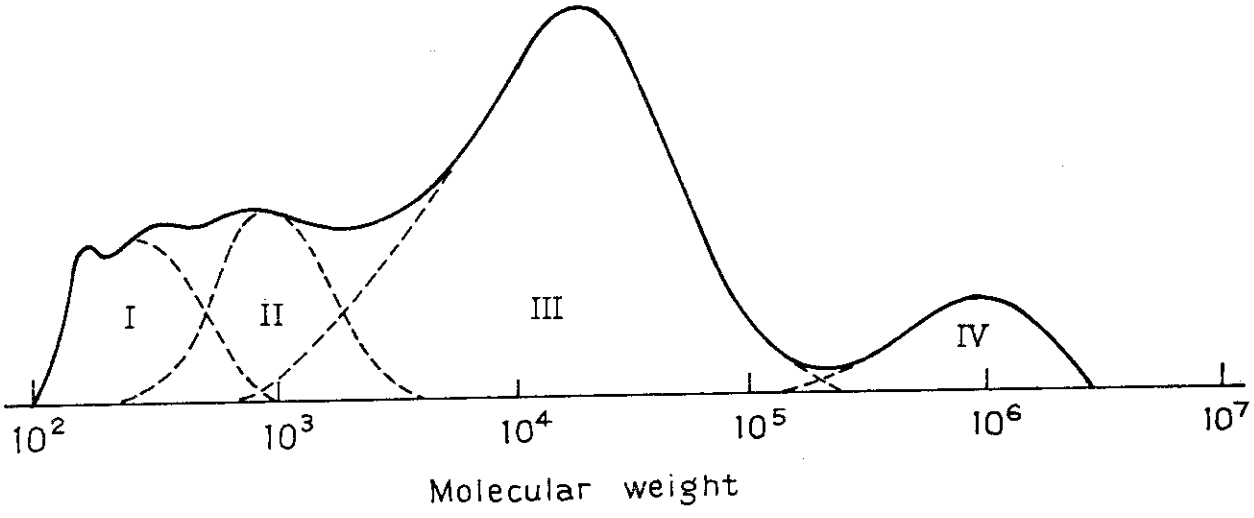

Fig. 1. GPC molecular weight distribution curve of polymerization product of water-saturated styrene at a dose rate of 1.8×10^7 rad/sec.

content of styrene between $10^{-3} \sim 10^{-2}$ mol/l may be useful to elucidate the mechanism of the polymerization of the super polymer; however it had to be postponed due to experimental difficulty.

Polymerization of the water-saturated styrene in a wide range of dose rate was carried out to know the lowest dose rate necessary for the super-polymerization and the dependence of the rate of super-polymerization on the dose rate. The experimental results are summarized in Table 1. It is seen from the table that the super polymer is not detected at a dose rate of 1.2×10^3 rad/sec, its formation is quantitatively measured

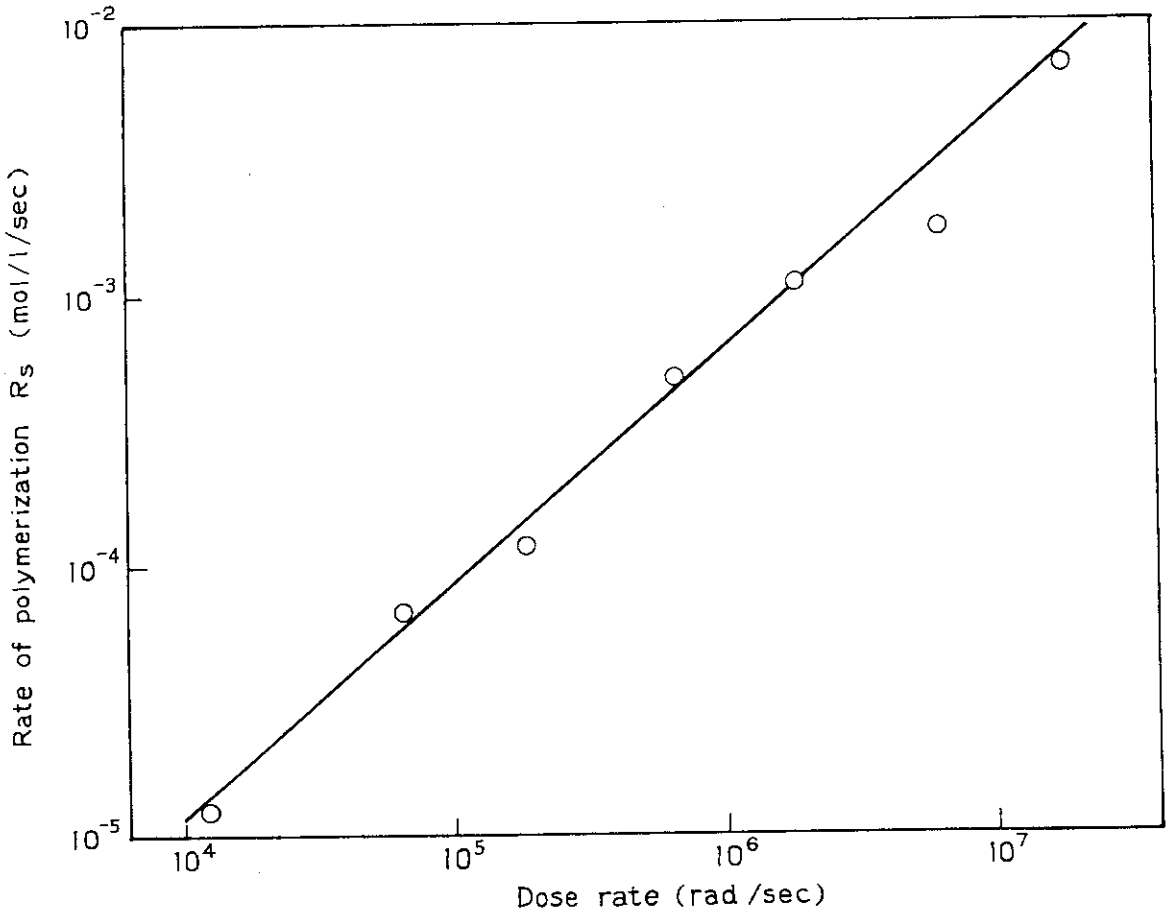

Fig. 2. Dependence of the rate of super polymerization (R_s) on the dose rate for the bulk polymerization of water-saturated styrene.

Table 1. Radiation-Induced Polymerization of Water-Saturated Styrene in a Wide Range of the Dose Rate

Dose Rate (rad/sec)	1.2×10^{3}	1.2×10^{4}	6.0×10^{4}	1.8×10^{5}	6.0×10^{5}	1.8×10^{6}	6.0×10^{6}	1.8×10^{7}
Irrad. Time (sec)	2.5×10^{3}	10^{3}	500	300	50	30	10	2
Total conv. (%)	2.18	3.08	3.50	5.15	3.75	4.88	3.84	1.94
Fraction of four kinds of polymer (%)								
Oligomer, I	12.4	8.9	10.3	11.3	12.3	14.9	15.1	13.8
Radical, II	87.6	63.9	53.3	41.9	27.6	31.8	15.4	15.3
Ionic, III	0	22.8	25.8	39.5	52.5	45.7	64.1	62.2
Super, IV	0	4.4	10.7	7.5	7.6	7.6	5.4	8.6
Rate of polymerization of super polymer R_s mol/l/sec	——	1.17×10^{-5}	6.53×10^{-5}	1.11×10^{-4}	4.96×10^{-4}	1.08×10^{-3}	1.83×10^{-3}	7.26×10^{-3}
Molecular weight of super polymer MW (10^{6})	——	1.0	1.0	0.8	1.0	0.82	0.75	0.55
Super polymer content in the reaction mixture 10^{-2} mol/l	——	1.2	3.2	3.4	3.3	3.2	1.8	1.4

above 1.2×10^4 rad/sec up to the highest dose rate of 1.8×10^7 rad/sec. The rate of polymerization of the super polymer R_s increases with increasing dose rate. Fig. 2 shows the dependence of the rate of polymerization of super polymer on the dose rate. It is seen that the exponent of the dependence is 0.87, this is in good agreement with our previous report[1].

Super polymer is characterized by its very high molecular weight of about 1×10^6; Table 1 contains also the molecular weights corresponding to the super polymer peaks of the GPC curves. It is noteworthy that the molecular weight decreases slowly with increasing dose rate. Super polymer content of the polymerization mixture is given, as in the case of the calculation of the rate of polymerization, not in the polymer mole but in the basic mole (C_8H_8) per liter. The value of the super polymer content is by no means a constant but it changes with the time of polymerization as will be shown below. However, it is useful from practical point of view to produce the super polymer in satisfactory yield.

To obtain time-conversion curve of the super polymer, water-saturated styrene was irradiated at a dose rate of 1.2×10^5 rad/sec at room temperature for various duration of time between 80 and 1200 seconds. The experimental results are shown in Table 2 and Fig. 3. The dependence of the S.P. content on the irradiation time is very important; it has a high value at the beginning, is almost constant up to 600 seconds and then it drops rather rapidly to 0 at 1200 seconds.

The curve shown in Fig. 3 suggests apparently that at the very beginning of the irradiation the water-saturated styrene contains a certain amount of super polymer; however, it is impossible. The explanation is that an appreciable amount of super polymer is formed in a very short time, arrives at a stationary state within 80 seconds. In the present experiment ca. 0.1% of the starting styrene is converted to the super polymer within 80 seconds, therefore there is some difficulty to shorten the reaction time, nevertheless it is worth trying. From the presence of a stationary state and the disappearance of the super polymer by the irradiation we have to assume the

decomposition of the super polymer, though we have not yet direct experimental evidence for it.

Some experiments were carried out under employment of methanol instead of water. Corresponding to water content of moderately dried ($[H_2O] = 3.0 \times 10^{-3}$ mol/l) and water saturated ($[H_2O] = 3.5 \times 10^{-2}$ mol/l) styrene, methanol concentrations were, $[CH_3OH] = 6.2 \times 10^{-3}$ and 3.7×10^{-2} mol/l. Irradiation was carried out at a dose rate of 1.8×10^5 rad/sec for 3×10^3 seconds at room temperature. Experimental results are shown in Table 3. As can be seen from the table, methanol has similar effect as water to depress ionic polymerization and produce super polymer. When a larger amount of methanol as for example

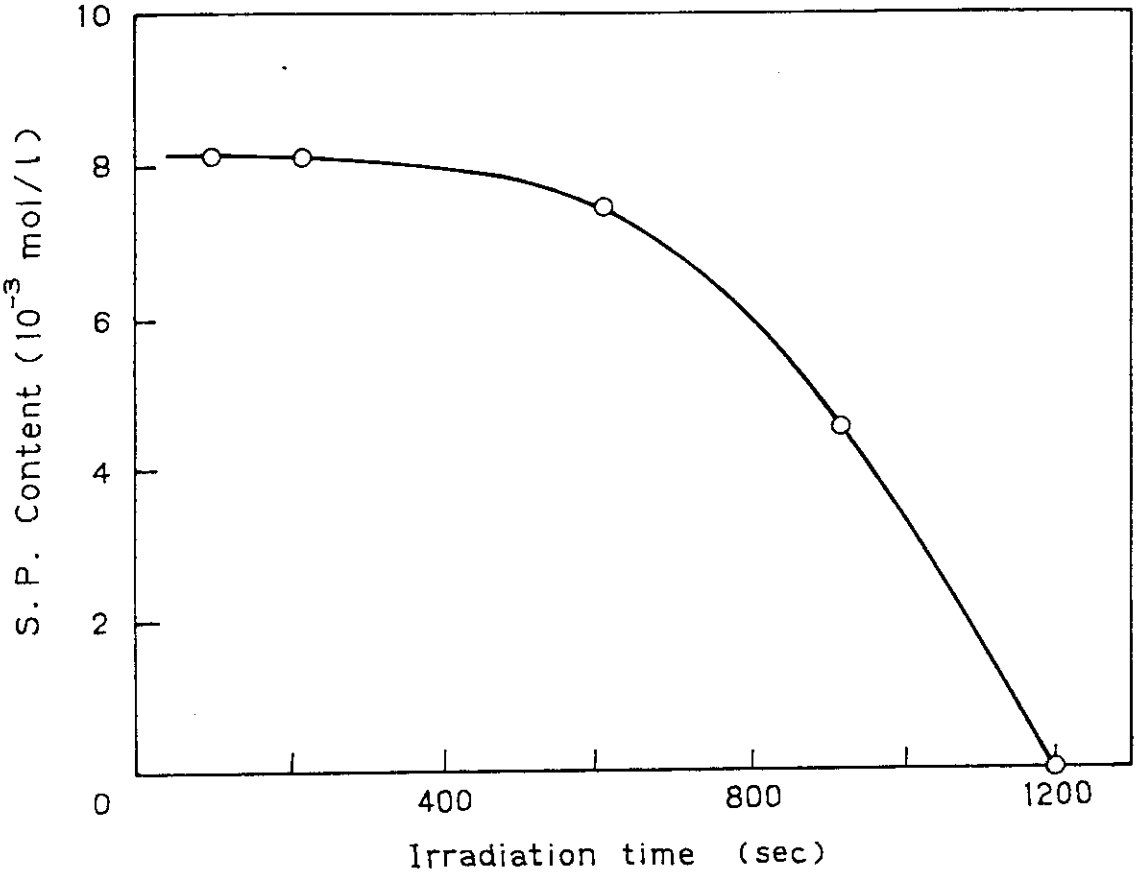

Fig. 3. Polymerization of super polymer (S.P.) by the irradiation of water-saturated styrene at room temperature: Dose rate, 1.2×10^5 rad/sec.

Table 2. Change of the Amount of Super Polymer with the Irradiation Time in the Radiation-Induced Polymerization of Water-Saturated Styrene.

Irradiation Time (sec)	80	200	600	800	1200
Total Conversion (%)	1.07	1.93	6.15	7.42	12.4
Fraction of four kinds of polymer (%)					
Oligomer, I	9.2	15.5	18.2	22.4	11.2
Radical, II	21.3	33.2	51.0	58.2	49.5
Ionic, III	60.9	46.5	29.4	18.7	39.3
Super, IV	8.6	4.8	1.4	0.7	0
Molecular weight of super polymer					
MW(10^6)	1.2	1.2	1.5	1.6	—
Super polymer content in the reaction mixture					
10^{-3} mol/l	8.0	8.1	7.5	4.5	0

Table 3. Formation of Super Polymer by Irradiation of Styrene Containing a Small Amount of Methanol

Additive	Water	Methanol	Methanol
Concentration (mol/l)	3.5×10^{-2}	6.2×10^{-3}	3.7×10^{-2}
Total conversion (%)	5.15	5.88	3.25
Fraction of four kinds of polymer (%)			
Oligomer, I	11.3	13.1	7.32
Radical, II	41.9	22.4	84.4
Ionic, III	37.4	61.7	4.9
Super, IV	7.5	4.9	3.4
Rate of polymerization of super polymer R_s mol/l/sec	1.13×10^{-4}	8.79×10^{-5}	3.21×10^{-5}
Molecular weight of super polymer MW (10^5)	8.0	8.0	8.0
Super polymer content in the reaction mixture 10^{-2} mol/l	3.33	2.50	0.86

20 ml is added to 80 ml styrene and irradiated at a dose rate of 7.5×10^4 rad/sec, super polymer was not formed.

The above metnioned experimental results do not give sufficiently useful information. However, it suggests that methanol is indirectly useful as a tool to study the role of water molecule for the formation of super polymer.

(J. Takezaki, T. Okada, and I. Sakurada)

1) J. Takezaki, T. Okada, and I. Sakurada, J. Appl. Polym. Sci., 22, 3311 (1978).

2. Radiation-Induced Formation of Styrene Super Polymer in Binary Mixtures with Solvents

Formation of styrene super polymer by irradiation of binary mixtures of styrene with solvents was studied. Though the formation of the styrene super polymer was found at first in the case of bulk polymerization of styrene which contained a small amount of impurities such as water or methanol, it will be described in the present report that formation of the super polymer was found in solution polymerization.

The first example is the super polymer formation by irradiation of the styrene/ethylene dichloride (80/20 in vol); the irradiation was carried out at various dose rates to know the dose rate dependence of the rate of polymerization of the super polymer. The results are summarized in Table 1. It is seen from the table that the formation of the super polymer is observed first at the dose rate of 2.4×10^4 rad/sec, it is noteworthy that radical polymerization which has been playing a dominant role varied to ionic polymerization near this dose rate. The dose rate dependence of the rate of polymerization of the super polymer is shown in Fig. 1; it is seen that the exponent of the dependence is 0.84, which is practically the same as to the case of the water-saturated styrene.

Effect of the ethylene dichloride content of the reaction mixture on the formation of the super polymer was investigated and the results are shown in Table 2. Reaction conditions are also included in the table. Figure 2 shows the super polymer content in the reaction mixture after the irradiation. It is seen clearly that increasing amount of the super polymer is formed with increasing content of ethylene dichloride showing a maximum at about 50/50 of styrene/ethylene dichloride. When the styrene content is less than 20% no formation of the super polymer is detectable.

Next binary mixtures with ethylene glycol was studied because the glycol was interesting in connection with methanol. Table 3 shows results of experiments which were carried out in the same manner as binary mixture of styrene-ethylene dichloride.

Table 1. Dose Rate Dependence of Polymerization of Styrene in Styrene/Ethylene Dichloride (80/20 vol.), Fractions of the Four Kinds of Polymer and Polymerization Rate of Super Polymer

Dose Rate (rad/sec)	1.1×10^{3}	2.4×10^{4}	1.2×10^{5}	4.8×10^{5}	2.4×10^{6}	8.4×10^{6}	3.0×10^{7}
Irradiation Time (sec)	3×10^{3}	5×10^{2}	1×10^{2}	50	10	5	2
Total Conversion (%)	3.00	4.24	4.64	12.4	7.18	6.24	6.89
Fractions of four kinds of polymer (%)							
Oligomer	18.5	8.0	7.6	8.3	7.0	17.0	17.5
Radical	73.1	29.0	15.2	9.0	23.7	0	0
Ionic	8.4	60.5	75.9	81.4	67.7	81.6	81.1
Super	0	2.0	1.3	1.3	1.6	1.4	1.4
Rate of polymerization of super polymer							
R_s (mol/l/sec)	0	1.18×10^{-5}	4.22×10^{-5}	2.25×10^{-4}	8.04×10^{-4}	1.23×10^{-2}	3.32×10^{-3}

Table 2. Relation between the Formation of the Super Polymer of Styrene and the Content of Ethylene Dichloride
Irradiation: Dose rate, 6.0×10^6 rad/sec; Time, 10 sec;
At room temperature

Content of ethylene dichloride (vol.%)	0	40	50	60	80
Total Conversion (%)	13.1	10.9	13.3	23.2	35.4
Fractions of four kinds of polymer (%)					
Oligomer	10.7	12.7	17.3	11.1	14.6
Radical	0	7.5	8.6	9.2	20.4
Ionic	89.3	76.3	68.5	78.4	64.2
Super	0	3.5	5.6	1.3	0.8
Molecular weight of super polymer MW(10^6)	—	0.85	0.70	1.0	0.9
Super polymer content in the reaction mixture 10^{-2} mol/l	0	2.00	3.24	1.05	0.04

Table 3. Relation between the Formation of the Super Polymer of Styrene and the Content of Ethylene Glycol
Irradiation: Dose rate, 6.0×10^6 rad/sec; Time, 10 sec,
At room temperature

Content of ethylene glycol (vol.%)	0	20	40	60	80
Total conversion (%)	13.1	1.70	2.66	3.04	6.20
Fractions of four kinds of polymer (%)					
Oligomer	10.7	25.6	33.3	54.0	68.6
Radical	0	36.5	34.1	31.0	27.1
Ionic	89.3	16.0	11.9	1.1	0
Super	—	21.9	20.7	13.9	4.3
Molecular weight of super polymer MW(10^6)	—	1	0.64	0.50	0.34
Super polymer content in the reaction mixture 10^{-2} mol/l	—	2.59	2.88	1.48	0.46

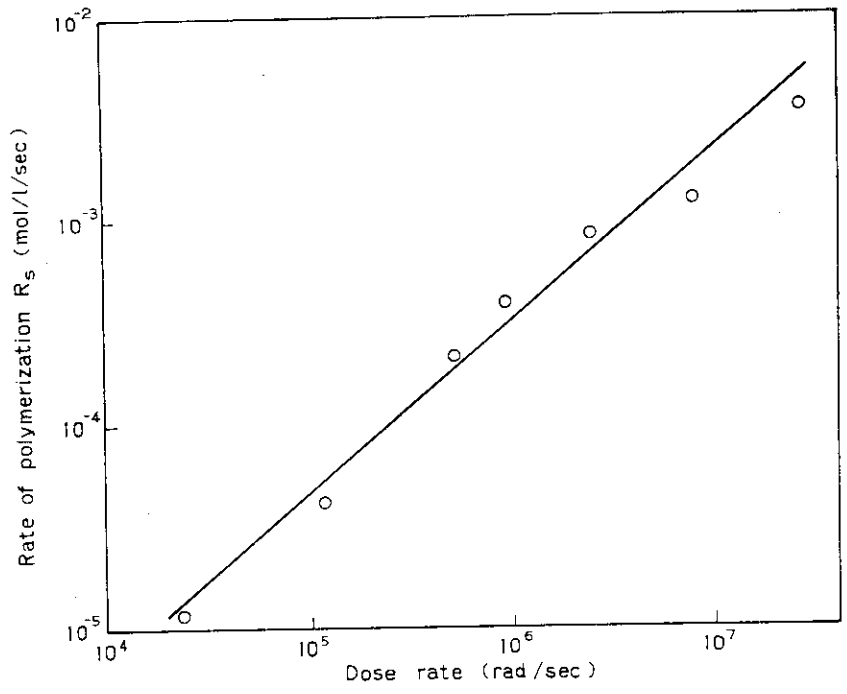

Fig. 1. Dependence of the rate of super polymerization of styrene (R_S) on the dose rate in styrene/ethylene dichloride (80/20 vol).

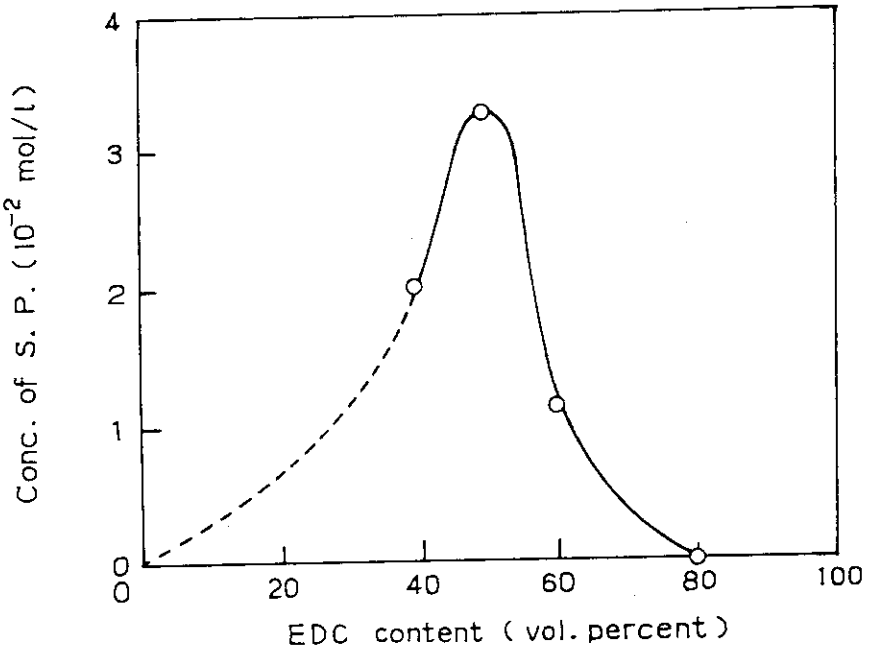

Fig. 2. Formation of styrene super polymer (S.P.) in styrene/ethylene dichloride (EDC) of various ratios by the irradiation: Dose rate, 6.0×10^6 rad/sec; 10 seconds; at room temperature.

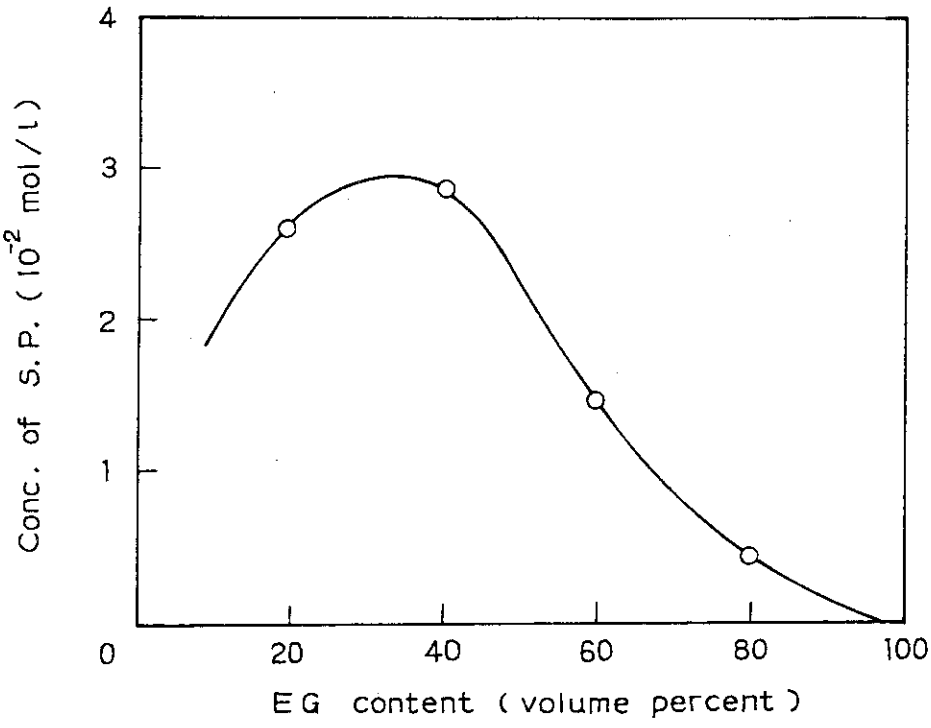

Fig. 3. Formation of super polymer (S.P.) in styrene-ethylene glycol (EG) of various ratios by the irradiation: Dose rate, 6.0 x 10^6 rad/sec; 10 seconds; at room temperature.

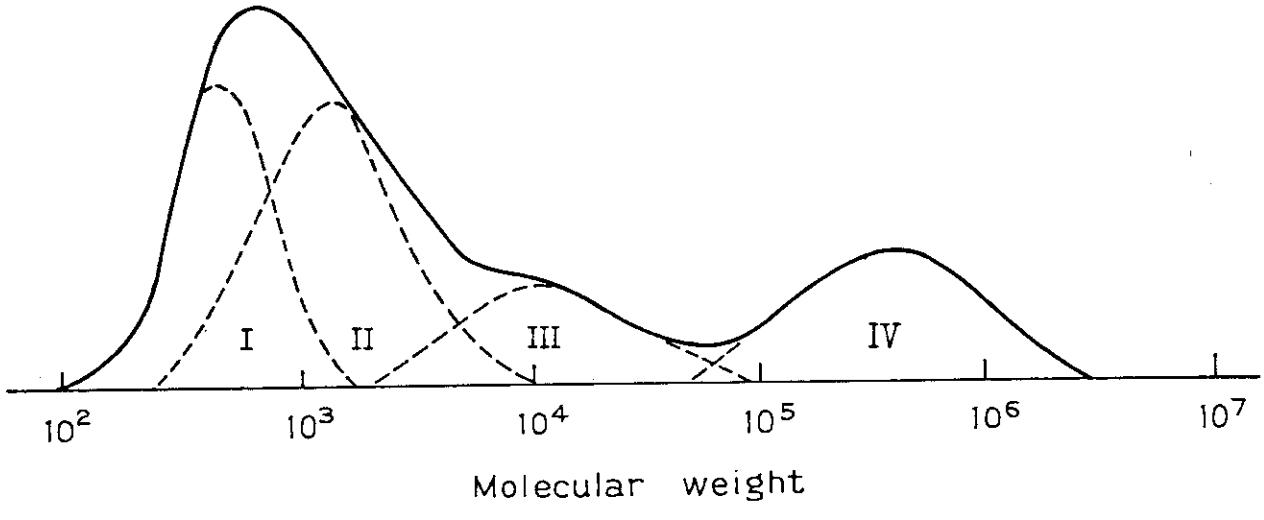

Fig. 4. GPC molecular weight distribution curve of polystyrene in styrene/ethylene glycol (80/20 vol) at 6.0 x 10^6 rad/sec (dose, 6.0 x 10^7 rads).

Table 4. Formation of Super Polymer of Styrene in Binary Mixtures with Benzene, Dichloro- and Nitrobenzene

I. Styrene/Benzene
(Dose rate, 1.2×10^5 rad/sec; time, 10 sec)

Content of solvent (vol%)	20	40	60	80
Total conversion (%)	—	10.4	15.5	13.1
Fractions of four kinds of polymer (%)				
Oligomer	—	9.1	12.9	8.9
Radical	—	67.8	75.7	91.1
Ionic	—	19.6	10.7	0
Super	—	3.5	1.4	0

II. Styrene/o-Dichlorobenzene
(Dose rate, 6.0×10^6 rad/sec; time, 10 sec)

Total conversion (%)	7.05	—	62.1	—
Fraction of four kinds of polymer (%)				
Oligomer	43.5	—	21.4	—
Radical	27.8	—	21.9	—
Ionic	24.3	—	55.7	—
Super	4.4	—	1.0	—

III. Styrene/Nitrobenzene
(Dose rate, 6.0×10^6 rad/sec, time, 10 sec)

Total conversion (%)	4.50	—	8.55	3.76
Fraction of four kinds of polymer (%)				
Oligomer	3.44	—	50.0	70.9
Radical	15.3	—	15.7	15.3
Ionic	42.9	—	29.4	13.8
Super	7.4	—	4.9	0

Content of the super polymer in the reaction mixtures changes with concentration in a similar way. The most important result obtained in the styrene-ethylene glycol system is that the percent of the super polymer in the total polymer is much larger in this case than in the cases of water-saturated styrene and the binary mixture of styrene/ethylene dichloride. The highest value found in the former cases was about 10%, but in the present case it is greater than 20% (see Figure 4). Discussion on the mechanism is, for the present, unable due to the lack of experiments; however it may be a key to solve the problem.

Binary mixtures of styrene/benzene, styrene/*o*-dichlorobenzene and styrene/nitrobenzene were also employed for the experiments. Experimental conditions and results are briefly summarized in Table 4; it is noteworthy that nonpolar compound benzene is also capable of forming the super polymer.

(J. Takezaki, T. Okada, and I. Sakurada)

3. Cationic Oligomerization of Butadiene in the Presence of Halogenated Hydrocarbons

In the preceding papers, polymerization of butadiene by electron beam irradiation was reported in bulk[1] and in n-hexane solution[2]. In these systems it was found that the polymerization proceeded with cationic mechanism and $\bar{M}n$ of the products was not so high, 2000 ∿ 2500. The residual unsaturation in the polymer was 84 and 69% for bulk and n-hexane system respectively in contrast to ca. 20% in the catalyst-initiated cationic polymerization. In this study, cationic oligomerization of butadiene was carried out using halogenated hydrocarbons as chain transfer agents.

n-Hexane, which was used as solvent to obtain a mixture of butadiene and halogenated hydrocarbons, and chain transfer agents were dried with calcium hydride. Butadiene was used as received. All the samples were sealed in a metal cells[3] for electron beam irradiation after degassing in a vacuum system.

Irradiation was carried out at -10°C by 1.5 MeV electron beams from a Van de Graff accelerator.

$\bar{M}n$ value of the product was evaluated by a GPC measurement applying an MW calibration curve for polybutadiene which was obtained by fractionated butadiene oligomers. Quantitative determinations of terminal- and micro-structure of the products were made by ^{1}H-NMR measurements (60 MHz) in $CDCl_3$ solution at room temperature.

It is considered that cationic oligomerization of butadiene (B) proceeds with the following mechanisms. Here RCl and S mean a chain transfer agent containing chlorine atom and solvent, respectively.

$$RCl\ (B,S) \xrightarrow{\sim\sim} R^+(B^+,S^+) \qquad (1)$$

$$R^+(B^+,S^+) + B \longrightarrow RB^+ \qquad (2)$$

$$RB_n^+ + B \longrightarrow RB_{n+1}^+ \qquad (3)$$

$$RB_n^+ + RCl \longrightarrow RB_nCl + R^+ \qquad (4)$$

$$RB_n^+ + X \longrightarrow RB_n + X^+ \qquad (5)$$

By the repetition of reactions (2) ∿ (4), oligomers of an RB_nCl type are formed. The chain oligomerization is eventually terminated by the reaction (5), the degradative chain transfer to water, X, which is contained in the system as an impurity. As a chain transfer agent, four chlorinated hydrocarbons were used as shown below.

1-Chloro-2-butene (1C2B)

CH_3-CH = CH-CH_2Cl

Benzyl chloride (BC)

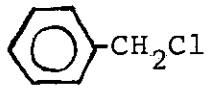

Epichlorohydrin (ECH)

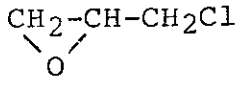

Cumyl chloride (CC)

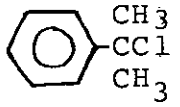

In Figs. 1 and 2, changes of the relative R_p and $\bar{M}_n$ in the presence of these chain transfer agents are shown. In Fig. 1 R_p divided by initial concentration of butadiene, [B] is plotted against [RCl]/[B] since [B] is different in each sample. When 1C2B is used, the relative rate once attains a maximum value, then decreases and finally it increases again very slightly with increasing [RCl]/[B] ratio. Such a variation of R_p is also observed in the case of ECH and the situation may be similar for BC. The rapid increase of R_p at low [RCl]/[B] ratio can be accounted by an increase of initiating cation in consequence of the energy transfer from monomer and solvent to the chain transfer agent. The yield of the initiating cation is expected to level off with increasing [RCl]/[B] ratio. On the other hand, an addition of polar substance increases water concentration in the system resulting the decrease of R_p. The gradual increase of R_p at high [RCl]/[B] ratio is supposed to be related to the change of the dispersion state of water in the system by the increase of [RCl].

In Fig. 2, $\bar{M}_n$ decreases with increasing [RCl]/[B] ratio and at high [RCl]/[B] ratio, tends to converge to a constant value in the cases of 1C2B, BC and ECH. In CC, $\bar{M}_n$ already attains a constant value even at substantially low [RCl]. From Fig. 2, we can see that the chain transfer coefficients are in the following order.

$$CC > ECH > BC > 1C2B$$

Comparing Figs. 1 and 2, it seems that the higher the chain transfer coefficient, the lower the [RCl]/[B] ratio at which the maximum $R_p/[B]$ is attained.

In Fig. 3, NMR spectra of butadiene oligomers obtained in the presence of 1C2B are shown. The strong absorptions at 0.8 $\sim$ 2.5 and 4.8 $\sim$ 6.0 ppm are due to paraffinic and olefinic protons of polybutadiene unit, respectively. Relatively weak absorptions at 3.4 $\sim$ 3.7 and 4.0 ppm are due to the chloromethyl groups of alkyl and allyl type, respectively. These two absorptions are highly intense in low molecular weight product,

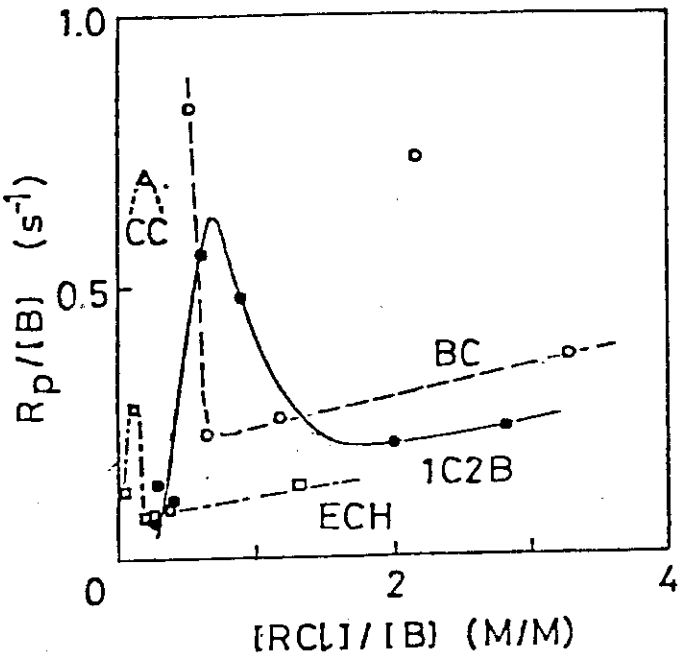

Fig. 1. Changes in relative R_p.

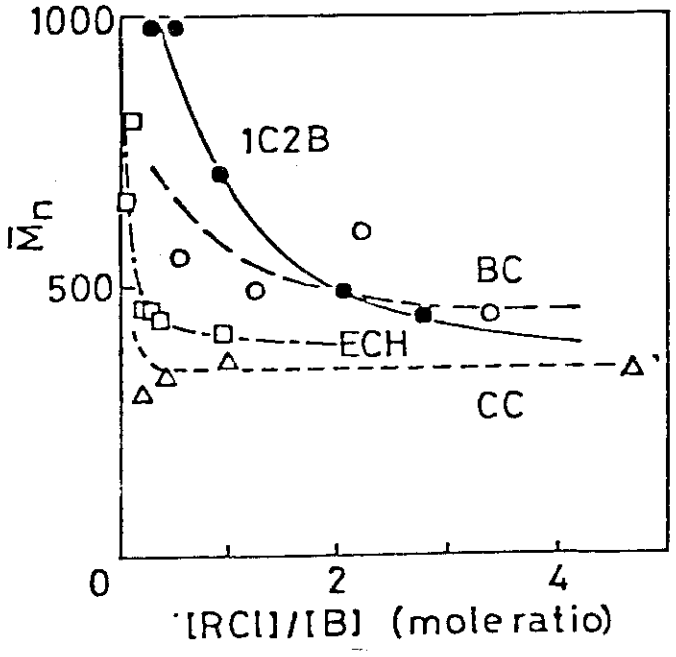

Fig. 2. Changes in MW.

suggesting that these groups are present mainly at a terminal of the oligomer. Chloromethyl group of alkyl type is considered to form through a hydrogen shift reaction from allyl type chloromethyl terminal.

In Table 1, results on 1C2B system are summarized. No systematic change in the ratio of the amounts of the two chloromethyl groups with [1C2B]/[B] but the sum is almost constant, about 1.3 per molecule, except the lowest [1C2B]/[B] case. The residual unsaturation decreases with increasing [RCl]/[B] ratio indicating an occurrence of cyclization reaction.

In Table 2, results on the structures of B-BC and -CC oligomers are given. In BC-oligomer, sum of two chloromethyl terminal is about 0.4 per molecule and total chlorine atom per molecule is 0.7 even when non-terminal -CHCl- is taken into account. On the other hand, the number of phenyl group i.e.,

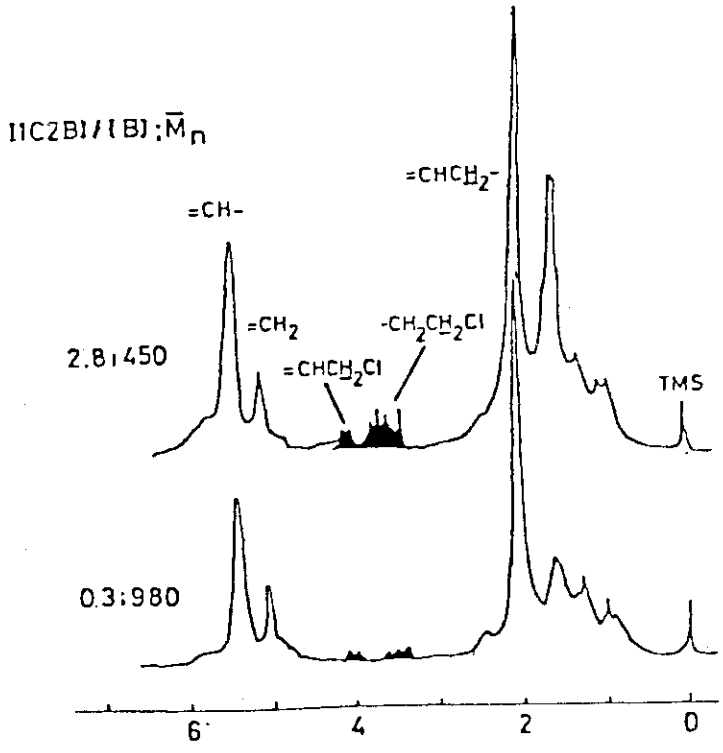

Fig. 3. NMR spectra of B-1C2B oligomers.

Table 1. MWs and Structures of Oligobutadienes Obtained in 1C2B-n-Hexane System: 2.2×10^5 rad/s, -10°C.

$\frac{[1C2B]}{[B]}$	$\bar{M}_n$	Terminal group per molecule			Residual unsat. (%)	Vinyl frac. (%)
		$=CHCH_2Cl$	$-CH_2CH_2Cl$	Sum		
0.28	980	0.34	0.50	0.84	76	28
0.49	980	0.74	0.61	1.35	65	26
0.89	710	0.62	0.55	1.17	64	25
2.03	490	0.36	0.91	1.27	59	24
2.82	450	0.50	0.79	1.29	37	21

Table 2. Structures of B-BC, CC Oligomers

RCl	Benzyl Chloride	Cumyl Chlrodie
[RCl]/[B]	0.74	0.98
$\bar{M}_n$	600	365
$=CHCH_2Cl$	0.25	0.31
$-CH_2CH_2Cl$	0.16	-
CHCl	0.32	-
	1.27	2.15
Residual unsat.(%)	73	5
Vinyl frac. (%)	25	ca. 16

another end of the molecule is about 1.3, which disagrees with the number of chlorine containing group. In CC-oligomer, no other chlorine containing group than allylic chloromethyl is observed and the unbalance between the numbers of two terminal groups is much greater. The microstructure of BC-oligomer is not much different from 1C2B-oligomer but most of double bond in the CC-oligomer is consumed by the cyclization reaction.

In NMR spectra of ECH-oligomers, a strong absorption due to diol $-CH(OH)-CH_2OH$ terminal is observed at 3.8 ppm but no absorption of epoxy ring is observed. The presence of chloromethyl terminals is uncertain since its absorption overlaps with diolone. The number of terminal diol structure is increased from 2 to 4 with increasing [RCl]/[B] from 0.05 to 0.35. The high number of diol terminal is partly due to the overlapping of chloromethyl terminal but it seems still too high. Microstructure of the oligomer are not much different from that of 1C2B-oligomer at low additive concentrations.

(K. Hayashi and S. Okamura)

1) K. Hayashi, Y. Tanaka, and S. Okamura, J. Polym. Sci. Polym. Chem. Ed., 19, 1435 (1981).
2) K. Hayashi, K. Kagawa, and S. Okamura, ibid, 19, 1977 (1981).
3) K. Hayashi, ibid., 18, 179 (1980).

4. Emulsion Polymerization of Styrene in a Flow System (2)

In the last issue of this report, it has been reported the kinetic behavior of the emulsion polymerization of styrene[1] and vinyl acetate[2] by high dose rate electron beam irradiation. In this report, polymerization of styrene is reinvestigated. Here, the reaction vessel[1] is fixed on a cassette type holder, which can be mounted to the scanner head of a Van de Graaf accelerator. This apparatus helps us to improve the reproducibility of the dose rate absorbed in a sample at each run of the experiment and hence gives more reliable results than the earlier work[1]. Further methods of experiment, apparatus and

procedures are almost the same as in the earlier report[1]. Sodium lauryl sulfate (SLS) is used as an emulsifier. Electron beam irradiation is carried out at the beam energy of 1.5 MeV with a variable beam current at the sample temperature of 40°C.

In Fig. 1, the change of the initial R_p with SLS concentration at the monomer concentration of 30 wt% is shown at two different dose rates. Here, R_p means the rate of polymerization when one liter of emulsion is irradiated in our experimental system. In the figure, the changes of R_p with SLS concentration at two dose rates are very similar each other. At lower [SLS] than 1 wt% to the monomer, R_p increases very slightly with [SLS]. It is noteworthy that no abrupt increase of R_p at the critical micellar concentration (CMC) of the emulsifier[3] is observed at high dose rate polymerization. At higher [SLS] than 1%, R_p increases violently and the dose rate exponent at [SLS] = 3 $\sim$ 5% is 1.2 at both dose rates. This suggests that the polymerization proceeds with a different reaction mechanism at low and high SLS concentration.

In Fig. 2, the change of R_p with dose rate is shown at two SLS concentrations. The dose rate exponents are approximately 0.3 and 0.4 for 1 and 3% SLS, respectively. The influence of the monomer concentration on R_p is shown in Fig. 3. At 1% SLS, the R_p increases proportionally to the monomer concentration when the weight fraction of styrene in the emulsion is 0.2 $\sim$ 0.4. At 3% SLS, R_p changes proportionally to [St] up to 30%.

In our system, it is hard to obtain the full conversion of monomer even after the irradiation of 16,000 sec. Generally, the polymerization ceases at 70 $\sim$ 80% conversion. With increasing the polymer conversion, the circulation rate of the emulsion decreases for the increase of the emulsion viscosity. The slower flow rate of the emulsion in a reaction vessel enhances the deposition of the polymer onto the beam window of the vessel resulting a further reduction of the flow rate.

The average molecular weight of the polystyrene depends mainly on dose rate. The $\bar{M}_n$ at 3.0×10^5 rad/sec is usually between 800 and 1000 as described in the earlier article[1].

The size of the polymer particles in the emulsion is

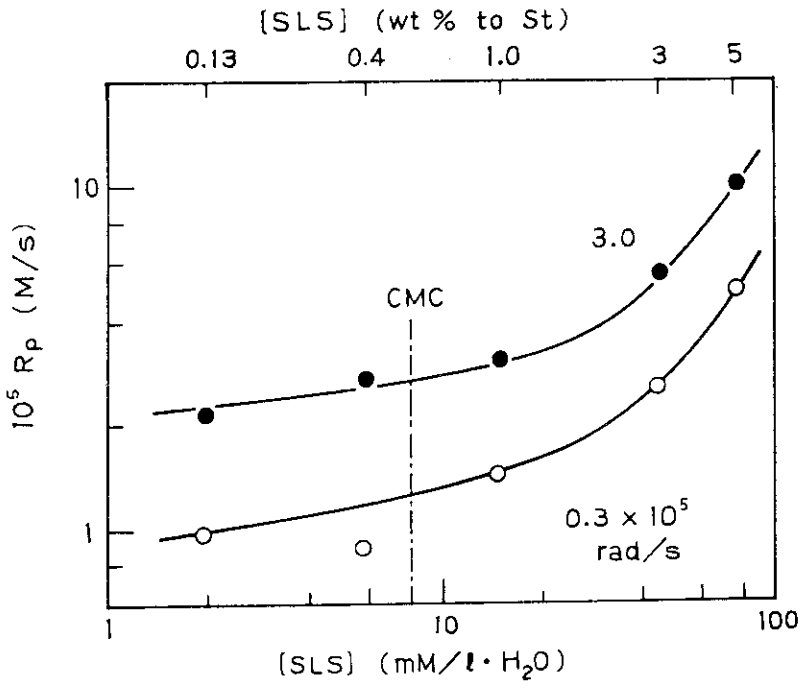

Fig. 1. Dependence of R_p on emulsifier concentration: Styrene conc., 30 wt%.

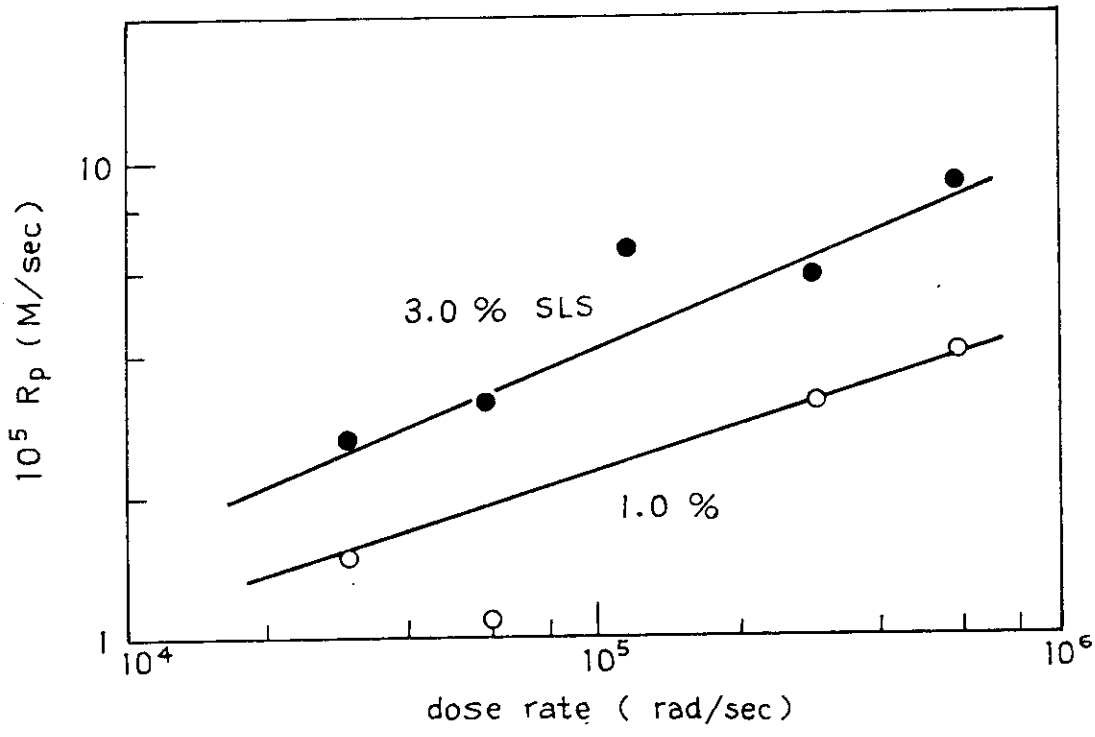

Fig. 2. Dose rate dependence of R_p: Styrene conc., 30 wt%.

determined by two methods, time-correlation light scattering method using Coulter "Nanosizer" and stopped flow method.[4] Agreements of the values by the two methods are fairly well as shown in Table 1. The values in the parentheses after the particle sizes by Nanosizer represent a relative unit of polydispersity in the particle size distribution and in present case, the values indicate substantially broad distribution. From the table, particle diameters of the emulsions are between 500 and 800 A, which is fairly small compared with those obtained in ordinary processes. Therefore we can say that the polymerization of high initiation rate yields an emulsion of fine particles.

The average number of radicals in a particle, $\bar{n}$ is calculated for the initiation rate of 1.3×10^{17} radicals/ml·sec, which is the rate of radical formation in water phase assuming

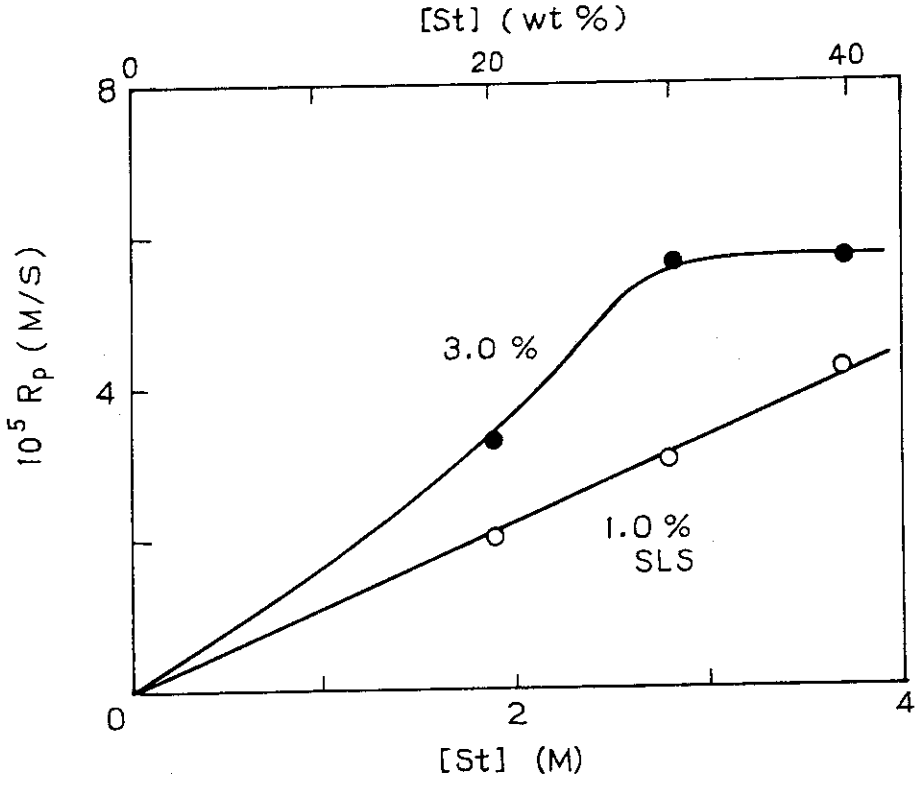

Fig. 3. R_p vs. monomer concentration:
Dose rate, 3.0×10^5 rad/sec.

Table 1. Preparation Conditions and Particle Diameters of Polystyrene Emulsions

Sample	[St] (wt%)	[SLS]/[St] (wt%)	Irradiation			Solid content (%)	Particle diameter (A)	
			E (MeV)	I (μA)	Time (s)		Stopped flow	Nanosizer
ES38	30	1.0	1.5	50	10,000	21.8	610	630 (6-7)
ES39	30	3.0	1.5	50	16,000	24.9	720	820 (4-6)
ES50	10	3.0	2.0	90	14,000	8.9	690	-
ES51*	10	3.0	2.0	50	16,000	7.0	700	-
ES52	10	3.0	2.0	50	16,000	7.6	560	-
ES57	20	3.0	1.5	100	16,000	17.3	530	-

* no reservoir system

$G(R\cdot) = 1$ at 3.0×10^5 rad/sec. Using Stockmeyer's equation[4], $\bar{n}$ values at 500 and 800 A are 0.75 and 1.1 radicals/ml·sec, respectively. This indicates that the present polymerization follows neither to the case 2 ($\bar{n} = 1/2$) nor to the case 3 ($n >> 1$) of Smith-Ewart theory[5]. Therefore, the reaction behavior we have observed corresponds to the intermediate stage of the two cases.

(K. Hayashi and S. Okamura)

1) K. Hayashi and S. Okamura, JAERI-M, 9214, 113 (1980).
2) K. Hayashi and S. Okamura, JAERI-M, 9214, 116 (1980).
3) S. Okamura and T. Motoyama, J. Polym. Sci., 58, 221 (1962).
4) S. Egusa, submitted to J. Colloid Interface Sci.
5) W. H. Stockmeyer, J. Polym. Sci., 24, 314 (1957).
6) W. V. Smith and R. H. Ewart, J. Ehcm., Phys., 16, 592 (1948).

5. Data Processing System for GPC Measurements

A new GPC system is introduced in this year. As schematically shown in Fig. 1, three types of detecting units, differential refractometer (RI), UV spectrometer (UV) and low angle laser light scaterring apparatus (LALLS) are installed. This system alllows us measurements of conventional GPC, copolymer analysis, functional and end group analysis and absolute MW determination. The outputs of each detector are recorded on a cassette type magnetic tape, which is processed later by a microcomputer.

First of all, a program is made to obtain a molecular weight distribution (MWD) curve in log MW unit as an abscissa. Since we are mainly concerned with oligomeric products, we used a calibration curve method rather than MW determination by LALLS. The procedures of the data processing is briefly shown in Table 1.

The original data tape, D1 on which three channels of data

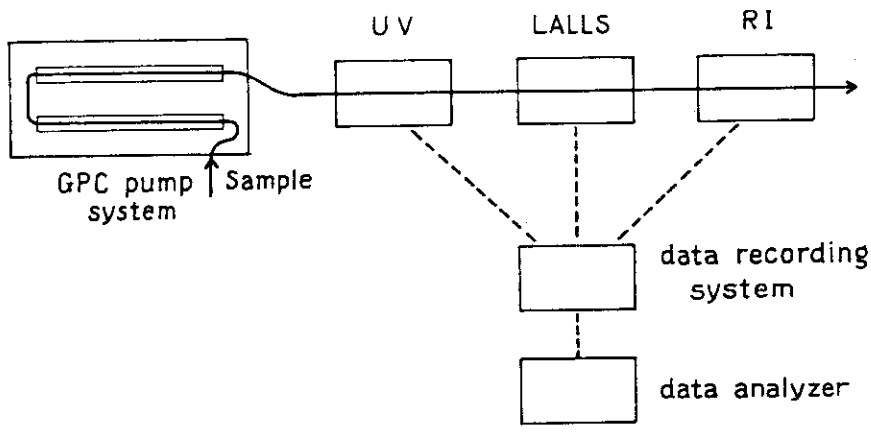

Fig. 1. Schematic illustration of the GPC system.

Table 1. Procedures of the Data Processing

Data tape	Program	Main operation
Original data D1		
	Program I	Binary → decimal MW calibration data MWD data (base line)
Second data D2		
	Program II	Approximation of MW calibration curve; MWD. and av. MW calc.; MWD output with comments
Final data D3		

are recorded in binomial code is treated by Program I. The data in some single channel, for example RI data, is converted into a decimal code, the peak positions of the standard polymers (usually monodisperse polystyrene) of known MW's are read in a unit of elution count and a base line is drawn for MWD data as shown in Fig. 2. These data for MW calibration and MWD data of the samples in study are recorded on D2 tape.

Then D2 tape is processed by Program II. First, the data for MW calibration (elution count-MW relationship) is displayed on a graphic display and the result is approximated with one of the three methods; polynomial function, a combination of linear-trinomial-linear functions and a set of linear functions simply connecting the successive data points. For the first two methods of approximation, a least-mean-square method is used. Therefore we obtain an MW calibration function as log

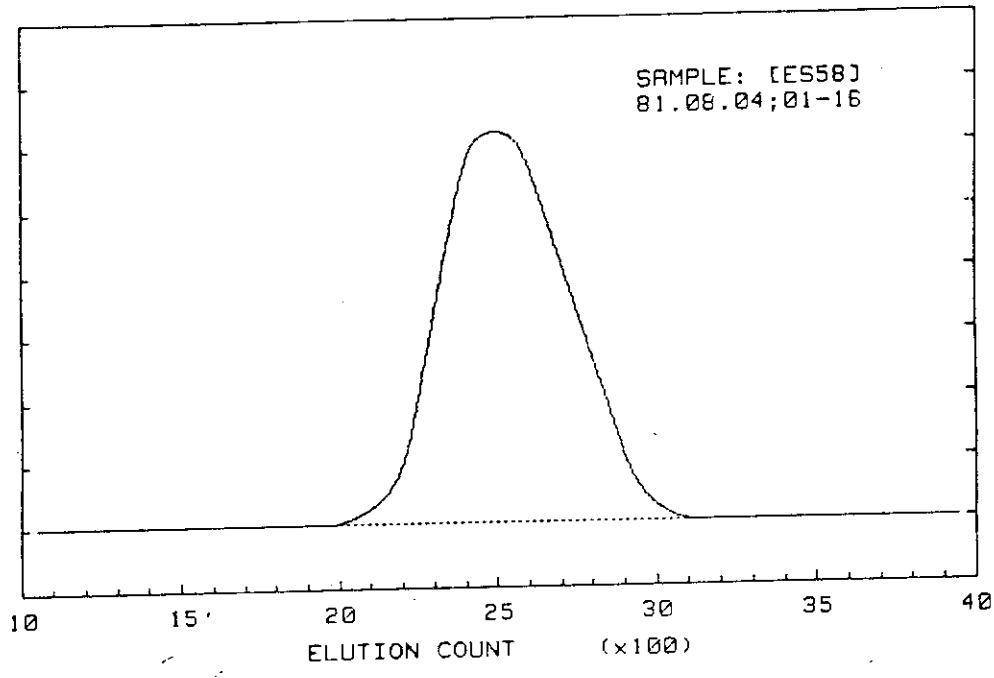

Fig. 2. MW-elution count relationship.

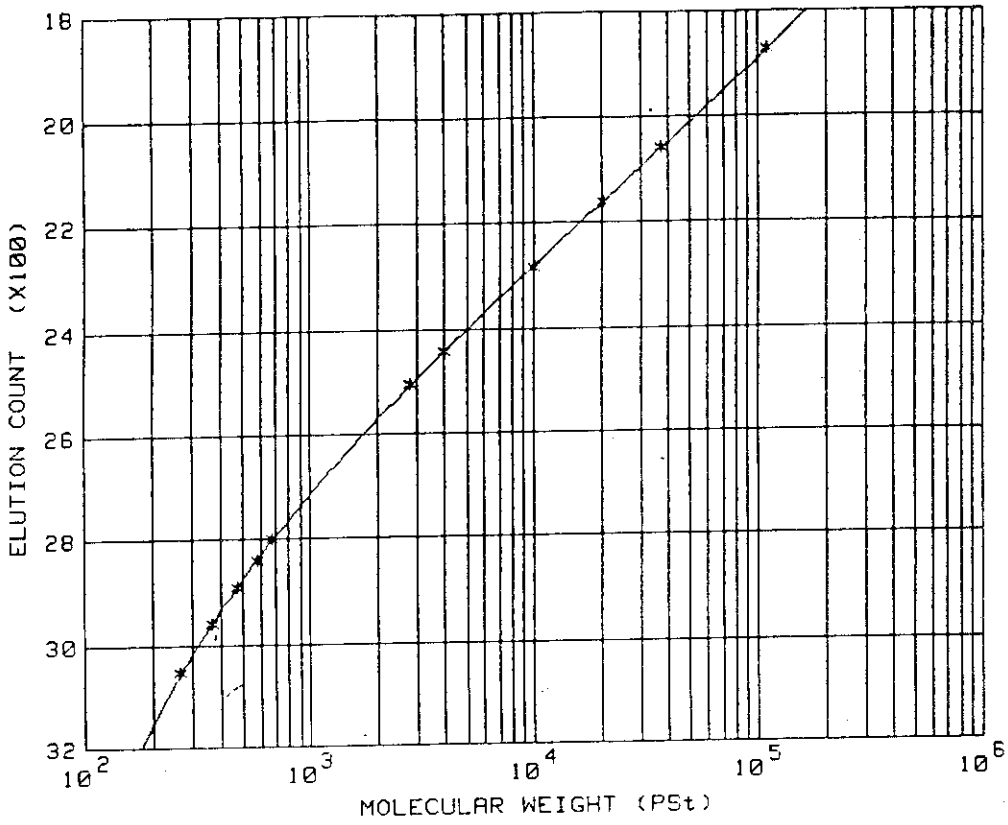

Fig. 3. MWD curve in elution count unit as an abscissa.

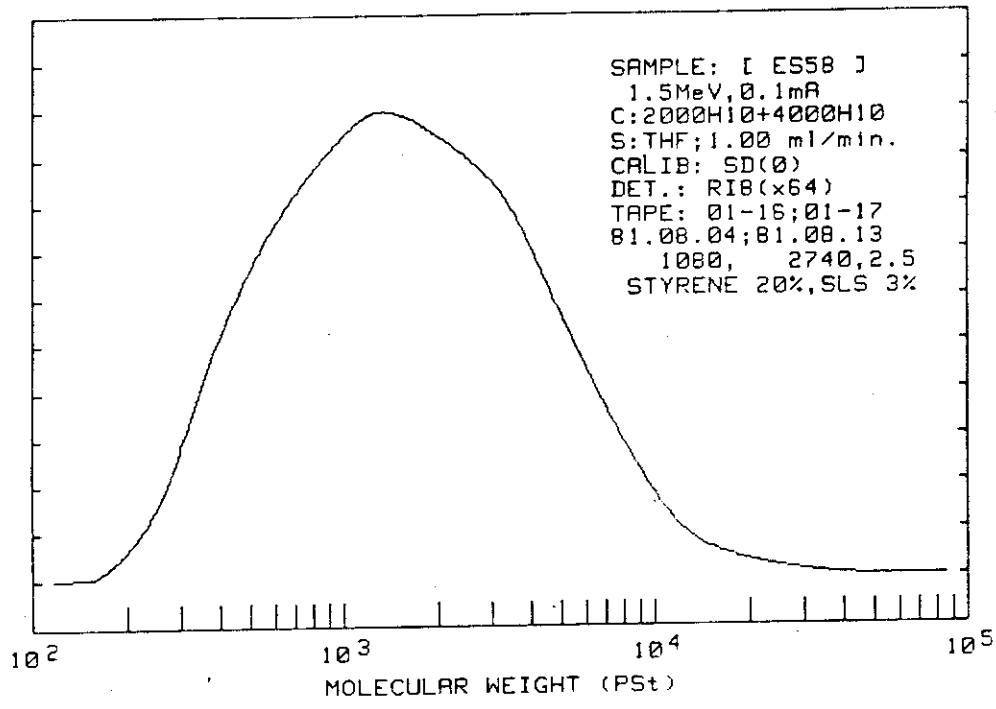

Fig. 4. MWD curve in log MW unit as an abscissa.

MW = f(el. ct.), as shown in Fig. 3. Next, the MWD in Fig. 2 is transformed into an MWD in log MW units as an abscissa. Here, the height of MWD in Fig. 2 at the elution count, ct_1 is converted into a height in new MWD (Fig. 4), $h'(MW_1)$ where $h'(MW_1) = a \cdot h(ct_1)/f'(ct_1)$ and $\log MW_1 = f(ct_1)$. (a: constant) Average MWs, $\bar{M}n$, $\bar{M}w$ and $\bar{M}w/\bar{M}n$ are also calculated. Then hard copy of MWD is obtained with several comments concerning the nature of the sample, instrumental- and data processing-conditions, dates of measurement and processing and MWs as shown in Fig. 4. All of these data including comments are recorded on D3 tape. In Fig. 3, MWD of polystyrene oligomer obtained in high dose rate emulsion polymerization is shown as an example. When MW-elution count is once known for a polymer other than polystyrene, for instance, polybutadiene, the MW calibration curve for polystyrene can be easily converted into that for polybutadiene and MWD of polybutadiene against log MW of polybutadiene as an abscissa is obtained.

The largest advantage of obtaining MWD in log MW unit is that the MWD is free from the fluctuation of elution count-MW relationship, which arises from the variation of pump speed, room temperature and aging of the gel columns. Therefore we can make a detailed comparison of MWDs which are measured on different day. Second advantage is an ease of keeping MWD. We can easily find any data in tapes D1 - D3 and reprocessing of these data is also probable.

(K. Hayashi)

[3] Modification of Polymers

1. Preparation of Cation-exchange Resin by Graft Copolymerization

It has been reported that polyvinyl chloride (PVC) powder grafted by acrylic acid showed a good cation-exchange property, especially its high rate of metal adsorption.[1,2] The correlation between the conditions of the graft copolymerization and the adsorption behavior of cupric ion was well explained by the results of microscopic observation of the dyed cross sections of the grafted particles.[2] High ion-exchange rate is obtained when grafted mainly onto the surface.

Introduction of sulfonyl groups onto a polymer by graft copolymerization is studied to obtain a cation-exchange resin of strong acid type, being useful in a wide pH range. Here, as a trunk polymer, poly(vinyl chloride, 83%, -vinyl acetate, 17%) copolymer is used expecting easier grafting than PVC.

Among three commercial vinyl compounds having a sulfonyl group, two sodium salts of vinyl sulfonic acid, and of p-styrene sulfonic acid and one free acid of 2-acrylamido-2-methylpropane sulfonic acid (AMPS), it was unsuccessful to obtain over 10% grafting in the first two monomers so far tried. The selection of swelling agent of the trunk polymer seems to be important in the present study since relative diffusion rates of monomer and inhibitor into the trunk polymer is controlled by the swelling state of the system for determining the site of graft reaction. Graft copolymerizations with AMPS in water-DMF, -THF, or -EDC mixture can not give high graft percentage while 10 - 20% grafting is obtained in water-acetone mixture. As an irradiation temperature, 35°C is found to be suitable since room temperature is too low for reaction, and 50°C, induces gelation. As an inhibitor of the homopolymer formation mainly in solution, cupric sulfonate is found to be much better than Mohr's salt.

At first, irradiation is made under static condition, i.e.,

without mixing. By static irradiation, however, graft yield never exceeds above 20% because of the difficulty of monomer diffusion at the later stage of the polymerization. Increase of the initial monomer concentration simply yields an increase of the amount of homopolymer. Then, a device is tried to irradiate the sealed ampoules under rotation. By this system of irradiation, as shown in Fig. 1, copolymerization at 0.4 g/ml AMPS concentration can be made without forming gel whereas by static irradiation, 0.1 g/ml is an optimum condition.

In Fig. 2, adsorption behavior of cupric ions by the grafted resin is shown in comparison with that by Amberlite

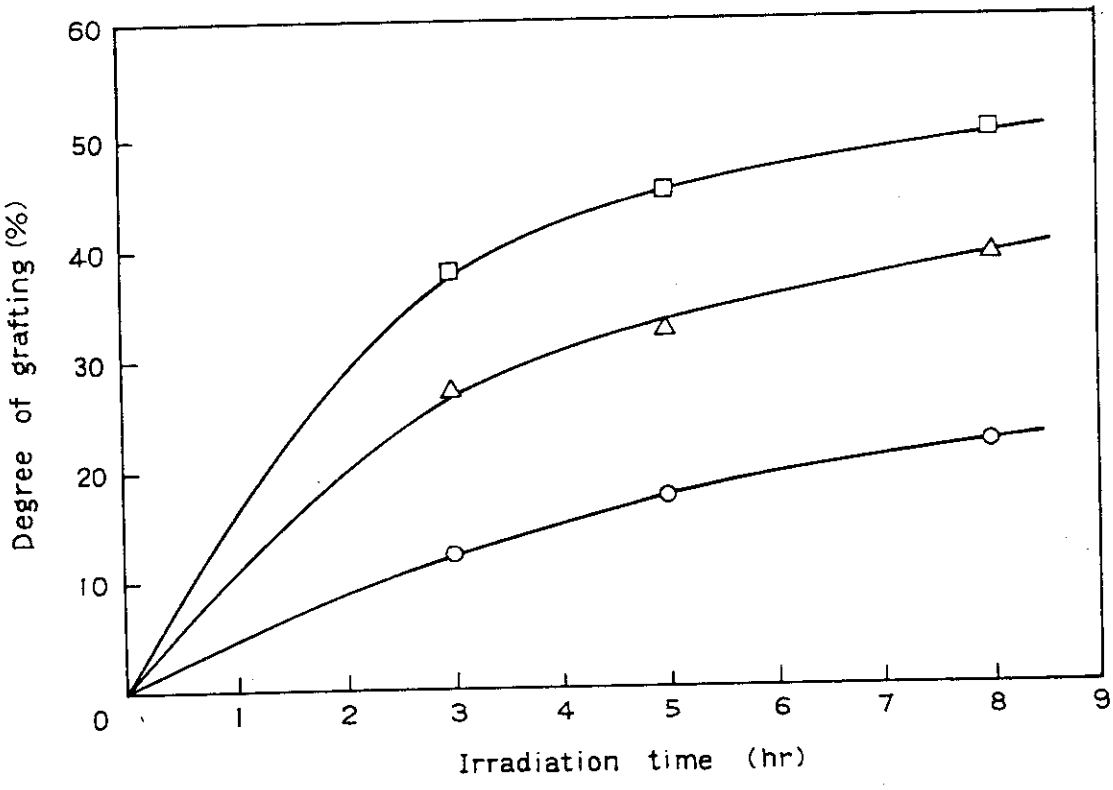

Fig. 1. Graft copolymerization of AMPS onto vinyl chloride-vinyl acetate copolymer at 35°C: Dose rate, 5 x 10^4 R/hr; H_2O/acetone = 3/7 in volume; $CuSO_4$, 0.01 wt% to water. AMPS concentrations are, 0.2 (○), 0.3 (△) and 0.4 (□) g/ml.

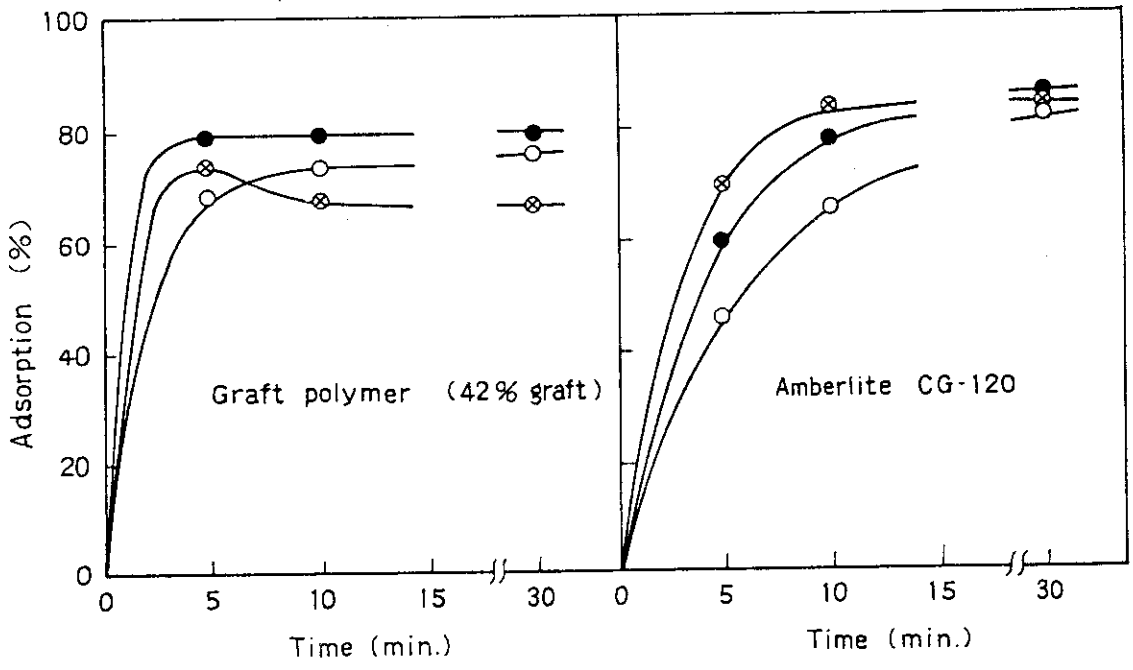

Fig. 2. Adsorption of cupric ion by the graft polymer (AMPS graft, 42%) and Amberlite CG-120 at various temperatures. $[Cu^{2+}]$ = 100 ppm; $[Cu^{2+}]/[SO_3H]$ = 1/2. Temperatures are ca. 0 (o), 25°C (●) and 50°C (⊗).

CG-120, a typical commercial cation-exchange resin of strong acid type. It is notable that the grafted resin adsorbs cupric ion much faster than Amberlite. A slight decrease of the amount of adsorption at 50°C is probably related to the softening of the grafted resin at this temperature. The resin of 50% graft adsorbs 1.5 meq/g of cupric ion, which is approximately a third of that by Amberlite. A study to obtain a grafted resin of high ion-exchange rate at the temperature higher than 50°C is now in progress.

(T. Yagi, K. Hayashi, and S. Okamura)

1) Y. Kusama and T. Yagi, JAERI-M, 8569, 117 (1979).
2) Y. Kusama and T. Yagi, JAERI-M, 9214, 125 (1980).

2. Radiation-Induced Grafting of Acrylic Acid onto High Density Polyethylene Filaments

We have been studying radiation-induced grafting of acrylic acid onto high density polyethylene filaments in order to improve the heat resistance and to impart flame retardance and hydrophilic properties. As shown in the previous report, large grafting percent was obtained by mutual irradiation method when the grafting was performed at elevated temperature, whereas the rate of grafting was very slow at room temperature. The graft filaments obtained by such a method exhibited high heat-shrinkage temperature, flame-retardance and hydrophilic properties. These properties were further improved by converting the graft filaments to metallic salt. The mechanical properties of these filaments at high temperatures, however, were not sufficiently improved.

In the present study we attempted mainly to improve the mechanical properties at high temperatures as well as the other properties by combining grafting and crosslinking. For this purpose the polyethylene filaments were pre-irradiated by electron beams since a large dose was necessary to crosslink polyethylene. Subsequently those filaments were grafted using the remaining trapped radicals, peroxides and/or hydroperoxides.

High density polyethylene filaments of 337d were pre-irradiated in nitrogen gas or in air with electron beams from v.d.G. accelerator at a dose rate of 1.8×10^5 rad/sec at room temperature. Grafting was carried out in a mixture of acrylic acid-water-ethylene dichloride, using Mohr's salt as an inhibitor of homopolymerization of acrylic acid outside the filaments.

The effect of reaction temperature on the rate of grafting was the same as that in the case of grafting by mutual irradiation method reported previously. Namely the rate of grafting was very low at room temperature, while the large graft percent was easily obtained at higher temperatures. No effect of oxygen on the grafting was observed in this experiment, whereas when pre-irradiation was carried out with γ-rays at a dose rate

of 1.5 x 10^5 rad/h, the effect of oxygen on the grafting was observed. This may be related to the time for the diffusion of oxygen. The effect of the total dose was also investigated. The graft percent increased linearly with increasing total dose up to 5 Mrad, above which it levelled off.

Heat-shrinkage: The heat-shrinkage of the acrylic acid graft polyethylene filament was measured up to 300°C under a small load of 0.01 g/d. The results are shown in Fig. 1. The

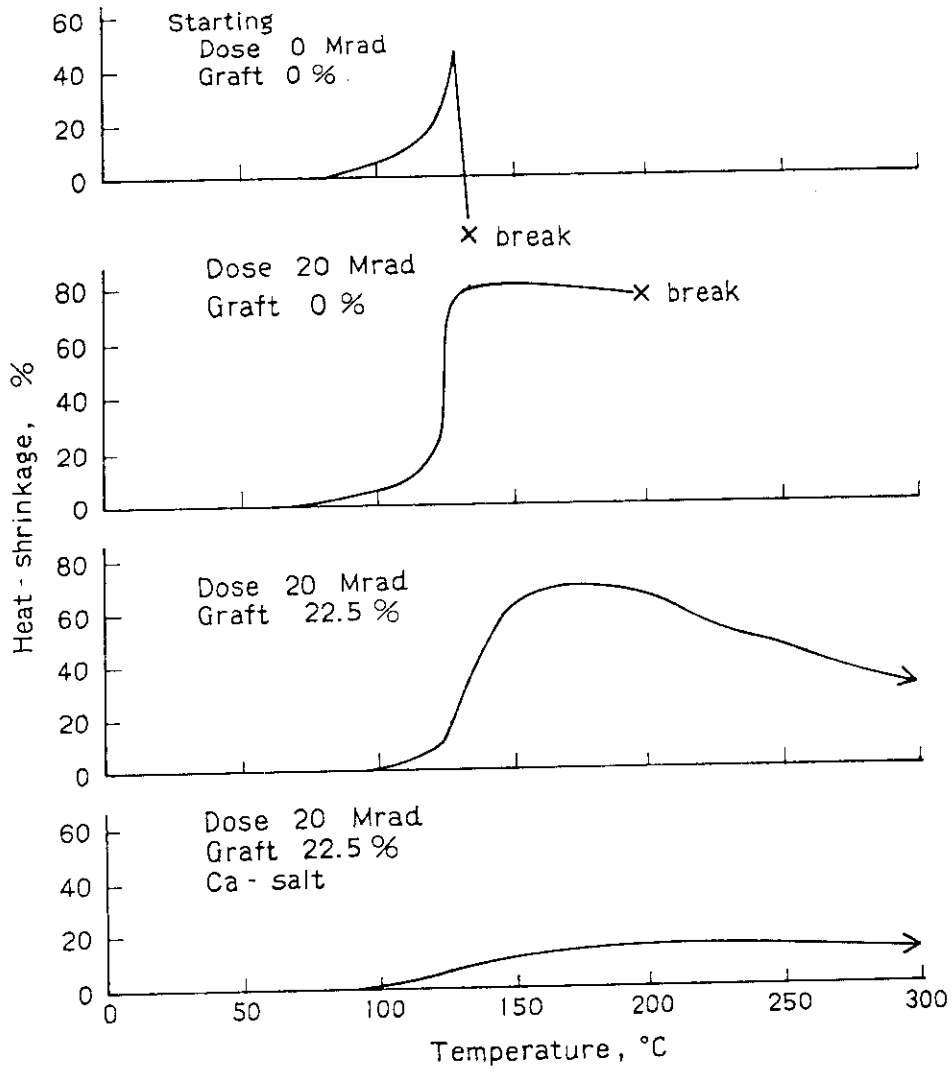

Fig. 1. Heat shrinkage of acrylic acid graft polyethylene filaments prepared by pre-irradiation method.

starting polyethylene begins to shrink at 70°C, reaches a maximum shrinkage of 50% at 130°C, and breaks at 137°C. The crosslinked filament, which was obtained by irradiation of electron beams of a total dose of 20 Mrad at a dose rate of 0.18 Mrad/sec in nitrogen gas, breaks at 200°C, though the maximum shrinkage reaches 80%. For the filaments irradiated at dosages ranging from 10 to 30 Mrad in nitrogen gas or in air, similar heat-shrinkage curves were obtained. The filament of 23% graft, obtained by pre-irradiation of 20 Mrad in nitrogen gas, does not break even at 300°C, though it shows still a rather large shrinkage of 70%. As already reported, ca. 50% graft was necessary to obtain such an effect only by grafting. Fig. 1 d shows the heat-shrinkage for the calcium salt of the above 23% graft filament. The heat shrinkage is less than 15% and it keeps its filament form even above 300°C.

Mechanical properties: The tensile strength of high density polyethylene filament decreases remarkably with increasing temperature from room temperature to the melting point. This behavior was not sufficiently improved by grafting of acrylic acid and its conversion to metallic salts, though the graft filament showed some tensile strength even above the melting point of the starting polyethylene.

The effect of crosslinking by electron beams was, therefore examined. Though the strength at room temperature slightly decreased with increasing total dose of irradiation, on the contrary the strength at 100°C increased. Fig. 2 shows temperature dependence of strength of the starting, 30 Mrad irradiated and subsequently grafted filaments. The strength of 30 Mrad irradiated filament decreases more gradually with temperature than that of the starting filament and the strength at 100°C is about 0.8 kg. The strength of the 35% acrylic acid graft filament is at any temperature higher than that of the irradiated filament. The conversion of this graft filament to calcium salt changes the strength only a little. The strength of the calcium salt of the 35% acrylic acid graft polyethylene filament is about 1 kg, corresponding to more than 2 g/d in

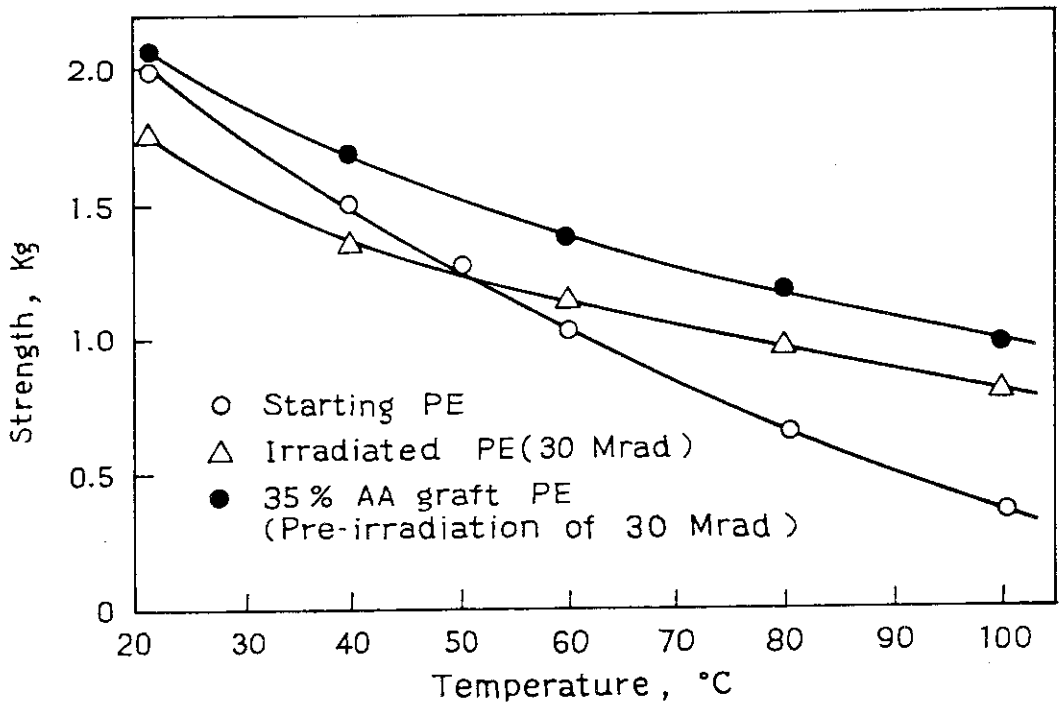

Fig. 2. Temperature dependence of strength for acrylic acid graft polyethylene filament prepared by pre-irradiation method.

tenacity, since this graft filament is 490d. This value is enough to use as apparel.

As above described, the tensile strength of polyethylene filament at elevated temperatures as well as heat resistance, flame retardance, and hydrophilic properties could be improved by combining radiation crosslinking and grafting.

(K. Kaji and T. Okada)

[4] Studies on Radiation Dosimetry

1. Light Emission from Argon Containing Small Amounts of N_2 and H_2O by Electron Beam Irradiation

In the study[1-2] on W value and energy transfer of binary mixture of argon and ethane under electron beam irradiation, emissions from $OH(A^2\Sigma^+)$ and $N_2(C^3\Pi_u \rightarrow B^3\Pi_g)$ always appeared in the spectrum of Ar due to a trace of H_2O and N_2 contained in argon gas. Studies were carried out this year in an attempt to elucidate the reactions involving Ar and these impurities. A combination of a new reaction chamber and a grating spectrometer manufactured by Murata Optical Instrument Co., Ltd. with a photomultiplier used in the experiments is schematically shown in Fig. 1. The reaction chamber is of 4.5 ℓ volume made of stainless steel, having an irradiation window (100 μm thickness aluminium) through which the electron beam penetrated into the vessel. The optical emission was introduced into the monochrometer which gives higher resolution than that (Shimadzu GF-16R) used last year and the grafting of the spectrometer oscillated automatically to allow display of the emission spectrum on an x-y recorder at a scanning rate from 20 to 400 nm/min. The irradiation was carried out using an electron beam of 15 μA and 0.6 MeV from a VdG electron accelerator.

Argon gas was obtained from Takachiho Chemicals Co., (Zero U Grade, estimated impurities: $N_2 \sim 5$ ppm, $H_2O \sim 5$ ppm) and used as received or after purification by passing an active carbon trap at -196°C or a P_2O_5 trap at room temperature.

Figure 2 a shows a typical emission spectrum of Ar obtained at 1 atm., where a broad peak from Ar_2^* and sharp peaks due to $OH(A^2\Sigma^+ \rightarrow X^2\Pi_i)$ and $N_2(C^3\Pi_u \rightarrow B^3\Pi_g)$, respectively. The emissions of the latter two were difficult to eliminate even after purification of Ar by passing it through active carbon trap cooled at -196°C, or by drying it over phosphor pentoxide. The intensity of the emission due to $OH(A^2\Sigma^+ \rightarrow X^2\Pi_i)$ decreased as the irradiation continues, while the intensities of the emission due to $N_2(C^3\Pi_u)$ remained constant during the irradiation (Fig. 2 b and

c). This result indicates that $OH(A^2\Sigma^+)$ is produced by irradiation from H_2O and H_2O is consumed by the irradiation, while $N_2(C^3\Pi_u)$ regenerates N_2 molecule after deexcitation from the $N_2(C^3\Pi_u)$ state with emission.

Figure 3 a through f show the emission spectra of argon gas immediately after the initiation of irradiation at different gas pressures. The intensities of the peaks due to Ar_2^* and $OH(A^2\Sigma^+)$ increase with increasing gas pressure, while the emission intensity due to $N_2(C^3\Pi_u)$ increases with increasing pressure up to 200 Torr, and then decreases when the gas pressure increases further.

These changes of the emission intensities are more quantitatively shown in Figs. 4 and 5. As may be seen in Fig. 4, the emission intensity of Ar_2^* is proportional to the 2.4th power of gas pressure, indicating that a ter-molecular reaction may partly contribute to the formation of Ar_2^* in addition to the

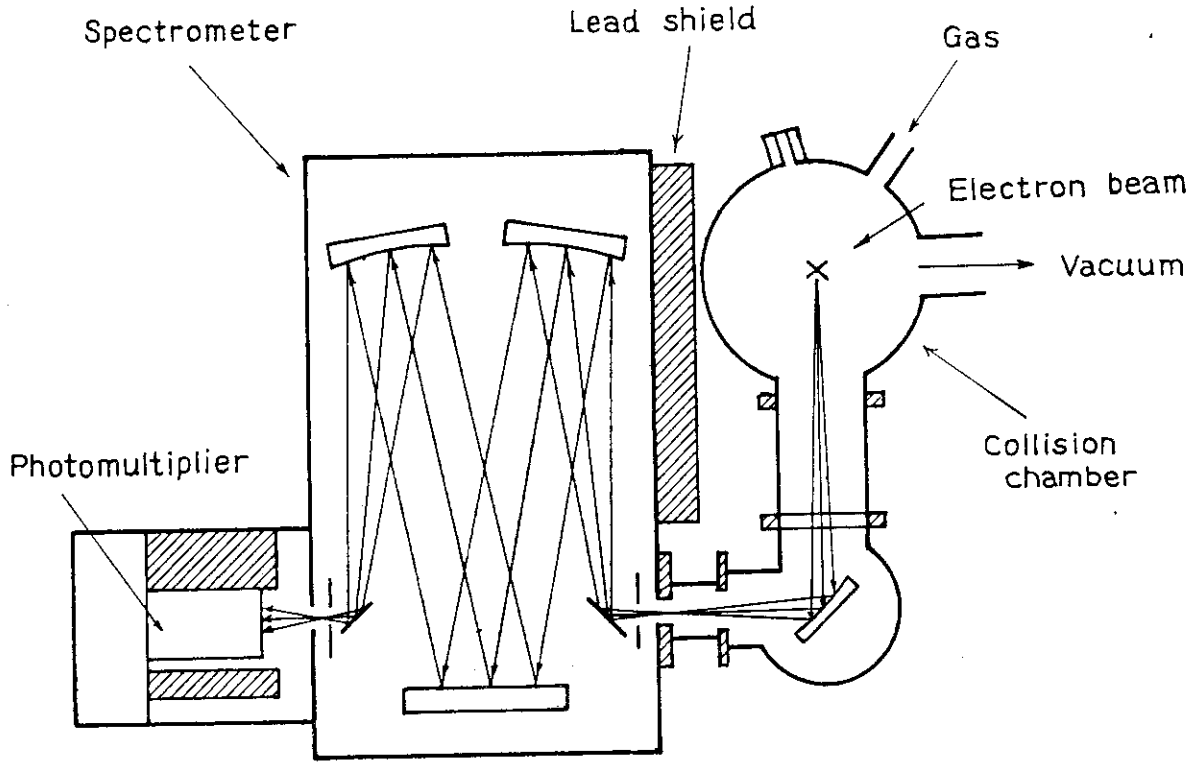

Fig. 1. Optical system and reaction chamber.

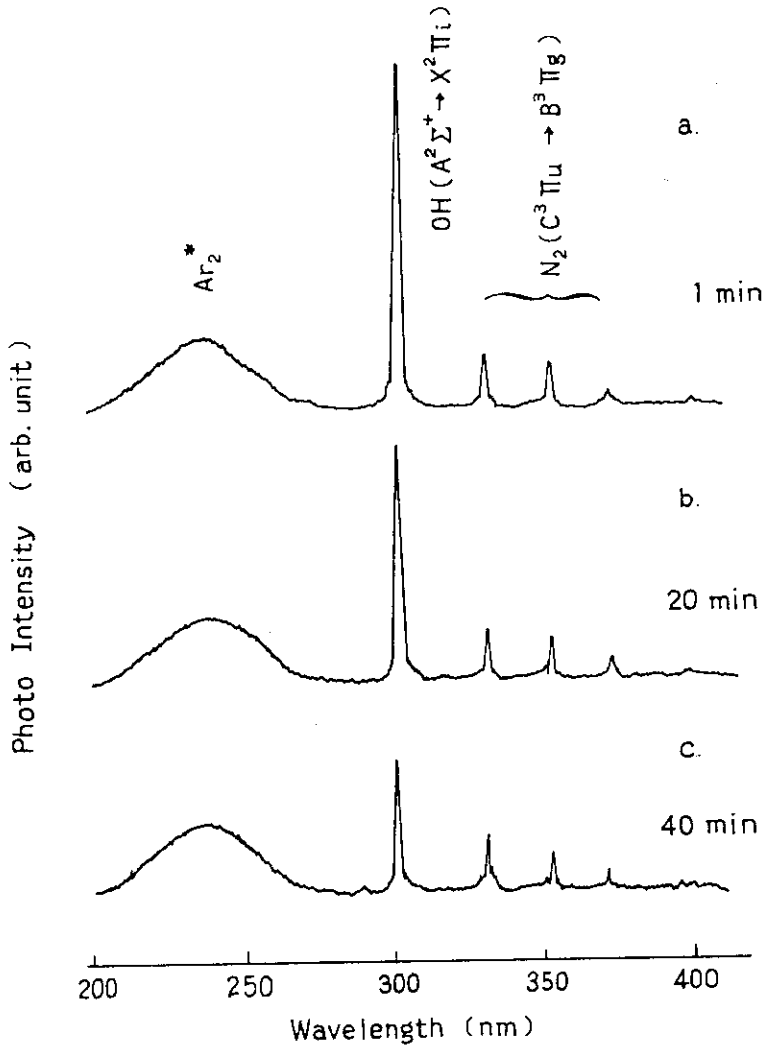

Fig. 2. Change of optical emission spectrum of argon containing trace amounts of N_2 and H_2O during irradiation: Electron energy, 0.6 MeV; Beam current, 15 μA.

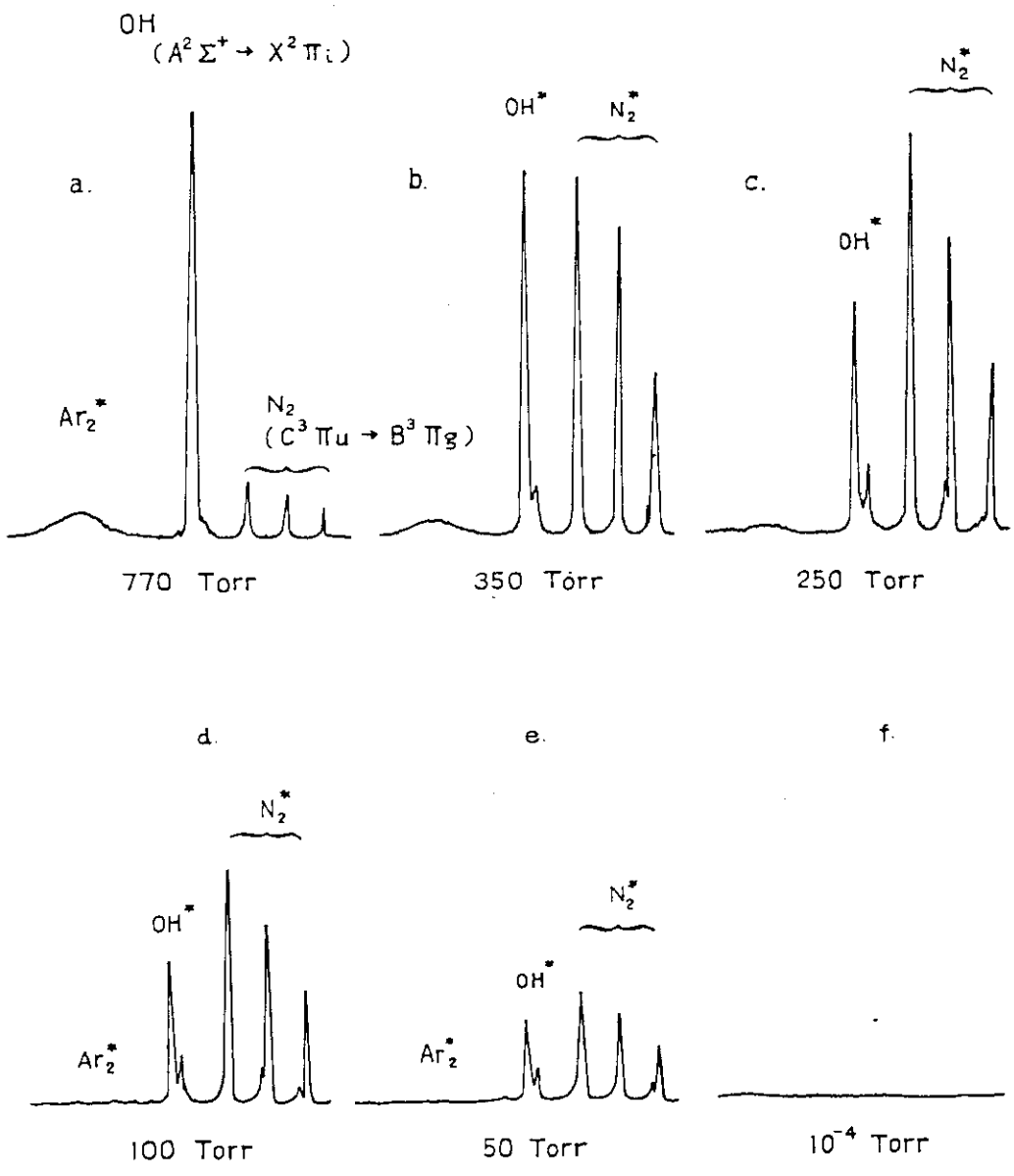

Fig. 3. Optical emission spectra of argon during irradiation at different pressures: Electron energy, 0.6 MeV; Beam current, 15 μA; Ar, 770 Torr; H_2O, 5 ppm; N_2, 5 ppm.

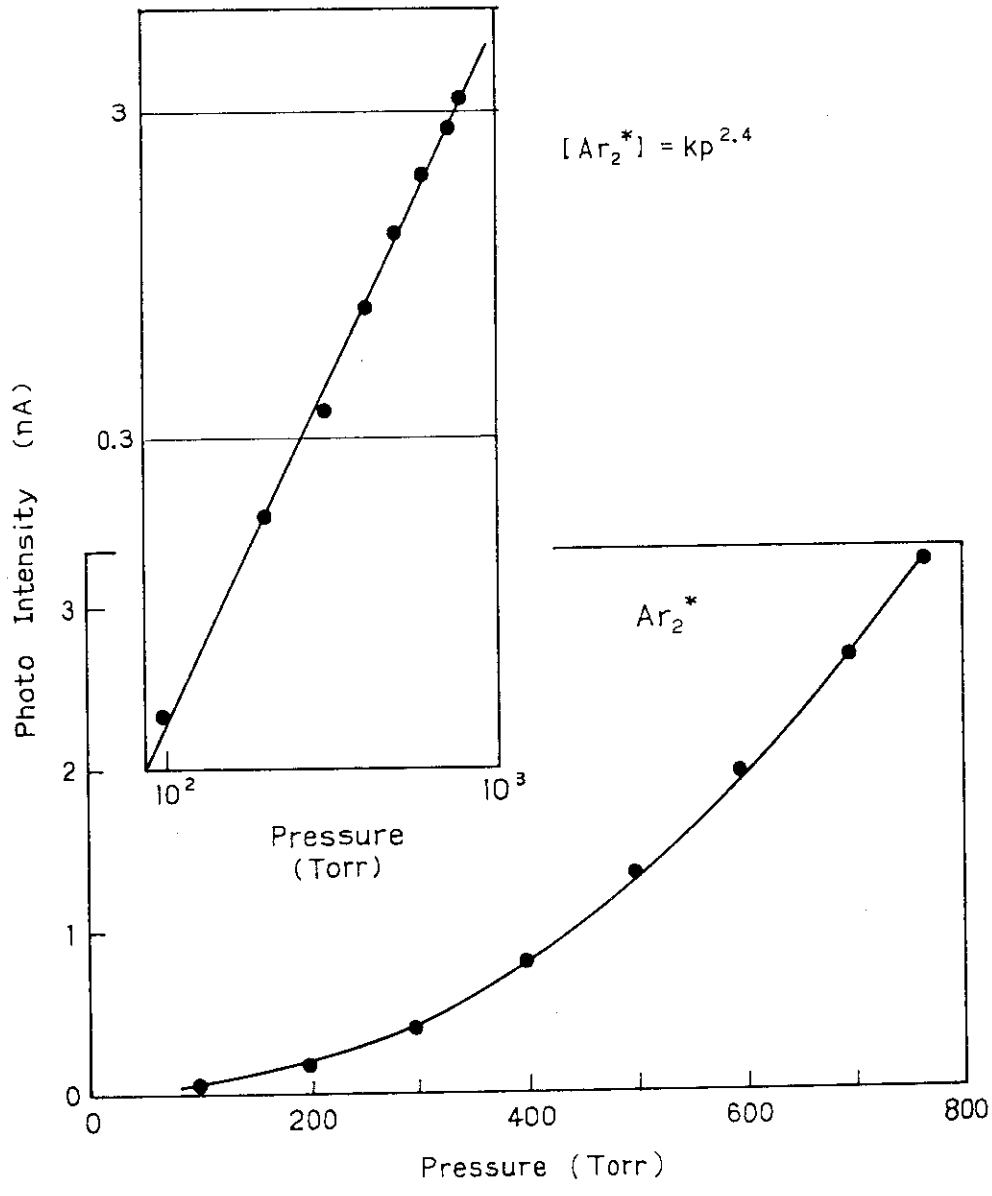

Fig. 4. Emission intensity of Ar_2^* as a function of pressure.

bimolecular reaction suggested in the earlier reports[1,2].

The pressure dependence of emission intensities of $OH(A^2\Sigma^+)$ and $N_2(C^3\Pi_u)$ are complicated as shown in Fig. 5.

The reaction scheme shown in Table 1 is tentatively assumed for the explanation of the pressure dependence of $N_2(C^3\Pi_u)$ emission. No interference seems to occur between N_2^* and OH^*, because the concentrations of these species are quite low. Assuming the steady state of reactive intermediates,

$$\frac{d[N_2]}{dt} = k_4[N_2][Ar^*] + k_1[N_2] - k_5[N_2^*][Ar] - k_6[N_2^*] \quad (1)$$
$$= 0$$

$$\frac{d[Ar^*]}{dt} = k_2[Ar] - k_3[Ar^*][Ar]^2 - k_4[Ar^*][N_2] \quad (2)$$
$$= 0$$

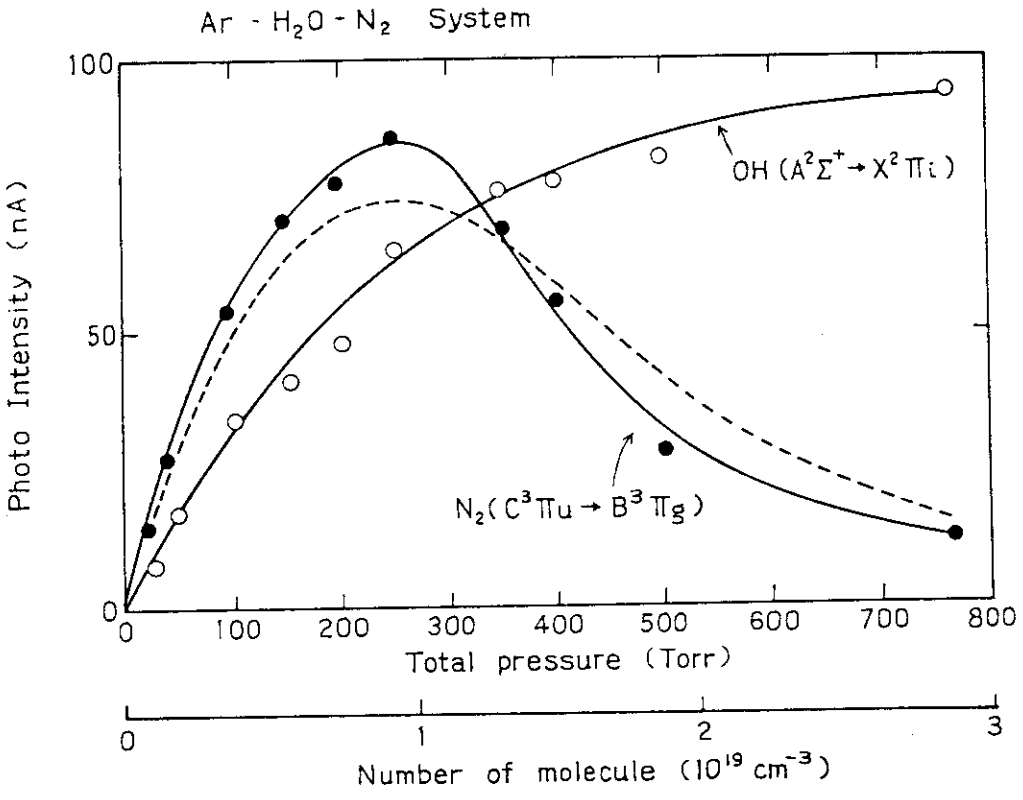

Fig. 5. Emission intensities of $N_2(C \rightarrow B)$ and $OH(A \rightarrow X)$ as a function of pressure.

the steady state concentration of $N_2(C^3\Pi_u)$ can be written as

$$[N_2(C^3\Pi_u)] = \frac{\frac{[N_2]}{[Ar]}}{k_5 + \frac{k_6}{[Ar]}} \left\{ \frac{k_2 k_4}{k_3[Ar] + k_4 \frac{[N_2]}{[Ar]}} + k_1 \right\} \quad (3)$$

where $[N_2]/[Ar] \simeq 5 \times 10^{-6}$. Using the rate constants reported for the reactions involving N_2^* and Ar^* in the electron irradiation studies on binary mixtures of Ar and N_2, the steady state concentration of $N_2(C^3\Pi_u)$ are calculated as a function of gas pressure, the unknown values being as parameters. The best fitted curve obtained after trial calculations is shown by a broken line in Fig. 5.

In an attempt to elucidate the reactions of H_2O, the emission spectra were recorded for the gas containing different amounts of H_2O. The spectrum change upon addition of H_2O is shown in Fig. 6 where the emission intensity of $OH(A^2\Sigma^+)$

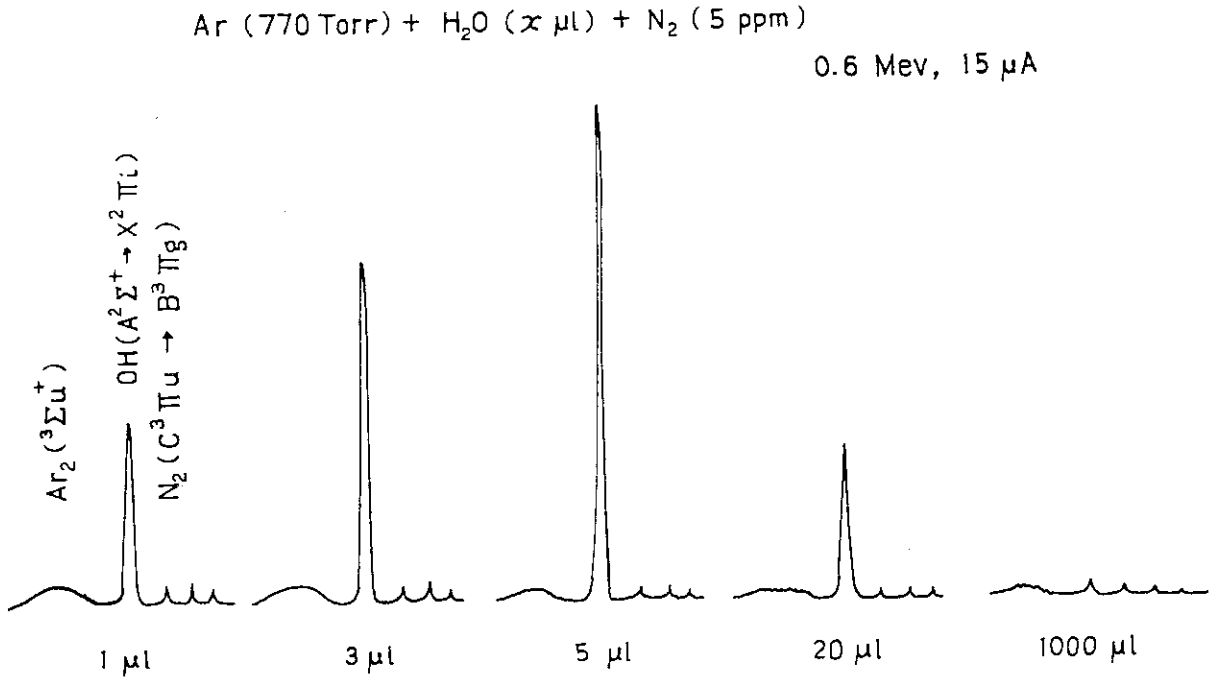

Fig. 6. Effect of amount of water added to the system on optical emission spectrum.

Table 1. The Reaction Scheme Involving $N_2(C^3\Pi u)$ in Ar-N_2-H_2O under Electron Irradiation

Reaction		Rate const.		References
N_2	$N_2(C^3\Pi u)$	k_1		This work
Ar	$Ar[^3P_{0,2}]$	k_2		This work
$Ar[^3P_{0,2}] + 2Ar$	$Ar_2(^3\Sigma u^+) + Ar$	k_3	6×10^{-33}	J. LeCalvé, et al. ('73)
$Ar[^3P_{0,2}] + N_2$	$N_2(C^3\Pi u) + Ar$	k_4	6×10^{-12}	S.K. Searles, et al. ('76)
$N_2(C^3\Pi u) + Ar$	$N_2 + Ar$	k_5	3×10^{-13}	D.W. Setser, et al. ('73)
$N_2(C^3\Pi u)$	$N_2 + h\nu$	k_6	2.5×10^{7}	A.W. Johnson, et al. ('70)

Table 2. The Reaction Scheme Involving OH(AΣ) in Ar-N_2-H_2O System under Electron Impact

Reaction		Rate const.		References
H_2O	OH* + H	k_1		
Ar	Ar*	k_2		
Ar* + 2Ar	Ar_2* + Ar	k_3		
Ar* + H_2O	OH* + H + Ar	k_4	7.5×10^{-11}	O. J. Dunn, et al. ('75)
Ar_2* + H_2O	OH* + H + 2Ar	k_5		
OH* + Ar	OH + Ar	k_6		
OH*	OH + hν	k_7		
Ar_2*	2Ar + hν	k_8		

changes considerably, while little change is observed for the emission intensities due to $N_2(C^3\Pi_u)$. The result supports the previous assumption that there is no interference between H_2O and N_2 or any related species produced from H_2O and N_2.

The reactions leading to the formation and decay of $OH(A^2\Sigma^+)$ are summarized in Table 2. The steady state assumption on the reactive intermediates gives eq. (4) for a steady concentration of $OH(A^2\Sigma^+)$ as a function of pressure.

$$[OH^*] = \frac{a}{b + \frac{c}{P}} \left[d + \frac{e}{fP + g} + \frac{h}{i + \frac{j+k}{P} + \frac{\ell}{P^2}} \right] \qquad (4)$$

where $[Ar] = P$, $\frac{[H_2O]}{[Ar]} = C$

$a = C$	$e = k_2k_4$	$i = k_3k_5C$
$b = k_6$	$f = k_3$	$j = k_3k_8$
$c = k_7$	$g = k_4C$	$k = k_4k_5C$
$d = k_1$	$h = k_2k_3k_5$	$\ell = k_4k_8C$

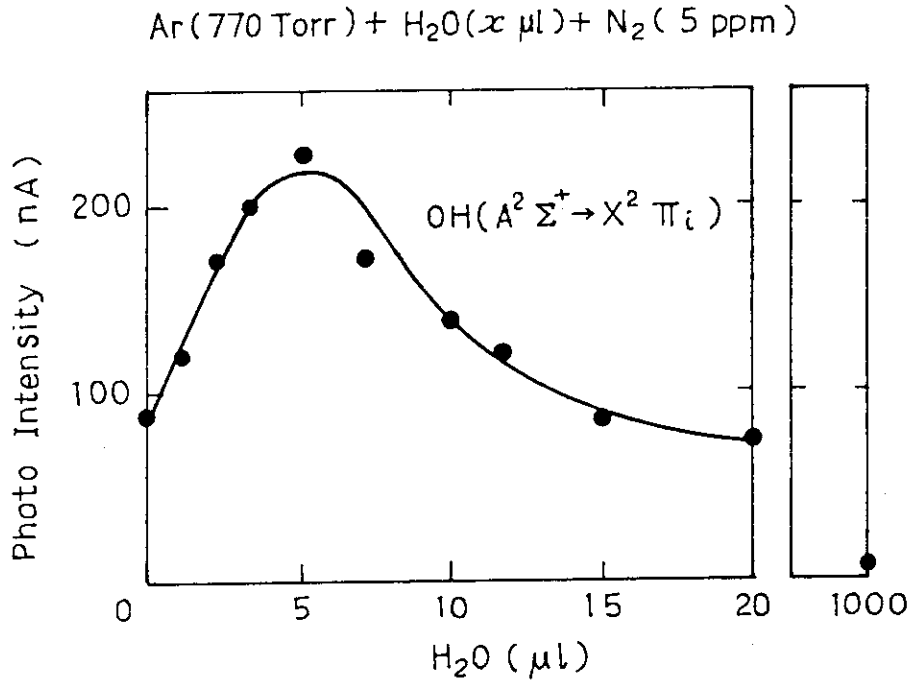

Fig. 7. Emission intensity of $OH(A \rightarrow X)$ band as a function of H_2O concentration in the system.

Since $[OH(A^2\Sigma^+)]$ of eq. (4) becomes zero at P = 0 and k_2/k_6 ($k_1 \simeq 0$), respectively, the curve of $[OH^*]$ as a function of pressure in Fig. 5 agrees qualitatively with eq. (4), but unfortunately little data was reported in the literature concerning the rate constants of these reactions and therefore detailed examination of the reactions involving OH remains as a future study.

(K. Matsuda)

1) K. Matsuda, JAERI-M 9214, 137 (1980).
2) K. Matsuda and T. Takagaki, Int. J. Appl. Rad. Isotopes, 32, 233 (1981).

III. LIST OF PUBLICATIONS

[1] Published Papers

1. H. Arai, S. Nagai, K. Matsuda, and M. Hatada, "Effect of Irradiation Temperature on Radiolysis of Methane", Radiat. Phys. Chem., 17, 151 (1981).

2. K. Matsuda and T. Takagaki, "W Value and Energy Transfer of Argon-Ethane Gas Mixtures", Int. J. Appl. Radiat. and Isotopes, 32, 233 (1981).

3. K. Hayashi, M. Tachibana, and S. Okamura, "Cyclization and Crosslinking of Polybutadiene in Solution by Electron Beam Irradiation", J. Polym. Sci., Polym. Chem., Ed., 18, 2785 (1980).

4. K. Hayashi, M. Tachibana, and S. Okamura, "Radiation-Induced Polymerization at High Dose Rate. IV. Chloroprene in Bulk", J. Polym. Sci., Polym. Chem. Ed., 18, 3297 (1980).

5. K. Hayashi, M. Tachibana, and S. Okamura, "Radiation-Induced Polymerization at High Dose Rate. III. Isoprene in Bulk", J. Polym. Sci., Polym. Chem., Ed., 18, 3381 (1980).

6. H. Iwata and Y. Ikada, "Interpretation of Rates of Polymer-Polymer Reactions in Terms of Statistical Thermodynamics of Dilute Polymer Solutions", Makromol. Chem., 181, 517 (1980).

7. W. Taki, H. Handa, S. Yamagata, M. Ishikawa, H. Iwata, and Y. Ikada, "Radiopaque Solidifying Liquids for Releasable Balloon: A Technical Note", Surgical Neurology, 13, (No. 2) 140 (1980).

8. T. Matsunaga and Y. Ikada, "Surface Modifications of Cellulose and Polyvinyl Alcohol and Determination of the Surface Density of the Hydroxyl Group", ACS Symposium Series, 121, 391 (1980).

9. Y. Ikada, M. Suzuki, and H. Iwata, "Water in Mucopolysaccharides", ACS Symposium Series, 127, 287 (1980).

10. Y. Ikada, H. Iwata, S. Nagaoka, F. Horii, and M. Hatada, "Mono-layers of Graft and Block Copolymers", J. Macromol. Sci.-Phys., B 17, (2) 191 (1980).

* * * * *

11. T. Okada, "Radiation-Induced Polymerization of Monomers at High Dose Rates", in Present Status and Future Scope High Dose Rate Effects of Radiation, S. Okabe (ed), Atomic Energy Society of Japan (1980).

12. I. Sakurada, T. Okada, and K. kaji, "Method for Manufacturing Heat-Resistant and Flame-Retardant Synthetic Fiber", U.S. Pat., 4,212,649 (1981).

[2] Oral Presentations

1. S. Sugimoto and M. Nishii, "Effects of Gas Composition and Pressure on the G values of the Products in Electron Irradiation of Circulated CO-H_2 Mixture", The 41st Annual Meeting of Chemical Society of Japan, Apr. 3, 1980.

2. S. Sugimoto and M. Nishii, "Synthesis of Simple Organic Compounds from CO-H_2 Mixture by Electron Irradiation", The 42nd Annual Meeting of Chemical Society of Japan, Sep. 17, 1980.

3. M. Nishii and S. Sugimoto, "Irradiation Technique for Circulating CO-H_2 Mixture at Elevated Pressure", The 23rd Discussion Meeting on Radiation Chemistry, Oct. 3, 1980.

4. S. Nagai, H. Arai, and M. Hatada, "Effect of Silica Gel on Radiation-Induced Reaction of CO-H_2 Mixture", The 23rd Discussion Meeting on Radiation Chemistry, Oct. 3, 1980.

5. S. Nagai, H. Arai, and M. Hatada, "Radiation-Induced Reaction of CO-H_2 Gas Mixtures over Various Solid Catalysts", The 3rd International Meeting on Radiation Processing, Oct. 28, 1980.

6. H. Arai, S. Nagai, K. Matsuda, and M. Hatada, "Radiation-Induced Reaction of CO-CH_4 Mixture —— Formation of Organic Acids", The 23rd Discussion Meeting on Radiation Chemistry, Oct. 3, 1980.

7. H. Arai and H. Hotta, "Effects of Addition of Gases on Interaction between Rare Gases and Pulsed Electrons", The 23rd Discussion Meeting on Radiation Chemistry, Oct. 3, 1980.

8. H. Arai and H. Hotta, "Numerical Analysis of Pulsed Electron Beam-Induced Ionization of Argon and the Effect of Gaseous Additives", The 4th Symposium on Swarm, Oct. 17, 1981.

9. K. Hayashi and S. Okamura, "Emulsion Polymerization of Styrene by Electron Beams", The 1st Polymer Microsphere Symposium, Nov. 1, 1980.

10. K. Hayashi, K. Kagawa, and S. Okamura, "Polymerization of Butadiene in n-Hexane Solution", The 29th Annual Meeting of the Polymer Society, Japan, May 28, 1981.

11. K. Hayashi, K. Kagawa, and S. Okamura, "Polymerization of Butadiene in n-Hexane Solution", The 23rd Discussion Meeting on Radiation Chemistry, Oct. 4, 1981.

12. K. Hayashi and S. Okamura, "Polymerization of Vinyl and Diene Monomers by Electron Beams", The 3rd International

Meeting on Radiation Processing, Oct. 30, 1980.

13. J. Takezaki, T. Okada, and I. Sakurada, "Radiation-Induced Polymerization of Styrene in Amine", The 3rd International Meeting on Radiation Processing, Oct. 30, 1981.

14. K. Kaji and T. Okada, "Properties of Acrylic Acid Graft High Density Polyethylene Filament", Annual Meeting of the Society of Fiber Science and Technology, Jun. 17, 1980.

15. K. Kaji, S. Hyon, and R. Kitamaru, "Graft Copolymerization and Molecular Mobility in the Non-crystalline Components of High Density Polyethylene Filament", Annual Meeting of the Society of Fiber Science and Technology, Jun. 17, 1981.

16. K. Kaji, T. Okada, and I. Sakurada, "Radiation-Induced Grafting of Acrylic Acid onto Polyethylene Filaments", The 3rd International Meeting on Radiation Processing, Oct. 27, 1980.

17. Y. Ikada, M. Suzuki, M. Taniguchi, H. Iwata, W. Taki, H. Miyake, Y. Yonekawa, and H. Handa, "Interaction of Blood with Radiation-grafted Materials", The 3rd International Meeting on Radiation Processing, Oct. 26-31, 1980.

18. Y. Ikada, T. Mita, H. Iwata, and S. Nagaoka, "Synthesis of Polymers with Terminal Functional Groups by Radiation Polymerization", The 3rd International Meeting on Radiation Processing, Oct. 26-31, 1980.

19. Y. Ikada, H. Iwata, M. Taniguchi, M. Suzuki, and F. Horii, "Effect of Surface Structure on Thromboresistance", The 29th Polymer Discussion Meeting, Oct. 14-16, 1980.

* * * * *

20. S. Okamura, "Advances in Applied Radiation Chemistry", The 3rd International Meeting on Radiation Processing, Oct. 26, 1980.

IV. EXTERNAL RELATIONS

During the fiscal year 1980, the laboratory welcomed oversea visitors listed below:

Prof. Ma Zue-Teh	Shanghai University of Science and Technology, China
Prof. Feng Yong-Kiang	Shanghai University of Science and Technology, China
Dr. Lu Wen-Yi	Shanghai University of Science and Technology, China
Dr. L. Chia	University of Singapore, Singapore
Dr. G. Ellinghorst	Institute für Physikalische Chemie, Germany
Dr. H. Christensen	Studsvik Energiteknik AB, Sweden
Mr. A. Miller	Risø National Laboratory, Denmark
Mr. E. Svendsen	Raychem Herstedoester, Denmark

The laboratory also welcomed trainees from industrial companies for 2 week training course on pure and applied radiation chemistry from Oct. 7 through Oct. 23.

At the laboratory seminar, the following lectures were made by two guest speakers:

"Tacticity of polymers as studied by NMR spectroscopy" by Prof. K. Hatada of Osaka University

"Catalytic activities of polymer complexes" by Prof. A. Nakamura of Osaka University

Prof. I. Sakurada was elected as an honorable chairman of the 3rd International Meetings on Applied Radiation Processes held at Tokyo on Oct. 26 - 31, 1980, where he was awarded the silver plate for his distinguished contribution to radiation and polymer chemistry.

Prof. S. Okamura presented an invited paper "Advances in Applied Radiation Chemistry" at the 3rd International Meeting on Radiation Processing.

Mrs. K. Kaji was the winner of the Sobue Memorial Award from the Society of Fiber Science and Technology of Japan for her outstanding contribution to the modification of synthetic fiber by radiation-induced grafting.

V. LIST OF SCIENTISTS

(Mar. 31, 1981)

[1] Staff Members

Yunosuke OSHIMA	Dr., radiation physicist, Head
Ichiro SAKURADA	Professor emeritus, Kyoto University, Ex-head
Seizo OKAMURA	Professor emeritus, Kyoto University
Toshio OKADA*	Dr., polymer chemist, Deputy Head
Motoyoshi HATADA	Dr., physical chemist
Kanae HAYASHI	Dr., polymer chemist
Siro NAGAI	Dr., physical chemist
Shun'ichi SUGIMOTO	Physical chemist
Koji MATSUDA	Radiation physicist
Jun'ichi TAKEZAKI	Physical chemist
Masanobu NISHII	Dr., polymer chemist
Hidehiko ARAI**	Physical chemist
Torao TAKAGAKI	Radiation physicist
Kanako KAJI	Polymer chemist
Yuichi SHIMIZU	Physical chemist
Toshiaki YAGI	Engineering chemist

[2] Advisors

Yoshito IKADA	Assoc. Professor, Kyoto University, Advisor

Present address:

*) Department of Engineering, Ohita University

**) Takasaki Radiation Chemistry Research Establishment